DISSERTATION

TAX ABOLISHES HISTONE H1 REPRESSION OF p300 ACETYLTRANSFERASE ACTIVITY AT THE HTLV-1 PROMOTER

Submitted by
Kasey L. Konesky
Department of Biochemistry and Molecular Biology

In partial fulfillment of the requirements
For the Degree of Doctor of Philosophy
Colorado State University
Fort Collins, CO
Spring 2006

Reproduced with permission of the copyright owner. Further reproduction prohibited without permission.

UMI Number: 3226138

INFORMATION TO USERS

The quality of this reproduction is dependent upon the quality of the copy submitted. Broken or indistinct print, colored or poor quality illustrations and photographs, print bleed-through, substandard margins, and improper alignment can adversely affect reproduction.

In the unlikely event that the author did not send a complete manuscript and there are missing pages, these will be noted. Also, if unauthorized copyright material had to be removed, a note will indicate the deletion.

UMI®

UMI Microform 3226138

Copyright 2006 by ProQuest Information and Learning Company.

All rights reserved. This microform edition is protected against unauthorized copying under Title 17, United States Code.

ProQuest Information and Learning Company
300 North Zeeb Road
P.O. Box 1346
Ann Arbor, MI 48106-1346

Reproduced with permission of the copyright owner. Further reproduction prohibited without permission.

COLORADO STATE UNIVERSITY

April 3, 2006

WE HEREBY RECOMMEND THAT THE DISSERTATION PREPARED UNDER OUR SUPERVISION BY KASEY L. KONESKY ENTITLED "TAX ABOLISHES HISTONE H1 REPRESSION OF p300 ACETYLTRANSFERASE ACTIVITY AT THE HTLV-1 PROMOTER" BE ACCEPTED AS FULFILLING IN PART REQUIREMENTS FOR THE DEGREE OF DOCTOR OF PHILOSOPHY.

Committee on Graduate Work

Dr. Jennifer Nyborg

Dr. Norm Curthoys

Dr. Karolin Luger

Dr. Alan Van Orden

Dr. Paul Laybourn, Advisor

Dr. Marv Paule, Department Head
(signed by Dr. Paul Laybourn, acting chair)

Reproduced with permission of the copyright owner. Further reproduction prohibited without permission.

ABSTRACT OF DISSERTATION

TAX ABOLISHES HISTONE H1 REPRESSION OF p300 ACETYLTRANSFERASE ACTIVITY AT THE HTLV-1 PROMOTER

Upon infection of human T-cell leukemia virus type-1 (HTLV-1), the provirus is integrated into the host cell genome and subsequently packaged into chromatin that contains histone H1. Consequently, transcriptional activation of the virus requires overcoming the environment of chromatin and H1. To efficiently activate transcription, HTLV-1 requires the virally-encoded protein Tax and cellular transcription factor CREB. Together Tax and CREB interact with three *cis*-acting promoter elements called viral cyclic-AMP response elements (vCREs). Binding of Tax and CREB to the vCREs promotes association of p300/CBP into the complex and leads to transcriptional activation. Therefore, to fully understand the mechanism of Tax transactivation, it is necessary to examine transcriptional activation from chromatin assembled with H1. Using a DNA template harboring complete HTLV-1 promoter sequence and a highly defined recombinant assembly system, we demonstrate proper and stoichiometric incorporation of histone H1 into chromatin. Addition of H1 to the chromatin template reduces HTLV-1 transcriptional activation two-fold through a novel mechanism. Specifically, H1 does not inhibit CREB or Tax binding to the viral CREs or p300 recruitment to the promoter. Rather, H1 directly targets p300 acetyltransferase activity. Interestingly, in determining the mechanism of H1 repression, we have discovered a previously undefined function of Tax, which is

Reproduced with permission of the copyright owner. Further reproduction prohibited without permission.

to overcome the repressive effects of H1-chromatin. Tax specifically abrogates the H1 repression of p300 enzymatic activity in a manner independent of p300 recruitment and without displacement of H1 from the promoter.

Kasey L. Konesky
Department of Biochemistry and Molecular Biology
Colorado State University
Fort Collins, CO 80523
Spring 2006

Reproduced with permission of the copyright owner. Further reproduction prohibited without permission.

ACKNOWLEDGEMENTS

I am indebted to those who have contributed to my success as a graduate student. It is impossible to obtain a Ph.D. without the help of others. Fortunately, I have been influenced by people with a true and infectious passion for science. I would like to thank my advisor, Dr. Paul Laybourn, for teaching me to keep an open mind. Data is what it is. My thesis spawned from a fortuitous collaboration between Dr. Laybourn and Dr. Nyborg, which has been instrumental to the success of my project. I am also thankful for the support from my committee members, Drs. Jennifer Nyborg, Norm Curthoys, Karolin Luger, and Alan Van Orden. I want to thank Stephanie Abernathy and Dr. Sara (Georges) Hanson for teaching me the tricks of the trade and for their friendship. I am also glad to have had the chance to work with Dr. Nicholas Polakowski. His humor, well, it speaks for itself, while his "theories" kept me on my toes. Finally, I sincerely appreciate the encouragement from those near and dear to me – Mom, Dad, Kelly, Uncle Jim, and my fiancé, Matt. I am especially grateful to Matt.

Reproduced with permission of the copyright owner. Further reproduction prohibited without permission.

TABLE OF CONTENTS

Title Page i
Signature Page ii
Abstract of Dissertation iii
Acknowledgments v
Table of Contents vi

Chapter 1: Introduction 1

1.1 HTLV-1 2
1.2 HTLV-1 Associated Diseases 3
1.3 HTLV-1 Replication 4
1.4 Genomic Organization of HTLV-1 6
1.5 Transcriptional Activation of the Provirus 6
1.6 The Role of Coactivators in HTLV-1 Transcriptional Regulation 11
1.7 Chromatin: The Major and Minor Players 16
1.8 Linker Histone Structure and Function 18
1.9 Histone H1: A Mediator of Gene Regulation 22
1.10 Statement of Purpose 24

Chapter 1 Figures

Figure 1.1 HTLV-1 genome 7
Figure 1.2 Tax and CREB domains 9
Figure 1.3 Transcriptional regulatory elements 10
Figure 1.4 CBP/p300 domains 13
Figure 1.5 From nucleosome to chromosome 17
Figure 1.6 H1 binding models 21

Chapter 2: Materials and Methods 26

2.1 Baculovirus Maintenance 27
2.2 Protein Expression and Purification 31
2.3 Recombinant Chromatin Methods 37
2.4 *In Vitro* Assays on Chromatin Templates 43

Reproduced with permission of the copyright owner. Further reproduction prohibited without permission.

Chapter 2 Figures

Figure 2.1 Plaque visualization 28
Figure 2.2 Purified histones 31
Figure 2.3 Purified dNAP-1 33
Figure 2.4 Purified ACF 34
Figure 2.5 Purified p300 35
Figure 2.6 Purified Tax and CREB 36
Figure 2.7 Promoter schematic 37

Chapter 3: Recombinant Chromatin: Optimization of Chromatin Containing Histone H1 48

3.1 Abstract 49
3.2 Introduction 50
3.3 Results 52
3.4 Discussion 61

Chapter 3 Figures

Figure 3.1 H1 sequence anaylsis 53
Figure 3.2 Topological assay 55
Figure 3.3 Micrococcal nuclease assay (MNase) with H1 57
Figure 3.4 MNase with CEM H1 58
Figure 3.5 Sucrose gradient with dNAP-1 60
Figure 3.6 Sucrose gradient with truncated yNAP-1 61

Chapter 4: Tax Abolishes Histone H1 Repression of p300 Acetyltransferase Activity at the HTLV-1 Promoter 65

4.1 Abstract 66
4.2 Introduction 67
4.3 Results 70
4.4 Discussion 93

Chapter 4 Figures

Figure 4.1 Histone H1 is properly incorporated into chromatin 71
Figure 4.2 Histone H1 represses transcriptional activation 74
Figure 4.3 Tax counteracts the H1-chromatin repression 78
Figure 4.4 CREB binding is not inhibited by H1 chromatin 82
Figure 4.5 H1 chromatin inhibits p300 acetyltransferase activity 83

Reproduced with permission of the copyright owner. Further reproduction prohibited without permission.

Figure 4.6 Tax completely overcomes H1 repression of p300 activity 87
Figure 4.7 Recruitment of p300 is not affected by H1 91
Figure 4.8 Model for HTLV-1 regulation in a chromatin context 98
Figure 4.9 H1 addition to naked DNA transcription 100
Figure 4.10 CREB DNase I footprinting on naked DNA 101
Figure 4.11 CREB DNase I footprinting on chromatin AA vs. DA 102
Figure 4.12 Tax and CREB DNase I footprinting on chromatin DA 103
Figure 4.13 Tax and CREB addition during assembly in MNase 104
Figure 4.14 Free H1 does not inhibit p300 acetyltransferase activity 105
Figure 4.15 H1 binding to immobilized template

Chapter 5: Future Directions 107

5.1 How does Tax Affect p300 in Overcoming H1 Repression? 108
5.2 CREB Binding *In Vitro* Versus *In Vivo*? 110
5.3 Can We Correlate H1 Structure With Function? 111

Appendix A: Histone Variant H2A.Bbd 112

A.1 Abstract 113
A.2 Introduction 113
A.3 Results and Discussion 114

Appendix A Figures

Figure A.1 MNase of H2A.Bbd nucleosomes 116
Figure A.2 H2A.Bbd nucleosomes are less repressive in transcription 117

Appendix B: Mass Spectrometry Analysis of *Drosophila* Histones 118

References 121

Reproduced with permission of the copyright owner. Further reproduction prohibited without permission.

Chapter 1

Introduction

Reproduced with permission of the copyright owner. Further reproduction prohibited without permission.

1.1 HUMAN T-CELL LEUKEMIA VIRUS TYPE-1 (HTLV-1)

The first human retrovirus was discovered in 1979. Poiesz et al. (1980) reported the presence of reverse transcriptase in a T-cell line established from a patient infected with adult T-cell leukemia (ATL) (125). Identification of reverse transcriptase confirmed retroviral infection and the virus was designated HTLV-1 (125). Roughly 10-20 million people worldwide are infected with HTLV-1 and infection is considered endemic in Southern Japan, the Caribbean and Africa (39). HTLV-1 varies from other transforming retroviruses in that it does not activate expression of a cellular proto-oncogene through integration and activation of downstream genes. Instead, production of the viral protein Tax contributes to malignant transformation (53, 54). Viral infection is linked to the pathogenesis of two distinct illnesses - ATL and HTLV-1 associated myelopathy/tropical spastic paraparesis (HAM/TSP). Transmission of HTLV-1 is thought to require the transfer of infected T-cells and can occur through several modes including breast feeding, sexual intercourse, and blood transfusions, of which the most common route is from a mother to her unborn child (114, 144, 148). There is currently no vaccine for humans, and therefore, no method for preventing new cases of HTLV-1. However, increased awareness of and testing for the virus has decreased the occurrence of viral infection from mother to child (66) and donated blood is now screened against HTLV-1.

Reproduced with permission of the copyright owner. Further reproduction prohibited without permission.

1.2 HTLV-1 ASSOCIATED DISEASES

1.2a ATL

ATL was discovered in 1976 in Japan prior to identification of HTLV-1 (154). As more cases of ATL were confirmed, the search for the etiology of the leukemia began. The connection between ATL and HTLV-1 was established by detecting unique serum antibodies from ATL patients and identifying HTLV-1 antigens that reacted with these antibodies (67, 166).

The cumulative risk of developing ATL upon HTLV-1 infection is approximately 4%, as most individuals remain lifetime asymptomatic carriers of the virus (146). Typically, the onset of ATL occurs decades after the initial infection. Diagnosis of ATL is dependent upon identification of abnormal T-cells that have hyperlobulated, flower-shaped nuclei, malignant cells harboring monoclonal proviral integration sites and HTLV-1 antibodies (149).

There are four subtypes of ATL - acute, chronic, smoldering and lymphoma that have been classified according to their clinical features (141). Acute ATL occurs in 55-75% of those persons with ATL, and is the most advanced form, as patients are typically resistant to chemotherapy and die within a year of onset (56, 159). Chronic and smoldering ATL are lesser degrees of disease but are capable of progressing to the acute stage after a long period. The fourth subtype is lymphoma ATL, which is characterized by the formation of tumors within the lymph system. While the exact symptoms of ATL vary, skin lesions, enlarged lymph nodes and infiltration of leukemic cells into various organs are common.

Reproduced with permission of the copyright owner. Further reproduction prohibited without permission.

1.2b HAM/TSP

Infection of HTLV-1 has also been associated with a neurological disorder - HAM/TSP (48, 116). This disease is characterized by demyelination of the long motor neuron tracts within the spinal cord and can ultimately lead to paralysis. The clinical features of HAM/TSP are similar to multiple sclerosis; therefore, confirmation of this disorder requires the presence of antibodies against HTLV-1 antigens. Like ATL, individuals often develop HAM/TSP long after the initial infection with HTLV-1 and have a 4% chance of disease progression (115).

Interestingly, individuals with HAM/TSP have a different antibody response to infection than those with ATL or who are asymptomatic carriers of the virus (12). Specifically, HAM/TSP patients have a greater immunological response and have certain types of human leukocyte antigens. Despite increased antibodies, these individuals have greater populations of infected T-cells that are able to infiltrate the spinal cord and cerebrospinal fluid (104). From there, the infected cells mediate destruction of neuronal tissue, which contributes to the clinical features of HAM/TSP (75).

1.3 HTLV-1 REPLICATION

HTLV-1 primarily infects CD4+ T-cells and to a lesser degree CD8+ lymphocytes (161). After endocytosis of the virion and uncoating, the two copies of single-stranded RNA are transcribed using reverse transcriptase from the virus into double-stranded DNA. The resulting DNA is randomly integrated into the host genome (113). More recently, data indicate that sites of proviral integration

Reproduced with permission of the copyright owner. Further reproduction prohibited without permission.

are not random with respect to the nucleotide sequence, as A/T-rich regions are preferred by the virus (90). Because HTLV-1 integrates into the host genome, the virus is able to escape destruction by the host, another characteristic of retroviruses. Subsequent to infection, HTLV-1 is replicated using the host cell DNA polymerase and not the viral reverse transcriptase. Interestingly, the mechanism for HTLV-1 propagation occurs through cell-to-cell contact, explaining the lack of virions in the serum of infected individuals (71).

The persistence of clinical latency and the low incidences of ATL and HAM/TSP are attributed, in part, to the continual cellular immune response to HTLV-1 infection (13). This steadfast response suggests that the virus does not enter a latent state but is continually producing proteins, and therefore, viral antigens. The anomaly with HTLV-1 infection has been the near undectable level of viral proteins like Tax (109) and verification of viral mRNA in only small populations of infected cells (49). A possible explanation for low protein and mRNA levels is through a Tax-specific cytotoxic T lymphocyte (CTL) response. When HTLV-1 infected cells are removed from patients and cultured *in vitro*, the percentage of CD4+ cells expressing Tax rises dramatically (11). In addition, CTLs have been shown to reduce the frequency of Tax-expressing cells *in vitro*, as the approximate half-life of these cells is less than one day (11). Since the CTL response is robust *in vivo*, these data suggest the mechanism behind clinical latency and reduced viral protein and mRNA levels is partly through the selected destruction of Tax expressing cells.

Reproduced with permission of the copyright owner. Further reproduction prohibited without permission.

1.4 GENOMIC ORGANIZATION OF HTLV-1

Housed between 5′ and 3′ long terminal repeats (LTRs) are the typical retroviral genes – *gag*, *pol* and *env*. These genes encode viral core proteins, reverse transcriptase and envelope proteins, respectively. The genome of HTLV-1 differs from most retroviruses in that it contains an additional sequence 3′ of the *env* gene, referred to as pX (Figure 1.1) (134, 136). Multiple proteins, including Tax and Rex, are encoded by the pX region and are produced by alternate splicing and multiple reading frames.

Each LTR can be further divided into three regions that are characteristic of retroviruses, the U3, R and U5 regions. Further, the U3 region contains the polyadenylation signal, the TATA box and viral promoter, while the U3/R boundary is the RNA transcription initiation site. Three 21 base pair repeats within the U3 region, termed viral cyclic AMP-response elements (vCREs), act as *cis*-acting regulatory sequences that are necessary for transcriptional activation of the virus (140).

1.5 TRANSCRIPTIONAL ACTIVATION OF THE PROVIRUS

Regulation of transcription is critical to viral replication. Coincidentally, HTLV-1 has a defined feedback system that relies on the functions of Tax and Rex. While Tax is a potent *trans*-activator of viral transcription, HTLV-1 down-regulates Tax-mediated activation through the effects of Rex (135). Rex does not repress transcription directly, but leads to increased translation of the viral

Reproduced with permission of the copyright owner. Further reproduction prohibited without permission.

structural genes (64). As a consequence, Rex inhibits expression of *tax/rex* mRNA and ultimately down-regulates transcriptional activation.

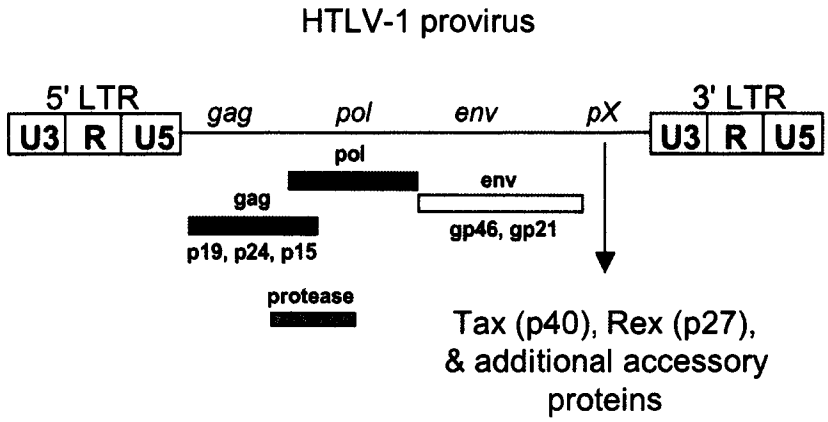

Figure 1.1. Schematic of the HTLV-1 genome. HTLV-1 contains typical retroviral elements including 5' & 3' LTRs and the *gag*, *pol*, and *env* gene products, which are listed. HTLV-1 differs from other retroviruses in that it contains an additional sequence termed pX. Transcriptional regulatory proteins Tax and Rex are encoded by the pX region in addition to other non-structural proteins, and are produced from alternative splicing of mRNA encoded by different open reading frames.

1.5a Tax and CREB-Mediated Transcriptional Activation

Activation of HTLV-1 transcription is not mediated by Tax alone. Rather, Tax interacts with transcription factors from the CREB/ATF (cyclic AMP-response element binding protein/activating transcription factor) family in stimulating viral transcription from each LTR (2, 44, 168). Efficient Tax transactivation requires both protein-protein as well as protein-DNA contacts.

A well-studied role for Tax is increasing the affinity of CREB to vCRE DNA (6, 22, 168). Tax also augments the stability of CREB dimers (15). As expected,

Reproduced with permission of the copyright owner. Further reproduction prohibited without permission.

these functions of Tax are directed through protein-protein contacts. Specifically, residues in the N-terminus of Tax are critical for CREB interactions, and the basic segment within the CREB b-ZIP domain is required for Tax binding (Figure 1.2) (2, 15, 52, 124). Together, Tax and CREB bind the three *cis*-acting vCREs within the U3 region of the HTLV-1 promoter, forming a ternary complex (Figure 1.3). Not only do they bind the 5′ LTR to activate transcription of viral proteins, but Tax and CREB also bind the 3′ LTR and potentially activate transcription of cellular genes that are positioned downstream of the integration site (96).

The vCREs are critical for Tax-mediated transcriptional activation (42, 128). At minimum, two vCREs are required for Tax transactivation (21). Although there are only one to two nucleotide differences between a cellular CRE and vCRE, formation of the ternary complex is highly specific to vCRE DNA (117). CREB binds as a dimer (or heterodimer with other CREB/ATF members) to the 8-nucleotide vCRE core within each 21 base pair element. And, Tax preferentially interacts with the GC-rich sequences immediately flanking the core CRE within the DNA minor groove (Figure 1.3) (77, 82, 97, 103, 117).

In addition to the effects on HTLV-1 gene activation, it is important to note that Tax regulates transcription of numerous cellular genes, both positively and negatively (reviewed in 164).

Reproduced with permission of the copyright owner. Further reproduction prohibited without permission.

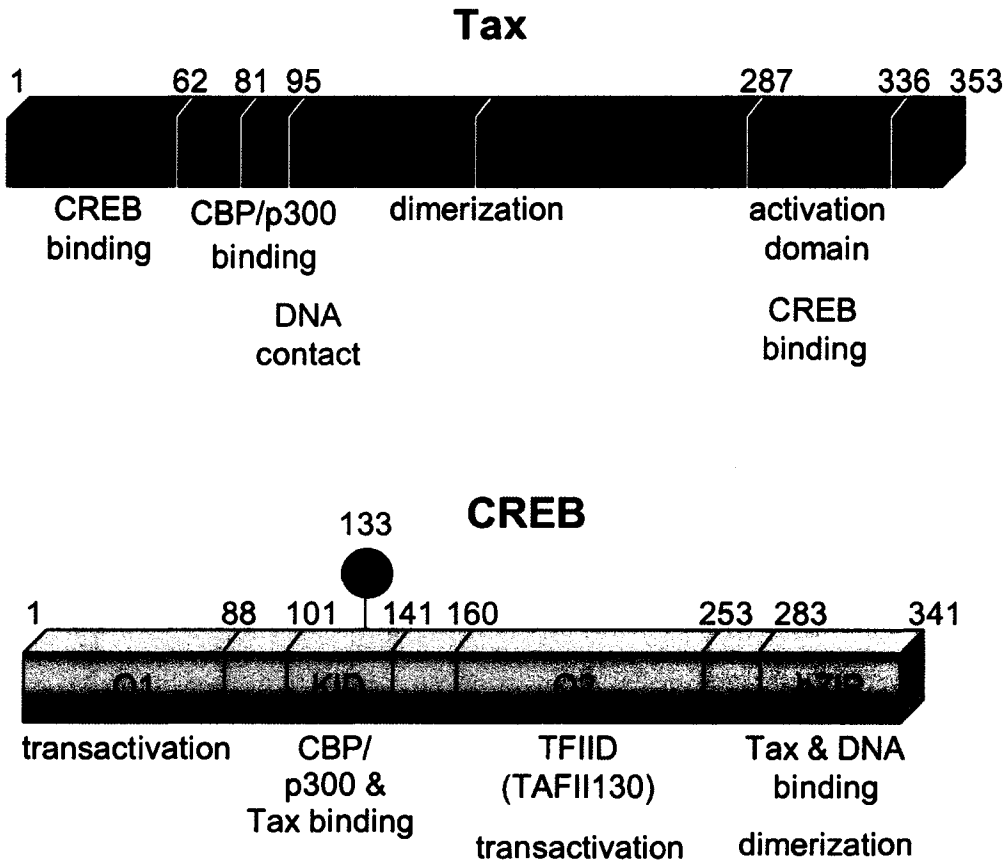

Figure 1.2. Critical domains within Tax and CREB. Tax is a 40kDa protein containing 353 amino acids. CREB is 341 amino acids in length and encodes a 42 kDa protein. Approximate amino acid positions are illustrated for the various functional domains within each protein.

Reproduced with permission of the copyright owner. Further reproduction prohibited without permission.

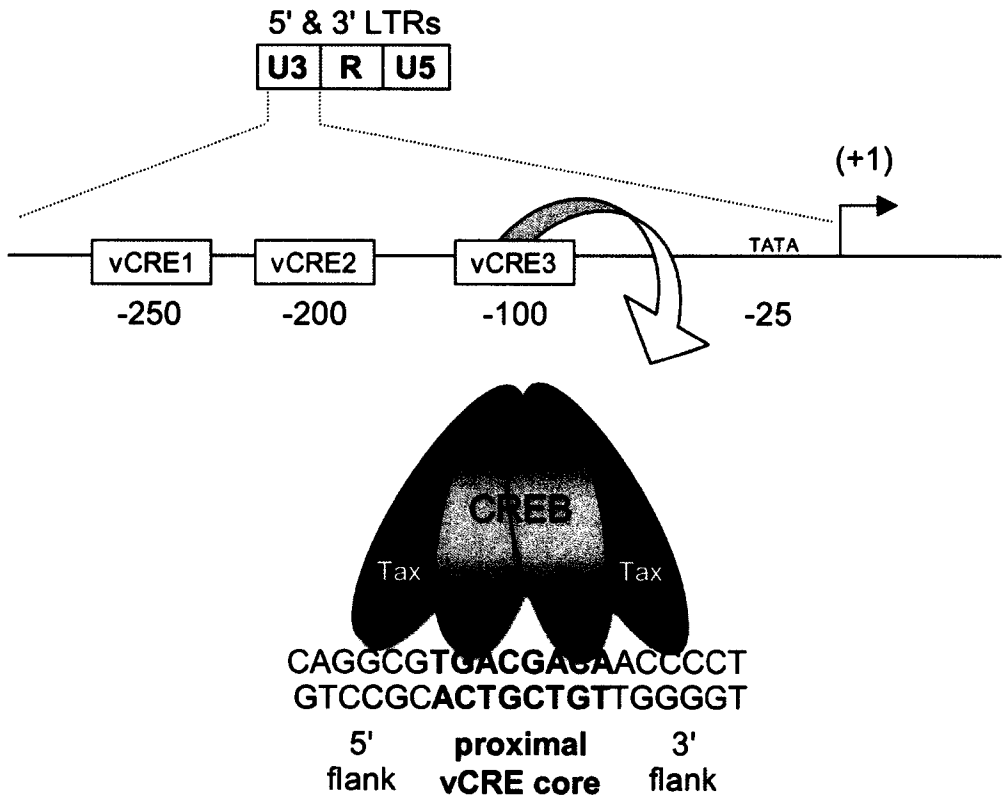

Figure 1.3. Transcriptional regulatory elements of the HTLV-1 promoter. The viral promoter is contained within the U3 region of each LTR. Approximate nucleotide positions for the vCREs and TATA box are indicated relative to the transcription start site (+1). A model of the Tax/CREB/DNA ternary complex is illustrated using the vCRE core and flanking sequences from the promoter proximal 21 bp element.

Reproduced with permission of the copyright owner. Further reproduction prohibited without permission.

1.6 THE ROLE OF COACTIVATORS IN HTLV-1 TRANSCRIPTIONAL ACTIVATION

1.6a The Coactivators CBP/p300

CBP (CREB binding protein) and p300, often referred to as CBP/p300, are considered paralogues. These large proteins exhibit a high degree of sequence similarity (63%), which suggests a functional overlap between these two proteins. However, while CBP and p300 do perform related functions, they also have distinct roles (reviewed in 80). Gene knockout studies in mice have demonstrated unique properties of each coactivator in development (160). Additionally, these studies confirmed the pleiotropic functions of CBP/p300, as homozygous and heterozygous CBP or p300 knockout mice are embryonic lethals (160). Therefore, it is no surprise that CBP/p300 are involved in biological processes that affect cell growth, transformation and development of multicellular organisms from worms to humans (reviewed in 51). Central to the various functions of CBP/p300 are their roles as transcriptional coactivators through recruitment by numerous nuclear proteins, including Tax and CREB.

1.6b Tax-Mediated Coactivator Recruitment

Classically, stimulation of the cyclic-AMP (cAMP) pathway leads to activation of protein kinase A (PKA) and subsequent phosphorylation of CREB at serine 133 within the KID domain (kinase inducible domain) (108). The phosphorylated form of CREB (P-CREB) specifically recruits the coactivator

Reproduced with permission of the copyright owner. Further reproduction prohibited without permission.

CBP/p300, resulting in enhanced transcriptional activation of genes harboring cellular CREs (10, 87). Interestingly, Tax bypasses the requirement for P-CREB in recruiting CBP/p300 to the vCREs, providing an alternative to cAMP-dependent transcriptional activation of the HTLV-1 promoter (86).

Tax interacts with three functionally distinct regions of CBP/p300 - C/H1, KIX, and SRC-1 (steroid receptor cofactor-1) (18, 50, 93, 133). Figure 1.4 illustrates the main functional domains of CBP/p300 and the approximate binding sites for various proteins. The KIX domain of CBP/p300 has been well studied, as this region also interacts with the KID domain of P-CREB (127). The interactions between Tax and KIX are mediated through a KID-like domain within Tax, encompassing amino acids 81-95 (Figure 1.2) (61). Tax recruits KIX in the presence of either CREB or P-CREB to vCRE DNA, forming a quaternary complex (18, 50). Interestingly, the KID domain of CREB is dispensable for complex formation and subsequent transcriptional activation, demonstrating the dependence on Tax for KIX recruitment to vCREs in the absence of CREB phosphorylation (50). Additionally, the role of CBP/p300 in Tax transactivation was demonstrated *in vivo*, as transfection of a KIX expression plasmid abrogated Tax transcriptional activation (50).

The interactions between Tax and SRC-1 of CBP/p300 have been less studied, but revealed Tax transactivation was also dependent on interactions with this C-terminal region within CBP/p300 (133). Additionally, the binding of Tax and the p53 family member p73 to the N-terminal C/H1 region of CBP is mutually exclusive (93). The ability of Tax to interact with both the N and C-terminal

Reproduced with permission of the copyright owner. Further reproduction prohibited without permission.

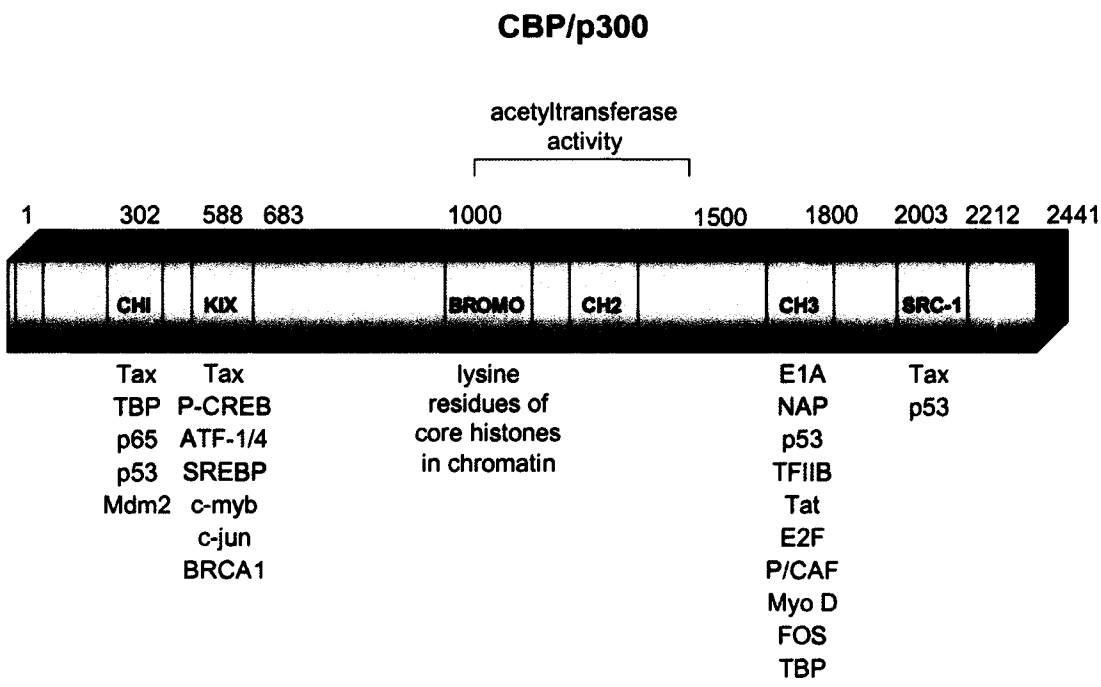

Figure 1.4. Conserved domains of CBP/p300. The approximate amino acid residues of functional regions within CBP/p300 are indicated and various proteins associated with each domain are illustrated.

regions of CBP/p300 suggest a mechanism in which two Tax/CREB complexes bind the coactivator simultaneously during transcriptional activation. Currently, how many molecules of CBP/p300 that are tethered to the HTLV-1 promoter via interactions with Tax remain unknown.

1.6c Transcriptional Regulation by CBP/p300

As coactivators, CBP/p300 function in augmenting transcriptional activation by stimulating RNA polymerase II recruitment to promoter elements. There are three main mechanisms for transcriptional regulation by CBP/p300

Reproduced with permission of the copyright owner. Further reproduction prohibited without permission.

(reviewed in 31). The first is a bridging model in which the coactivators interact with transcription factors and the basal transcription machinery. Secondly, CBP/p300 have been shown to act as scaffolds, nucleating formation of a multiprotein complex that function in recruiting the polymerase. Additionally, these coactivators rely on their intrinsic histone acetyltransferase activity (HAT) in promoting transcriptional activation.

Importantly, *in vivo* studies using chromatin immunoprecipitation (ChIP) assays detected the presence of both CBP and p300 on the HTLV-1 promoter of infected cells (95). Similar studies also demonstrated increased promoter occupancy of p300 upon transfection of a Tax expression plasmid into cells containing an HTLV-1 LTR luciferase construct (94). Furthermore, the presence of RNA polymerase II at the promoter increased four-fold upon Tax expression (94). Given the known interactions between Tax and CBP/p300 and the fact that the coactivators interact with various subunits of RNA polymerase II including TBP, TFIIB, TFIIE, and TFIIF (51), the data support a model in which CBP/p300 bridges Tax/CREB to the transcription machinery and promotes transcriptional activation.

1.6d The Intrinsic Histone Acetyltransferase Activity of CBP/p300

Interestingly, Tax directly contacts TFIIA, TBP (TATA binding protein) and the TAFII28 subunit of TFIID, which correlates with increased transcriptional activation (26, 34). Because Tax interacts with the RNA polymerase transcription machinery, CBP/p300 may not stimulate transcription solely through its apparent

Reproduced with permission of the copyright owner. Further reproduction prohibited without permission.

bridging function at the HTLV-1 promoter. However, specific protein-protein contacts between Tax and the transcription machinery in the presence of CBP/p300 remain to be determined. Alternatively, the intrinsic acetyltransferase activity of CBP/p300 is a widely accepted mechanism for the action of these coactivators at the HTLV-1 promoter (47, 99).

The HAT activity of CBP/p300 specifically functions to acetylate lysine residues within the core histone amino-terminal tails (112). This modification is proposed to "open" the chromatin structure, rendering nucleosomal DNA more accessible to transcription factor binding (58-60). Additionally, regions of hyperacetylated chromatin have been correlated with actively transcribed genes (110). Consistent with these results are the presence of CBP and p300 at active HTLV-1 promoters *in vivo* and the corresponding acetylation of histones H3 and H4, as compared to the lack of coactivators and modified histones on an inactive promoter (95). Further, the HAT activity of p300 is essential for strong transcriptional activation from a chromatin context *in vitro* (47, 99).

While the HAT activity of CBP/p300 contributes to activation of the HTLV-1 provirus that is assembled into chromatin, it is important to note that previous data demonstrated an additional requirement for transcriptional activation involving p300-mediated acetylation of non-histone substrates (46). The other targets of p300 acetyltransferase activity at the HTLV-1 promoter have yet to be identified. However, this factor acetyltransferase (FAT) activity of p300 is not uncharacteristic, as others have shown CBP/p300 to acetylate transcription factors and components of RNA polymerase II (143).

Reproduced with permission of the copyright owner. Further reproduction prohibited without permission.

1.7 CHROMATIN: THE MAJOR AND MINOR PLAYERS

To fully understand Tax-mediated activation of HTLV-1, studies must be performed in the context of chromatin, as the provirus is integrated into chromosomal DNA upon infection. Nucleosomes form the fundamental repeating unit of chromatin. They consist of a core histone octamer, which is composed of two H2B/H2A dimers and one H3/H4 tetramer wrapped by 146 base pairs of DNA in a 1.65 superhelical turn (102). In addition to the four major core histones, a fifth or linker histone, H1 contributes to the structure and function of chromatin. Incorporation of histone H1 increases the DNA associated with each nucleosome to two full superhelical turns, forming the chromatosome (152).

The initial deposition of nucleosomes onto DNA results in the formation of chromatin fibers that are often referred to as "beads on a string" (25). These 11 nM fibers further condense to 30 nM fibers in chromosomes (25). Less is known about the higher order structures that develop in subsequent levels of chromosome compaction (Figure 1.5). The core histone tails are vital to formation of the 30 nM chromatin fiber (132). Interestingly, histone H1 is not required for chromatin compaction but serves to stabilize the higher order structures (132).

Reproduced with permission of the copyright owner. Further reproduction prohibited without permission.

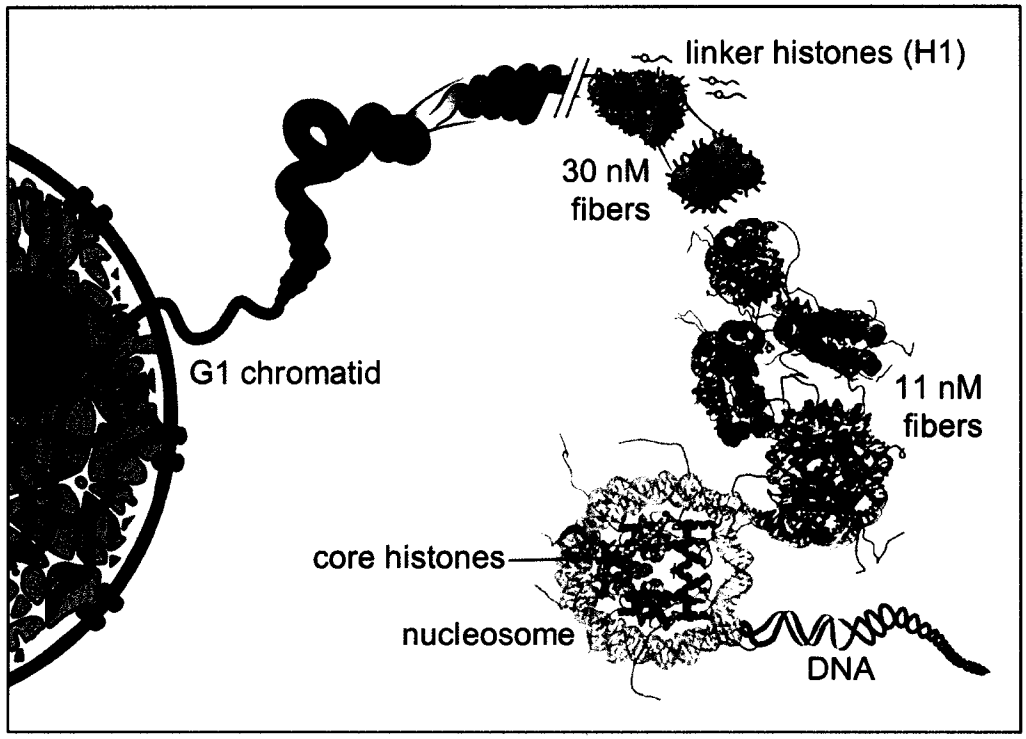

Figure 1.5. From nucleosome to chromosome - an illustration of the levels of chromatin structure. Nucleosomes form the fundamental unit of chromatin, allowing condensation of the genome. Linker histones function to stabilize higher order chromatin formations. (Figure courtesy of K. Luger)

Generally, organization of the DNA into chromatin represses cellular processes like transcription, replication, repair and recombination. To mediate these functions in the context of chromatin, cells have evolved mechanisms that alter the relationship between chromatin structure and function. Typically, what comes to mind is the ability of the core histone tails to be post-translationally modified or the presence of chromatin remodeling complexes. However, the

Reproduced with permission of the copyright owner. Further reproduction prohibited without permission.

structure of chromatin can also be modified through the incorporation or presence of histone variants.

The best-characterized variants include those for H3, H2A and histone H1. H3 has four variants – H3.1, H3.2, H3.3, and CENP-A, whereas H2A has four variants – H2A.Z, H2A.X, macroH2A, and H2A.Bbd (reviewed in 126). Research on the core histone variants has quickly progressed since the structure of the nucleosome was solved in 1997, as both structural and functional data have been obtained for several core histone variants (3, 8, 9, 14, 145). The roles of individual histone H1 isoforms are more ambiguous, since the general function of histone H1 is not nearly as defined as that of the core histones. In mammals the eight different H1 isoforms include the following: somatic linker histones ($H1^S$-1, $H1^S$-2, $H1^S$-3 and $H1^S$-4), oocyte specific ($H1^\infty$), testis specific (H1t), differentiation specific ($H1^0$) and a thymus/spleen/testis specific linker histone (H1a) (119). There is preliminary evidence that certain H1 isoforms ($H1^S$-2 & $H1^S$-4) are depleted from regions of active chromatin, suggesting a role for linker histone variants in differential gene regulation (121). Additionally, knockout studies in mice demonstrated the importance of histone H1 as homozygous deletions in three H1 isoform genes led to embryonic lethality (40).

1.8 LINKER HISTONE STRUCTURE AND LOCATION

Early data collected on H1 revealed a tripartite structure composed of an N-terminal tail (~40 aa), a central globular domain (~80 aa) and a C-terminal tail (~100 aa) (62). The globular domain is responsible for making direct contacts

Reproduced with permission of the copyright owner. Further reproduction prohibited without permission.

with nucleosomal DNA, while the tails are important for positioning H1 on the nucleosome and function during chromatin folding (5). Binding of linker histones to nucleosomes is easily detected upon digestion with micrococcal nuclease, since H1 protects 10-20 additional base pairs from nuclease digestion as compared to that from nucleosomes lacking H1. The globular domain alone is sufficient in conferring protection of extra base pairs (4). In 1993, the crystal structure of the globular domain of H5 (avian erythrocyte H1) was solved, providing insights into the mechanism of DNA binding by H1 (55). These studies revealed that the globular domain forms a winged-helix motif that is similar in structure to the *E. coli* CAP (catabolic activator protein) and *Drosophila* HNF3 (hepatic nuclear factor-3) proteins, which interact with the DNA major groove (33, 105).

Despite over 30 years of research, the exact location of H1 on the nucleosome has not been determined. Studies from the late 1970's proposed a model in which H1 interacted close to the nucleosomal dyad where DNA enters and exits the nucleosome (151, 152). Today's model is somewhat refined in that it places H1 on the dyad axis of the nucleosome, with H1 either protecting additional base pairs from nuclease digestion in a symmetric or asymmetric fashion (Figure 1.6) (153). Additionally, there is another model that is specific to 5S rDNA, which places H1 inside of the DNA gyres in direct contact with the core histones (Figure 1.6) (153).

One molecule of H1 typically binds per nucleosome (16). Regardless of where histone H1 is located, H1 binding to chromatin is a dynamic process. The

Reproduced with permission of the copyright owner. Further reproduction prohibited without permission.

first *in vivo* binding studies used GFP-tagged H1 and photobleaching in determining that nearly all of the transfected H1-GFP was bound to chromatin at any given time (107). These researchers and others also found H1-GFP was continuously exchanged in both euchromatic and heterochromatic regions, and that H1-GFP had a residency time of several minutes (98, 107). A "stop and go" model for H1 interactions has emerged from these data (24). Specifically, the time H1 stays bound to chromatin is much longer than the time H1 spends finding another location on the chromatin fiber, supporting the fact that most nucleosomes contain linker histone at any give moment. Interestingly, the "stop" stage at the single nucleosome level can be influenced and shortened due to post-translational modifications of H1 (specifically phosphorylation) and from competition with other nuclear proteins like HMGs, which also interact with chromatin (28, 98).

Reproduced with permission of the copyright owner. Further reproduction prohibited without permission.

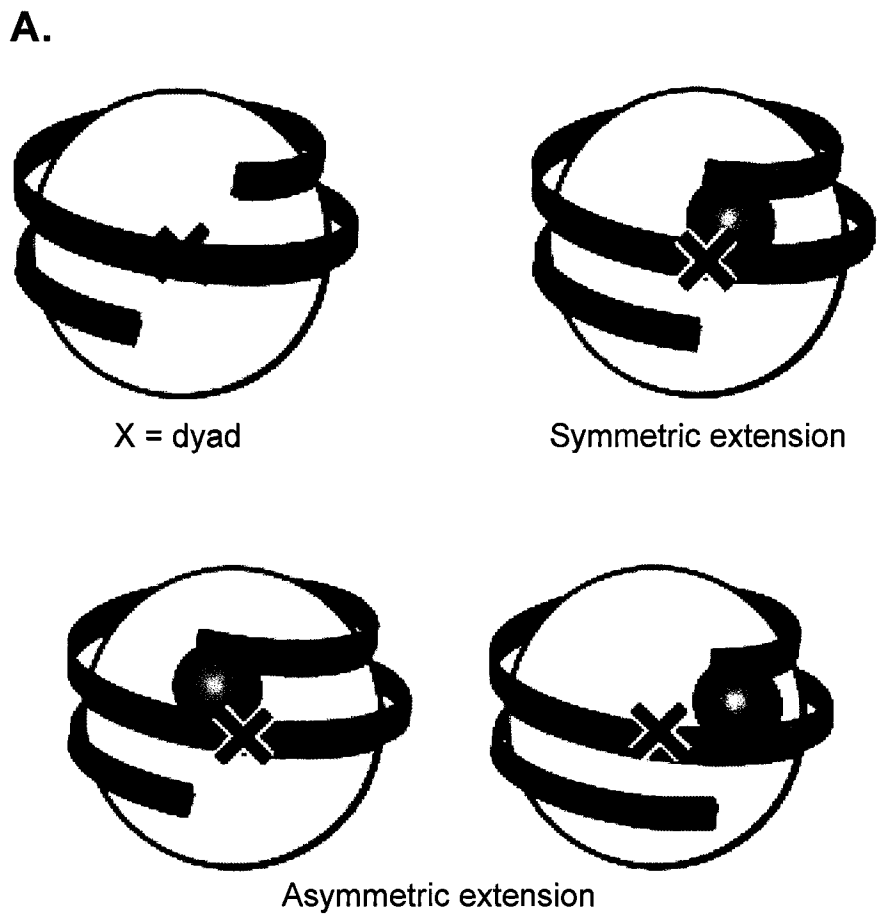

Figure 1.6. H1 binding models. (A) The "bulk chromatin" model places H1 at the nucleosomal dyad. The globular domain of H1 interacts with the DNA equally (symmetric extenstion) or unequally (asymmetric extension) in protecting additional base pairs from nuclease digestion. (B). The 5S rDNA model places H1 insides the DNA gyres.

Adapted from: **Travers, A.** 1999. The location of the linker histone on the nucleosome. TIBS. **24**:4-7.

Reproduced with permission of the copyright owner. Further reproduction prohibited without permission.

1.9 HISTONE H1: A MEDIATOR OF GENE REGULATION

1.9a The Role of Linker Histones in Transcriptional Repression

Chromatin assembled with only core histones is sufficient in repressing transcriptional activation. Incorporation of H1 into chromatin further represses transcription beyond that of the core histones (89). Therefore, H1 is classified as a transcriptional repressor. This function of histone H1 has been evident since the early 1980's, however, no general mechanism for H1 repression has come forth. In fact, the effects of H1 seem to be promoter specific. These findings, coupled with the contributions of H1 isoforms (although poorly understood) suggest a complex role for H1 in fine-tuning the aspects of gene regulation.

Early studies on the 5S RNA genes demonstrated chromatin containing H1 inhibited transcription factors from binding the DNA (131). Conversely, the assembly of transcription complexes onto chromatin stripped of H1 protected the 5S RNA genes from H1-mediated inactivation (139). Later research determined that H1 blocked transcription factors from binding to the oocyte-specific genes, but had no affect on TFIIIA binding to the somatic 5S RNA genes (137). Additionally, Juan et al. (1994) observed H1 inhibited a different transcription factor, USF (upstream stimulatory factor), from interacting with nucleosomal DNA (78, 79). More recently, a histone H1 isoform, H1b ($H1^S$-3), was found to interact with the transcription factor Msx1 to inhibit transcription of the MyoD promoter (91). In contrast, other researchers found no effect on estrogen receptor-α binding in the presence of chromatin containing H1 (32), and in one case, H1

Reproduced with permission of the copyright owner. Further reproduction prohibited without permission.

actually enhanced the interactions of the progesterone receptor to the MMTV promoter (83).

The effects of H1 extend beyond transcription factor binding, as H1-chromatin has been shown to selectively inhibit initiation of estrogen receptor transcriptional activation (32). Linker histones also inhibit the non-targeted histone acetyltransferase activity of PCAF (p300/CBP associated factor) to repress transcription (63). Yet another role for histone H1 in repressing transcription is through effects on chromatin remodeling complexes. H1 specifically inhibited SWI/SNF activity on a mononucleosome and an array, but failed to affect the ATP-dependent activity of ISWI along a nucleosomal array (65, 69, 156). However, in a different study with SWI/SNF, the authors observed no effect on chromatin remodeling in the presence of linker histone (155). Collectively, these studies confirm the lack of a general mechanism for H1 repression of transcriptional activation.

1.9b Histone H1 Phosphorylation

Histone H1 is phosphorylated during the cell cycle and also in response to transcriptional activation (19, 20). Interestingly, the levels of linker histone phosphorylation peak during mitosis when the chromosomes are condensing (130, 150). In contrast, phosphorylation of H1 on the MMTV promoter during transcription promotes activation, presumably through the disruption of H1/nucleosome interactions (19), while dephosphorylation leads to inactivation (92). Additionally, cyclin E/CDK2 (cyclin-dependent kinase 2) phosphorylation of

Reproduced with permission of the copyright owner. Further reproduction prohibited without permission.

H1 promotes H1 dissociation *in vivo*, increasing linker histone mobility (35). The effect of phosphorylation on histone H1 has very different consequences, and can be explained, in part, by a global versus localized effect. Phosphorylation during mitosis is most likely genome wide and clearly serves an important role in chromosome condensation, whereas histone H1 phosphorylation during transcriptional activation is probably confined to the promoter region.

While the extent and function of H1 modifications like phosphorylation, acetylation and ADP-ribosylation are poorly understood, new evidence demonstrated histone H1 becomes methylated at lysine 26 (85). With this finding, it is interesting to think of extending the "histone code" to linker histones. Despite the efforts by many, we are only beginning to scratch the surface of understanding histone H1 and its contributions to gene regulation.

1.10 Statement of Purpose

The established collaboration between Dr. Laybourn and Dr. Nyborg has provided insight into the mechanism of HTLV-1 gene regulation by examining contributions of the core histones and chromatin in transcriptional activation. To continue in furthering our understanding of HTLV-1 activation, we wanted to expand our studies by assembling chromatin containing linker histone. Therefore, the goal of my Ph.D. project was to define the role of histone H1 at the HTLV-1 promoter, which hinged upon successful incorporation of histone H1 into chromatin using a recombinant assembly system.

Reproduced with permission of the copyright owner. Further reproduction prohibited without permission.

To accomplish this task, we first optimized incorporation of histone H1 into chromatin using a recombinant assembly system, allowing us to examine the effects of H1 on transcriptional activation of HTLV-1. Specifically, we designed experiments to test whether chromatin containing H1 repressed transcriptional activation by Tax, and, if so, what step in activation is affected by H1. Biochemical approaches like *in vitro* transcription and histone acetyltransferase assays were used to verify histone H1 repressed activation and directly inhibited the acetyltransferase activity of p300. The data within this dissertation demonstrate the importance of histone H1 and provide a new platform from which to examine HTLV-1 transcriptional activation.

Reproduced with permission of the copyright owner. Further reproduction prohibited without permission.

Chapter 2

Materials and Methods

This chapter defines all of the experimental procedures described throughout this dissertation and compliments certain protocols with the addition of details often omitted in manuscripts. Also, this section serves as a comprehensive guide for maintenance of baculovirus stocks and subsequent protein expression and purification from Sf9 cells.

Reproduced with permission of the copyright owner. Further reproduction prohibited without permission.

2.1 BACULOVIRUS MAINTENENCE

2.1a Generating Baculovirus Clones

When expressing proteins from baculovirus, special care must be taken to ensure minimal passaging of each viral stock. If this guideline is not followed, mutations can occur in the baculovirus that ultimately cause a significant loss of protein expression. The first step in maintaining a low passage viral stock is to isolate new baculovirus clones from plaque assays. A detailed protocol explained in Baculovirus Expression Vectors: A Laboratory Manual (111) was followed for the plaque assays and picking of individual, isolated clones (pages 125-126). Clones were generated for all of our baculoviruses, which included dNAP-1_{His6}, Acf1, $ISWI_{FLAG}$ and $p300_{His6}$. Because these baculoviruses were kind gifts, we assumed the viruses had previously undergone several rounds of plaque purification. Therefore, we only performed one round of plaque assays for acquiring each clone.

2.1b Amplification of Viral Clones: Passage One Viral Stock

Passage one viral stocks were generated as described (111) (pages 128-129) with the following modification. Typically, viral supernatant was collected 7-9 days post infection as the cells began to lyse, instead of collecting at 4 days post infection. After harvesting the viral supernatant, there should be 1.5 to 2 ml of passage one virus. At this time, small-scale infections (described later) can be performed to select for one or two clones that produce high levels of the target

Reproduced with permission of the copyright owner. Further reproduction prohibited without permission.

protein. Ideally, the passage one virus is further amplified to a passage two stock before expression testing.

2.1c Amplification of Viral Clones: Passage Two Virus and Working Stocks

Generation of a second passage viral stock is necessary to further amplify the virus, both in titer and volume. The amplification was performed as described (pages 129-130) (111), but the infection was allowed to proceed until the cells began to lyse. After collecting the viral supernatant, plaque assays were performed to determine the titer of each virus. To better visualize and count plaques, the viable stain, neutral red, can be overlayed as described (111). However, neutral red should not be used when initially picking clones from which to generate new baculovirus stocks, as neutral red can potentially mutate the virus. Results from a typical plaque assay are shown in Figure 2.1.

The best time to perform small-scale infections is after calculating the titer

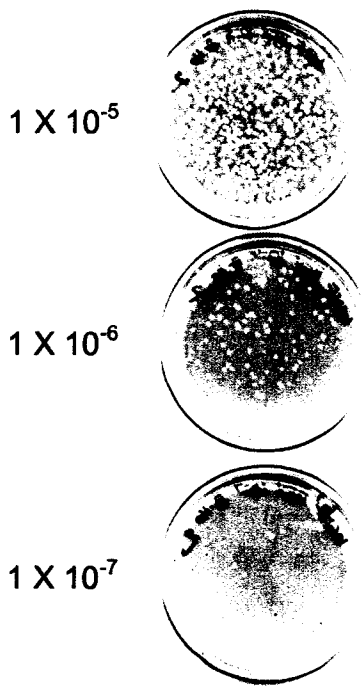

Figure 2.1. Plaque visualization is enhanced by neutral red staining. Serial dilutions of recombinant hSNF (RSF subunit) baculovirus were used in this plaque assay to calculate virus titer. Virus dilutions are indicated to the left of each plate. The titer was calculated from plaque counts at virus dilutions of 1 X 10^{-7} and 1 X 10^{-6}.

Reproduced with permission of the copyright owner. Further reproduction prohibited without permission.

of each passage two clone. Because the titer is known, cells can be infected with equivalent plaque forming units (pfu) of virus. For the small-scale infections, seed cells in log phase growth at a density of 1.0 X 10^6 cells/ml onto 6-well plates in a final volume of 2 ml of serum-free TNM-FH medium. Let the cells attach for 30 minutes to 1 hour in the serum-free medium and then aspirate the medium containing any cells that did not attach. Infect the cells with virus to a multiplicity of infection (MOI) of 5-10 and rock the plates at room temperature for 1 hour to ensure even infection. The virus may need to be diluted, as the cells should be covered with 0.5 – 1 ml of virus. After 1 hour, add complete TNM-FH media to 5 ml and place the cells at 27°C until they start to show signs of infection (typically 2-5 days, depending on the virus). The cells should appear visibly swollen and larger than control (uninfected) cells. Harvest the cells by scraping them off of each plate and collecting them into 15-ml conicals. Centrifuge 1000 x g for 5 minutes to pellet the cells, aspirate the supernatant, resuspend the cells in 50 μl SDS-PAGE loading dye and analyze protein expression by Western blot.

Importantly, if small-scale infections are performed with passage one virus, use 0.2 ml of virus to infect the cells. Since there is not enough passage one virus for both titer determination and amplification, the infections may not be of equal pfu. In addition, because passage one virus is very low in titer, visualizing cell growth is more difficult. Therefore, it is best to use passage two virus for these initial infections.

Reproduced with permission of the copyright owner. Further reproduction prohibited without permission.

After expression testing, select only the best clone from each virus to further amplify, and infect the cells at a low MOI of 0.1 to 1 to produce the working baculovirus stock as described (page 130) (111). It is important to infect working stocks at very low MOIs of 0.1 to 1 and infect for protein expression at high MOIs of 5 to 10. With our viruses, we found it necessary to carry this infection until the cells began to lyse (often days 7 to 9) before harvesting the viral supernatant for the working stock. Take special care in storing working stocks, as they must be protected from light to avoid compromising the viral titer (76). After working stocks are generated, perform another round of plaque assays to determine the virus titer. Working stocks are stable for six months, after which, a plaque assay should again be performed to determine any loss in viral titer. After a year, a new working stock can easily be made from an aliquot of passage two virus that is stored in liquid nitrogen. It is critical at this stage to store aliquots of the passage two clones that yielded the most protein in both -80°C and liquid nitrogen. This step is vital in maintaining low passage working stocks over several years and bypasses the need to isolate clones every year.

To further characterize each virus for optimal protein expression, cells should be infected at various MOIs between 5 and 10. This is readily accomplished using 100 ml spinners containing 50 ml of log phase cells at 1 X 10^6 cells/ml for each MOI. Allow the infections to proceed until the cells show signs of lysis. In the meantime, remove 1 ml of cells everyday until the cells begin to lyse. These cells will be used to determine the hours of infection required for optimal protein production and the best MOI. After removing the

Reproduced with permission of the copyright owner. Further reproduction prohibited without permission.

cells, pellet them, aspirate the media, resuspend in 50 μl SDS-PAGE dye and store at -20°C. When the last sample has been collected, analyze for maximum protein expression via western blot. Congratulations! You have finally determined the best MOI and infection time for optimal protein expression of one virus. Continue this process for every baculovirus in the laboratory.

2.2 PROTEIN EXPRESSION AND PURIFICATION

2.2a Native *Drosophila* Histones

Drosophila core histones (Figure 2.2) were purified from *Drosophila* embryos as described (23). Histone H1 (Figure 2.2) was also isolated and purified from *Drosophila* embryos as described by Croston et al. 1991 (36). We chose to use *Drosophila* H1 because they only have a single histone H1 isoform, unlike mammalian cells, which can contain as many as seven different isoforms (119).

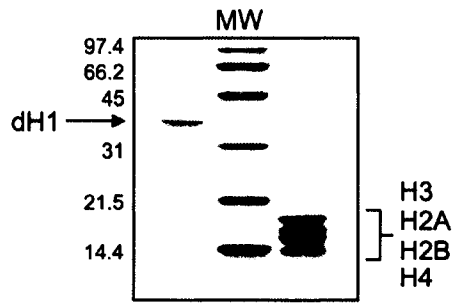

Figure 2.2. Purified native core histones and histone H1 from *Drosophila* embryos. Histones were resolved using 15% SDS-PAGE and visualized with coomassie brilliant blue. Positions of each histone are indicated and the sizes of molecular weight markers (MW) in kilodaltons are labeled on the left. The actual molecular weight of *Drosophila* H1 is 26343 kilodaltons. This histone runs higher than expected due to its high lysine content.

Reproduced with permission of the copyright owner. Further reproduction prohibited without permission.

2.2b *Drosophila* NAP-1 Expression and Purification

For dNAP-1 expression, one liter of Sf9 insect cells in log phase growth at 1 X 10^6 cells/ml was infected with dNAP-1_{His6} baculovirus to a MOI of five (the MOI will vary between 5-10, depending on the virus). The infection was allowed to proceed in spinner culture for 60-72 hours, upon which the cells were harvested by centrifugation at 1000 x g. Each cell pellet was washed with 30 ml 1X PBS, re-centrifuged, and either used immediately or frozen in liquid nitrogen and stored at -80°C for later use. To purify dNAP-1, we follow the protocol described by Fyodorov and Kadonaga 2003 (45) exactly (be certain to pH the buffers containing imidazole to pH 7.6). After isolating a new dNAP-1 baculovirus clone, typical yields were 5-6 mg of purified dNAP-1 per liter of Sf9 cells. The expected Source 15Q elution profile and purified dNAP-1 protein are shown in Figure 2.3.

2.2c ACF Expression and Purification

For ACF expression, log phase Sf9 cells were seeded at a density of 2 X 10^7 cells/plate and four plates were seeded per infection. Alternatively, log phase cells from spinner culture were diluted to 1 X 10^6 cells/ml and a total of 8 X 10^7 cells were infected in spinner culture. Cells were co-infected with Acf1 (w+) and $ISWI_{FLAG}$ baculoviruses. Typically cells were infected with Acf1 at a MOI of 5 and $ISWI_{FLAG}$ at an MOI of 10. To ensure stoichiometry of the purified ACF complex, the MOIs of each virus were adjusted accordingly and depended on the clones. Cells were infected for 44-46 hours and harvested by centrifugation at

Reproduced with permission of the copyright owner. Further reproduction prohibited without permission.

1000 x g, washed with 30 ml 1X PBS and usually frozen for later purification. ACF purification was performed as described (45) and our typical yields were 2-5 μg ACF per 2 X 10^7 cells (Figure 2.4).

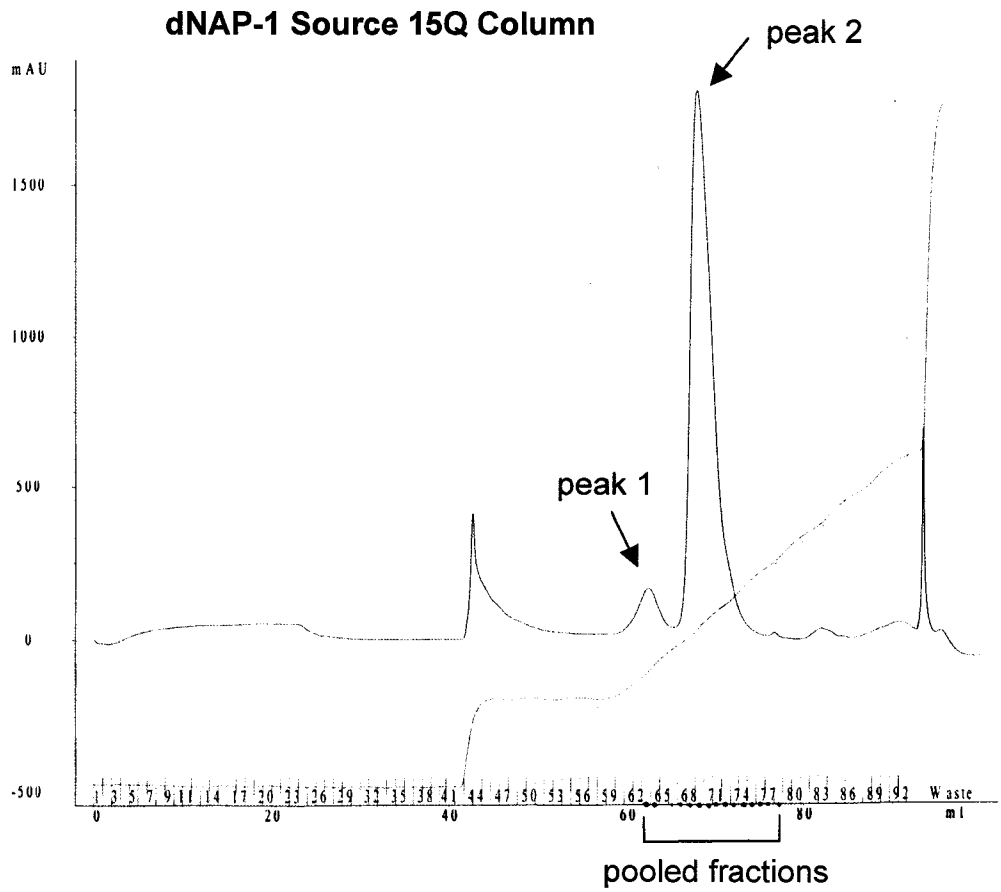

Figure 2.3. Recombinant dNAP-1_{His6} purification. A typical elution profile from Source 15Q column purification (top). Fractions in peak two of the elution step were pooled and concentrated. While peak one contains dNAP-1, some of the fractions also contain contaminating bands and were not pooled with the other fractions. The resulting dNAP-1 protein was resolved using 10% SDS-PAGE and visualized with coomassie brilliant blue. Molecular weight markers (MW) in kilodaltons are indicated to the left.

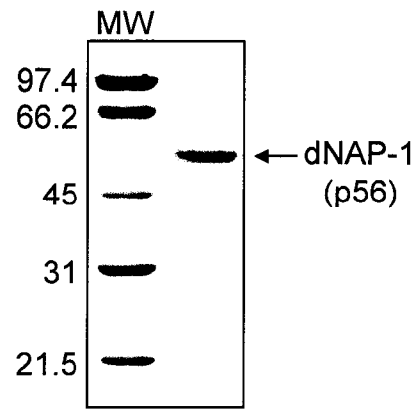

Reproduced with permission of the copyright owner. Further reproduction prohibited without permission.

2.2d p300 Expression and Purification

p300 was expressed and purified using a protocol defined by Kraus and Kadonaga, 1998 (84). For p300 expression, four 15 cm plates were seeded with cells at a density of 2 X 10^7 cells/plate. The cells were infected with $p300_{His6}$ baculovirus to a MOI of 5-10 and incubated at 27°C for about 72 hours. The cells were harvested by removing them from the plates into a 50-ml conical and pelleted by centrifugation at 1000 x g for 5 minutes. The cells were then washed with 30 ml 1X PBS and pelleted to remove the PBS. Cells pellets were either used immediately or flash frozen and stored at -80°C for later use.

Figure 2.4. Recombinant ACF purification. Acf1 and $ISWI_{FLAG}$ were co-expressed in Sf9 cells and the resulting ACF complex was affinity purified. ACF was resolved using 6.5% SDS-PAGE and visualized with coomassie brilliant blue. Molecular weight markers (MW) in kilodaltons are indicated to the left.

The cell pellet was resuspended in 1 ml of homogenization buffer per 15 cm plate (10 mM Tris-HCl, pH 7.5, 500 mM NaCl, 10 % glycerol, 0.1 % NP-40, 15 mM imidazole, 2 mM β-mercaptoethanol, 2 mM PMSF, 20 μg/ml leupeptin, and 20 μg/ml aprotinin). The cells were transferred to a homogenizer and dounced 10 times using a tight pestle on ice. The lysate was incubated 15 minutes on ice followed by clarification by centrifugation for 10 minutes at 4°C. The supernatant was transferred to a 15-ml conical containing 30 μl of a 50% Ni-NTA resin slurry per 15 cm plate that was previously washed with H_2O and

Reproduced with permission of the copyright owner. Further reproduction prohibited without permission.

equilibrated in homogenization buffer. The lysate was incubated with the equilibrated Ni-NTA resin for 2 hours on a rotator at 4°C. The resin was pelleted by centrifugation at 1000 x g and the flow through was removed. Four successive washes were performed, each with 1 ml wash buffer per 15 cm plate (10 mM Tris-HCl, pH 7.5, 200 mM NaCl, 10 % glycerol, 0.2 % NP-40, 15 mM imidazole, 2 mM β-mercaptoethanol, 2 mM PMSF). As much of the last wash as possible was aspirated before eluting the purified p300. The p300 was eluted with 100 μl elution buffer per 15 cm plate (10 mM Tris-HCl, pH 7.5, 100 mM NaCl, 10 % glycerol, 0.1 % NP-40, 250 mM imidazole, 2 mM β-mercaptoethanol, 2 mM PMSF), incubated on ice for 10 minutes and the elution was repeated. The purified p300 was divided into 5-10 μl aliquots, frozen in liquid N_2 and stored at – 80°C. A 4-plate infection produced 10-50 μg of purified p300 (Figure 2.5).

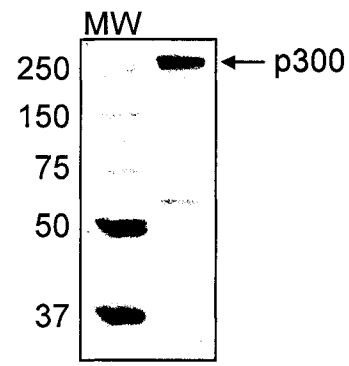

Figure 2.5. Purified recombinant p300. Sf9 cells were infected with $p300_{His6}$ baculovirus and purified using Ni-NTA resin. p300 was resolved using 6.5% SDS-PAGE and visualized with coomassie brilliant blue. Molecular weight markers (MW) in kilodaltons are indicated to the left.

Reproduced with permission of the copyright owner. Further reproduction prohibited without permission.

2.2f Topoisomerase I Expression and Purification

The topoisomerase I catalytic domain (ND423) that contains a C-terminal His6 tag and N-terminal truncation (138) was expressed and purified as described (45). The amount of topoisomerase I required to relax a supercoiled plasmid DNA template was empirically determined for each preparation.

2.2g Tax and CREB Expression and Purification

Tax and CREB were kind gifts from the Nyborg laboratory, prepared by Jeanne Mick and Dinaida Lopez. Recombinant CREB (Figure 2.6) (44) was expressed and purified from *E. coli* as previously described using the "boiling method" (68). Tax (Figure 2.6) (169) was expressed and purified as previously described (50).

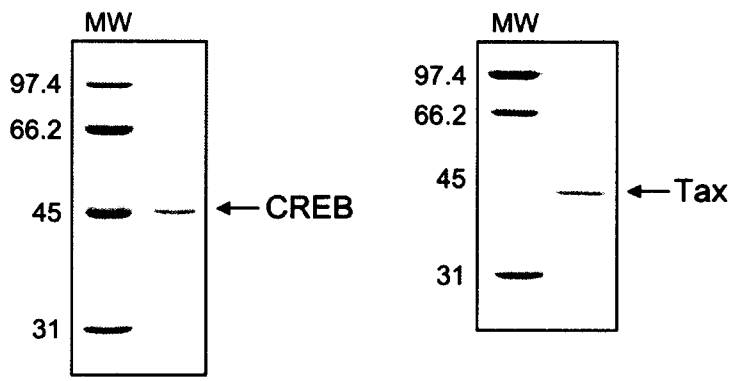

Figure 2.6. Recombinant CREB and Tax preparations. CREB (left) and Tax (right) were each resolved on 10% SDS-PAGE and visualized with coomassie brilliant blue. Molecular weight markers (MW) in kilodaltons are indicated to the left of each gel.

Reproduced with permission of the copyright owner. Further reproduction prohibited without permission.

2.3 RECOMBINANT CHROMATIN METHODS

2.3a Recombinant Chromatin Assembly

Core histones were deposited onto a p-306/G-less template (7) that contains HTLV-1 LTR sequence encompassing the three viral CREs and core promoter regions (Figure 2.7) using the NAP-1/ACF recombinant chromatin assembly system (45).

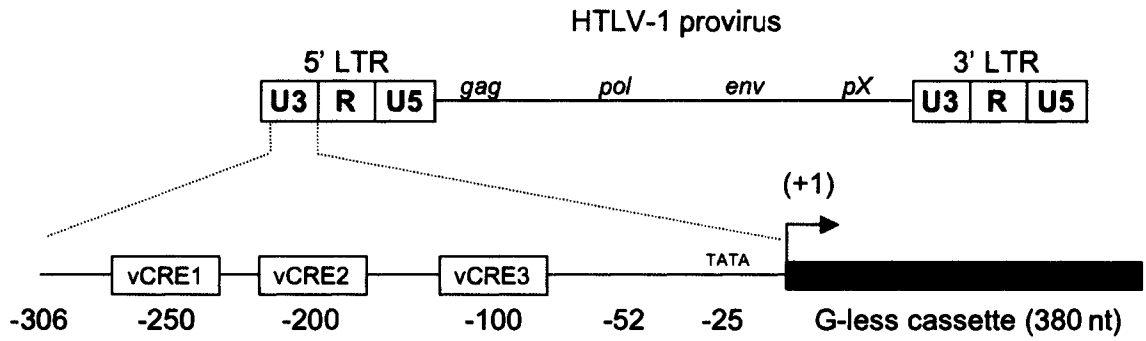

Figure 2.7. Promoter schematic. The p-306/G-less template is derived from the HTLV-1 genome and cloned into pUC13.

We used a 6:1 dNAP-1:core histone (wt/wt) ratio and 25 ng of ACF (Acf1/ISWI) per 150 ng plasmid DNA. To begin the assembly, core histones were pre-incubated with dNAP-1 on ice for 30 minutes in 25 mM HEPES (K+, pH 7.6), 0.05 mM EDTA and 5% glycerol. ACF was added to the core histone/dNAP-1 mix and mixed immediately, followed by the addition of an ATP-regenerating system (3 mM ATP, 30 mM phosphocreatine, 1 μg/ml creatine phosphokinase). Either supercoiled or relaxed plasmid DNA was added to the assembly reactions and incubated for 4-18 hours at 27°C under final conditions of 10 mM HEPES pH 7.6,

Reproduced with permission of the copyright owner. Further reproduction prohibited without permission.

50 mM KCl, 5 mM $MgCl_2$, 5% (v/v) glycerol, 1 % (wt/v) polyethylene glycol and 0.01% (v/v) NP-40. Histone H1 was added 1.5 hours post-assembly to the chromatin template where indicated at a 1.25 H1:octamer molar ratio. The order of factor addition is crucial for proper assembly, as is thorough mixing after each addition. Reactions were adjusted for assembling 150 ng (67 fmol) of DNA in a 7 μl volume (amount added to a single *in vitro* transcription reaction), however actual assembly volumes ranged from 50 to 600 μl. When necessary, ACF and CPK were freshly diluted in assembly buffer (10 mM HEPES pH 7.6, 50 mM KCl, 5 mM $MgCl_2$, 5% v/v glycerol, 1 % wt/v polyethylene glycol) and histones and dNAP-1 were diluted in buffer R (10 mM HEPES K+ pH 7.6, 10 mM KCl, 1.5 mM $MgCl_2$, 10% glycerol, 10 mM β-glycerophosphate, 1 mM DTT, 0.2 mM PMSF).

2.3b Topological (1-D) Supercoiling Assays

Chromatin was assembled as previously described with the following modifications. Supercoiled plasmid DNA (700 ng) was relaxed using recombinant topoisomerase I (clone ND423) in a 70 μl reaction volume with topoisomerase buffer (50 mM Tris-Cl pH 7.5, 50 mM KCl, 10 mM $MgCl_2$, 1 mM DTT, 0.5 mM EDTA, 30 μg/ml BSA). Typically, each reaction contained 3.5 μl of diluted topoisomerase I. The dilution of topoisomerase I varied between 1:10 to 1:100 depending on each enzyme preparation. The 70 μl relaxation reactions were incubated for 1 hour at 37°C. Immediately before adding relaxed DNA to the assembly, the DNA was "spiked" with an additional 20 μl of the appropriate topoisomerase I dilution. After chromatin assembly, the degree of supercoiling

Reproduced with permission of the copyright owner. Further reproduction prohibited without permission.

was measured by 1% TBE agarose gel electrophoresis, SYBR gold staining and STORM imaging. Relaxed DNA was only used in supercoiling assays and all subsequent assembly reactions were performed with supercoiled plasmid DNA.

2.3c Micrococcal Nuclease Digestion

Micrococcal nuclease (MNase) digestion was performed on 2.1 µg of assembled DNA (98 µl assembled chromatin). First, 135 µl of MNase buffer (1.74 mM HEPES pH 7.6, 121 mM KCl, 12 % v/v glycerol, 2.4 % wt/v PEG, 11.2 mM $CaCl_2$) were added to chromatin samples and incubated for 5 minutes at 37°C. Digestion was initiated by addition of 0.12 U MNase (Worthington) in a 7 µl volume to templates lacking histone H1 and 0.48 U MNase to H1-containing templates at 37°C. After 1, 2, 4, & 8 minutes, 60 µl aliquots were removed and digestion was stopped with 12 µl TE/EDTA (6 µl $T_{10}E_1$ / 6 µl 0.5 M EDTA). Samples were deproteinized with 9.6 µl 2.5 mg/ml proteinase K and 96 µl chromatin stop (20 mM EDTA, 200 mM NaCl, 1 % wt/v SDS, 0.25 mg/ml glycogen) for 30 minutes at 37°C. The DNA was extracted with phenol/chloroform followed by ethanol precipitation. Nucleic acids were analyzed on 1.2 % TBE agarose gels and visualized with SYBR gold. Gene ruler 100 bp plus markers (Fermentas) were used as DNA size standards. The nucleosome repeat length was calculated using Image Quant 5.1 software. Briefly, mobilities were measured for each standard and plotted against the corresponding base pair size. The data were fit to a logarithmic curve and nucleosome repeat lengths were extrapolated from the logarithmic equation. The positions of marker

Reproduced with permission of the copyright owner. Further reproduction prohibited without permission.

and nucleosomal DNA were determined from the number of pixels corresponding to the peak from each band. The nucleosome repeat lengths were calculated using DNA digested for 4 min. (3rd lane from the left in each set of 4) and data corresponding to mononucleosomes was omitted in the calculations. Three independent experiments were performed to determine the repeat length for chromatin assembled in the absence and presence of H1.

2.3d Sucrose Gradients

For sucrose gradient analysis, 4.2 µg of DNA was assembled into chromatin with varying H1:octamer molar ratios. Chromatin samples were resolved using 13 ml 15-40 % sucrose gradients (10 mM Tris-Cl pH 7.8, 0.1 mM EDTA, 1mM DTT, 0.1 mM PMSF, 0.1 mM benzamidine). Gradients were centrifuged at 4°C in an SW41Ti rotor (Beckman) at 40,000 rpm for 4 hours. Gradient fractions (11 tubes, each containing 1.2 ml) were collected from top to bottom. Proteins were TCA/DOC precipitated using 800 µl of each fraction, resolved on 15% SDS-PAGE and visualized with SYPRO ruby and STORM imaging or silver staining. DNA was deproteinized and precipitated from 200 µl of each gradient fraction, resolved on a 1% TBE agarose gel and visualized with SYBR gold.

2.3e Histone Extractions for Mass Spectrometry

Chromatin was assembled as previously described with or without H1 and the histones (including H1) were extracted using H_2SO_4 and TCA. Upon complete

Reproduced with permission of the copyright owner. Further reproduction prohibited without permission.

assembly, an equal volume of 0.4 M H_2SO_4 was added to the chromatin samples. The samples were placed on a rotator to mix for 1 hour at 4°C, typically in 15-ml conicals that were treated with silicone. After the extraction, the non-soluble proteins were precipitated by spinning in 1.7 ml siliconized eppendorf tubes at 4°C for 10 minutes at 14,000 rpm. The supernatant was transferred to glass corex tubes and TCA was added to a final concentration of 30% and mixed well by inversion. The samples were incubated on ice for 1 hour and centrifuged in the SS-34 rotor (Sorvall) at 4°C for 15 minutes at 12,000 rpm. The histone-containing pellets were washed once with 15 ml of acetone. The acetone was incubated with the pellets at room temperature for 10 minutes to help dissolve the TCA. The pellets were centrifuged again as described using the SS-34 rotor. The supernatant was carefully removed and the histone pellets were allowed to dry briefly on the bench top. They were resuspended in 200 μl H_2O and transferred to siliconized eppendorfs for -80°C storage. Our samples were analyzed by mass spectrometry in collaboration with Natalie Ahn at the University of Colorado in Boulder. Note: It might work better to leave the sample in pellet form and dissolve it immediately before use in the appropriate solvent for mass spectrometry analysis. I also experienced difficulty in extracting the histones from chromatin assembled with H1. For unknown reasons, these extractions were never as efficient as those from chromatin lacking linker histone.

Reproduced with permission of the copyright owner. Further reproduction prohibited without permission.

2.3f Preparation of Histone H1 for Mass Spectrometry Analysis

Drosophila histone H1 was treated with λ-phosphatase protein as described by the manufacturer (NEB - P0753S) and compared to the native form of H1 by mass spectrometry. Additionally H1 was phosphorylated using PKA (SIGMA P-2645) following the approach used for PKA treatment of CREB (described in section 2.4b). H1 protein (26 μg) was prepared for mass spectrometry after the appropriate enzymatic treatment by TCA/DOC precipitation as follows. TCA/DOC (1/4 of sample volume) was added to the sample, vortexed and incubated on ice for 30 minutes. The proteins were precipitated by centrifugation at 4°C for 20 minutes at 14,000 rpm. Siliconized eppendorfs were always used for precipitating H1. After centrifuging, the supernatant was removed and acetone was added (3-4 times the sample volume) and incubated at room temperature for 10 minutes. The sample was centrifuged as described and the resulting pellets were dried on ice and taken to the MRF (Macromolecular Resources Facility) at Colorado State University and analyzed by Drs. Phil Ryan and Jessica Prenni. Note: I found the TCA/DOC precipitations to work the best for mass spectrometry analysis of H1, as using perchloric acid to isolate and precipitate H1 interfered with the mass spectrometry analysis.

Reproduced with permission of the copyright owner. Further reproduction prohibited without permission.

2.4 *IN VITRO* ASSAYS ON CHROMATIN TEMPLATES

2.4a *In Vitro* Transcription

Following chromatin assembly, 150 ng (67 fmol) of DNA in a 7 μl volume were added to transcription reactions containing TM buffer (25 mM Tris-Cl pH7.9, 50 mM KCl, 6.25 mM $MgCl_2$, 0.5 mM EDTA, 10% glycerol, 1 mM DTT) and 50 μM acetyl-coenzyme A (AcCoA) in a 30-40 μl final volume. Exogenous Tax and CREB (1.6 pmol each) were added after or during the chromatin assembly where indicated. p300 (0.3 pmol) was also added to transcription reactions where indicated. Pre-initiation complexes were formed with the addition of 40 μg CEM (HTLV-1 negative T-cell line) nuclear extract (38) and samples were incubated for 60 minutes at 30°C. RNA synthesis was initiated with addition of 2.4 μl NTP mix (250 μM ATP, 250 μM CTP, 12 μM UTP & 0.8 μM [α-^{32}P] UTP 3000Ci/mmol) and incubated for 30 minutes at 30°C. Following RNA synthesis, 4 μl of RNase T1 (25U/μl) were added and samples were incubated for 30 minutes at 37°C. Proteins were digested for 30 minutes at 50°C with 8.5 μl proteinase K (10 mg/ml) and 10 μl transcription stop (250 mM NaCl, 1 % SDS, 20 mM Tris-Cl pH 7.5, 5 mM EDTA). A 622-bp DNA fragment, isolated from an *Hpa*II digest of pBR322 was end-labeled and added for a recovery standard. The amount of recovery standard added varied upon isotope decay and the number of reactions. RNA products and labeled DNA recovery standards were precipitated with 165 μl of a salt, ethanol and tRNA mix (140 μl 100% EtOH, 20 μl 4M NH_4OAc, 5 μl 10 mg/ml tRNA). The addition of tRNA helps prevent the loss of

Reproduced with permission of the copyright owner. Further reproduction prohibited without permission.

pellets. After precipitation and a 70% EtOH wash, the pellets were briefly dried on the bench top, resuspended in 7 μl formamide loading dye, and resolved on 6.5% sequencing urea-PAGE. Radiolabeled *Hpa*II-digested pBR322 served as molecular weight size markers. All radioactive data were imaged using STORM phosphorimaging and quantified with Image Quant 5.1 software. Experiments were performed a minimum of three times.

2.4b *In vitro* Histone Acetyltransferase (HAT) Assays

For *in vitro* acetylation assays, 2 μg of core histones were assembled into chromatin as described previously at an emperically determined core histone to DNA ratio that was properly assembled and responsive to transcriptional activation. Most reactions consisted of 2.8 μg of assembled DNA in a 40-60 μl volume. Tax and CREB (typically 30 pmol each) were included in the chromatin assembly reaction where indicated and were adjusted to the same levels used in transcription experiments, relative to the total DNA. A slight excess of p300 was used (8.4 pmol), compared to that used in transcription studies, relative to the DNA. Final reaction volumes varied from 100-150 μl and contained 75 μM ^{14}C-labeled AcCoA (56 mCi/mmol specific acitivity) under final conditions of TM buffer (25 mM Tris-Cl pH7.9, 50 mM KCl, 6.25 mM $MgCl_2$, 0.5 mM EDTA, 10% glycerol, 1 mM DTT) with 10 mM sodium butyrate and 1 mM PMSF. Samples were incubated for 60 minutes at 30°C. Proteins were methanol-chloroform precipitated and resolved on 18% SDS-PAGE. Free (unassembled) core histones were acetylated for a marker in a final volume of 20 μl.

Reproduced with permission of the copyright owner. Further reproduction prohibited without permission.

Phosphorylated CREB was added where indicated and was phosphorylated using the PKA catalytic subunit (SIGMA P-2645). Briefly, the final conditions for the phosphorylation reaction were as follows: 1 pmol/µl CREB, 8 mM DTT, 20 mM Tris-Cl pH 7.5, 1 mM NaF, 10 mM $MgCl_2$, 5 units of PKA/100 pmols CREB (PKA was dissolved according to the manufacturer), and 20 µM ATP. The reaction was incubated at 30°C for 1 hour and the PKA was inactivated by a 65°C incubation for 10 minutes. The resulting phosphorylated CREB was concentrated and the new concentration was determined via SDS-PAGE with BSA standards. Experiments were performed at least three times.

2.4c Deoxyribonuclease I (DNaseI) Primer Extension Footprinting

Experiments were performed as described (123) with the following modifications. Supercoiled plasmid DNA (p-306/G-less) was separated from nicked DNA using preparative-cell electrophoresis. The resulting purely supercoiled DNA (56 fmol) was assembled into chromatin in a 25 µl volume. CREB and Tax were added as indicated, either during or after chromatin assembly in a final volume of 50 µl in TM buffer. Binding reactions were incubated for 1 hour at 30°C. Digestion was performed as described (123), except digestion was stopped by placing samples in a dry ice/EtOH bath for 10 min. Digested DNA (10 fmol) was incubated with 50 fmol of [γ-^{32}P] ATP-labeled primer and primer extension was performed as described (123). To footprint the distal and middle vCREs, we used the following primer 5′-TCGATAAGCTTCTAGACCTCCCAGTG-3′, which binds ~70 bp upstream of the

Reproduced with permission of the copyright owner. Further reproduction prohibited without permission.

distal vCRE within pUC13. To footprint the proximal vCRE we used the following primer 5′-TCAGCCATATGCGTGCCATGAA-3′, which anneals to the promoter at position -47 relative to the transcription start site. Following primer extension, the DNA was precipitated and resolved on a 8% sequencing gel. The percent accessibility was quantified using the main band that disappears within each core vCRE region. Experiments were performed a minimum of three times.

2.4d Immobilized Chromatin Template Assays

Biotinylated DNA fragments from -288 to +408 (P) and -69 to +408 (C) of the HTLV-1 LTR were prepared by standard PCR using biotinylated forward primers. PCR products were purified using preparative-cell electrophoresis and bound to M 280 streptavidin Dynabeads (Dynal Biotech ASA, 10 μl beads/pmol DNA) as described by the manufacturer. Chromatin templates were assembled using 2 pmol biotinylated DNA. Tax (18 pmol), CREB or phospho-CREB (12 pmol), and H1 (1.25 molar excess per octamer) were added to the assembly reactions where indicated in a final volume of 50 μl in TM buffer. Chromatin was assembled for 4 hours at 27°C with constant rotation. After assembly, additional factors were added as indicated (0.75 pmol p300) and the volume was adjusted to 100 μl in TM buffer. Binding reactions were performed for 45 minutes at 27°C with constant rotation. Immobilized templates were washed twice with 100 μl TM buffer containing 100 mM KCl, resuspended in SDS- PAGE loading dye and processed by Western blotting. Experiments were performed at least three times. Antibodies against CREB (SC-186), P-CREB (SC-7978-R) and p300 (SC-

Reproduced with permission of the copyright owner. Further reproduction prohibited without permission.

584) were purchased from Santa-Cruz Biotechnology. H3 (Ab 1791) and H1 (V7013) antibodies were purchased from Abcam and Biomeda, respectively. A monoclonal Tax antibody (Hybridoma 168B17-46-92) was obtained from the NIH Aids Research and Reference Reagent Program.

Reproduced with permission of the copyright owner. Further reproduction prohibited without permission.

Chapter 3

Recombinant Chromatin: Optimization of Chromatin Containing Histone H1

This chapter focuses on the experiments required to optimize incorporation of histone H1 using a recombinant assembly system and contains negative results that cannot be published but are important to our understanding of proper H1 incorporation into chromatin. However, Figures 3.3 and 3.5 from this section appear in Chapter 4, which has been submitted for publication to the Journal of Virology.

Reproduced with permission of the copyright owner. Further reproduction prohibited without permission.

3.1 ABSTRACT

A recombinant chromatin assembly system was used to demonstrate that the single histone H1 isoform from *Drosophila* is properly incorporated into a chromatin template containing natural HTLV-1 promoter sequence. The degree of chromatin assembly in the absence and presence of histone H1 was measured using topological analysis. Assembly with H1 occurred at a lower core histone to DNA ratio compared to that lacking linker histone. Micrococcal nuclease digestion experiments were performed to confirm H1 incorporation and determine the quality of our *in vitro* chromatin templates. A 10-base pair increase in the nucleosome repeat length was observed, suggesting proper H1 incorporation. Micrococcal nuclease digestion experiments also demonstrated addition of H1 isolated from a mammalian T-cell line to the chromatin template, which contains at least four H1 isoforms. To verify H1 was stoichiometrically incorporated into chromatin, H1-containing chromatin samples were purified using sucrose gradients and ultracentrifugation. A slight molar excess of H1 to core histone octamer was required for stoichiometric incorporation of histone H1. Additionally, both yeast and *Drosophila* NAP-1 (yNAP-1 and dNAP-1, respectively) promoted association of H1 with chromatin. Specifically, only a truncated form of yNAP-1 lacking amino acids from both the N- and C-terminal tails was effective in H1 incorporation. Functional assays revealed that H1-chromatin assembled with truncated yNAP-1 did not repress Tax-mediated transcriptional activation like that observed from H1-chromatin assembled with dNAP-1. Therefore, subsequent experiments were performed using dNAP-1 as

Reproduced with permission of the copyright owner. Further reproduction prohibited without permission.

the histone chaperone. Together, these experiments confirm proper addition of H1 to the chromatin template using a recombinant assembly system, which provides an important tool for furthering our understanding of linker histone function.

3.2 INTRODUCTION

Eukaryotes package their DNA into chromatin to accommodate the tiny environment within a cell's nucleus. Structurally, the core histones combine with DNA to form the basic repeating unit of chromatin, the nucleosome (102). While the four core histones are vital to the structure and function of chromatin, so is the linker histone - H1. Histone H1 interacts with the nucleosome and functions to stabilize higher order structures within the chromosome (27). How cells manage to perform biological functions in the complex but organized nature of chromatin remains a central enigma in the field of molecular biology.

While much has been done to understand the role of the core histones, less is known about histone H1. Development of a recombinant system for assembling chromatin has further increased our understanding of the core histones, as the possibilities for octamer combinations and modifications are numerous (72, 73). Recently, this recombinant system has been used to incorporate histone H1 into a chromatin template (45). Prior to this development, H1 was typically incorporated into chromatin using either salt dialysis or crude extracts that contain chromatin assembly factors from *Drosophila* (S-190 extracts). There are limitations with both of these procedures. Specifically, salt

Reproduced with permission of the copyright owner. Further reproduction prohibited without permission.

dialysis is not very efficient when using large templates that are kilobases in length. The use of extracts overcomes the limitations of salt deposition but imposes additional obstacles. For example, after assembly, the chromatin template must be purified from the factors in the extract before performing functional studies such as transcription. Obviously, use of a recombinant system to assemble chromatin containing histone H1 would allow more studies on H1 and the ability to better correlate structure with function.

The protocol for recombinant assembly of H1-containing chromatin was not published until 2003. Our study originated in 2001. Therefore, to examine the functional role of histone H1 at the HTLV-1 promoter, we first optimized H1 incorporation into chromatin using the recombinant assembly factors dNAP-1 and ACF. We found H1 addition to chromatin templates increased the nucleosome repeat length about 10 base pairs, a characteristic associated with chromatosome formation. Further optimization revealed a slight molar excess of histone H1 relative to core histone octamer was necessary to achieve stoichiometric incorporation at roughly one molecule of H1 per nucleosome. Additionally, we compared the ability of y-NAP-1 to dNAP-1 for assembling chromatin containing H1. While dNAP-1 readily promoted incorporation of linker histone, only a truncated form of yNAP-1 produced chromatin containing H1. Unfortunately, chromatin assembled with truncated yNAP-1 failed to repress Tax-mediated transcriptional activation of HTLV-1, a functional characteristic of chromatin assembled using dNAP-1. Therefore, subsequent experiments were performed using dNAP-1 as the histone chaperone in assembling chromatin.

Reproduced with permission of the copyright owner. Further reproduction prohibited without permission.

The ability to successfully incorporate histone H1 into chromatin using recombinant assembly factors elevates our understanding of linker histone function and provides a new platform from which to study gene regulation.

3.3 RESULTS

3.3a H1 Sequence Comparison

Since mammalian cells possess as many as seven different H1 isoforms, *Drosophila* H1, which has only one type, was selected for incorporation into chromatin (120). *Drosophila* H1 is most like that of the mammalian H1 isoform – $H1^{s}$-4. Sequence analysis of $H1^{s}$-4 compared to *Drosophila* H1 revealed a 46% similarity in amino acid composition, with 36% of the sequence being identical (Figure 3.1). Additionally, $H1^{s}$-4 represents at least 60% of the total H1 content in mammalian T-cell lines that are not infected with HTLV-1 and comprises 67% of total H1 isolated from the T-cells of uninfected human blood (J. Bogenberger, personal communication).

3.3b Topological 1-D Supercoiling Assays

Core histones (23) and histone H1 (36) were purified from *Drosophila* embryos (Figure 2.2) and were assembled into chromatin using dNAP-1 (Figure 2.3) (72) and ACF (Figure 2.4) (73, 74). Since H1 is not as conserved as the core histones, the same species of linker and core histones were initially used to optimize our system. Additionally, *Drosophila* histones were readily accessible.

Reproduced with permission of the copyright owner. Further reproduction prohibited without permission.

To determine how to add histone H1 such that it would be incorporated into the chromatin template, topological supercoiling assays were performed.

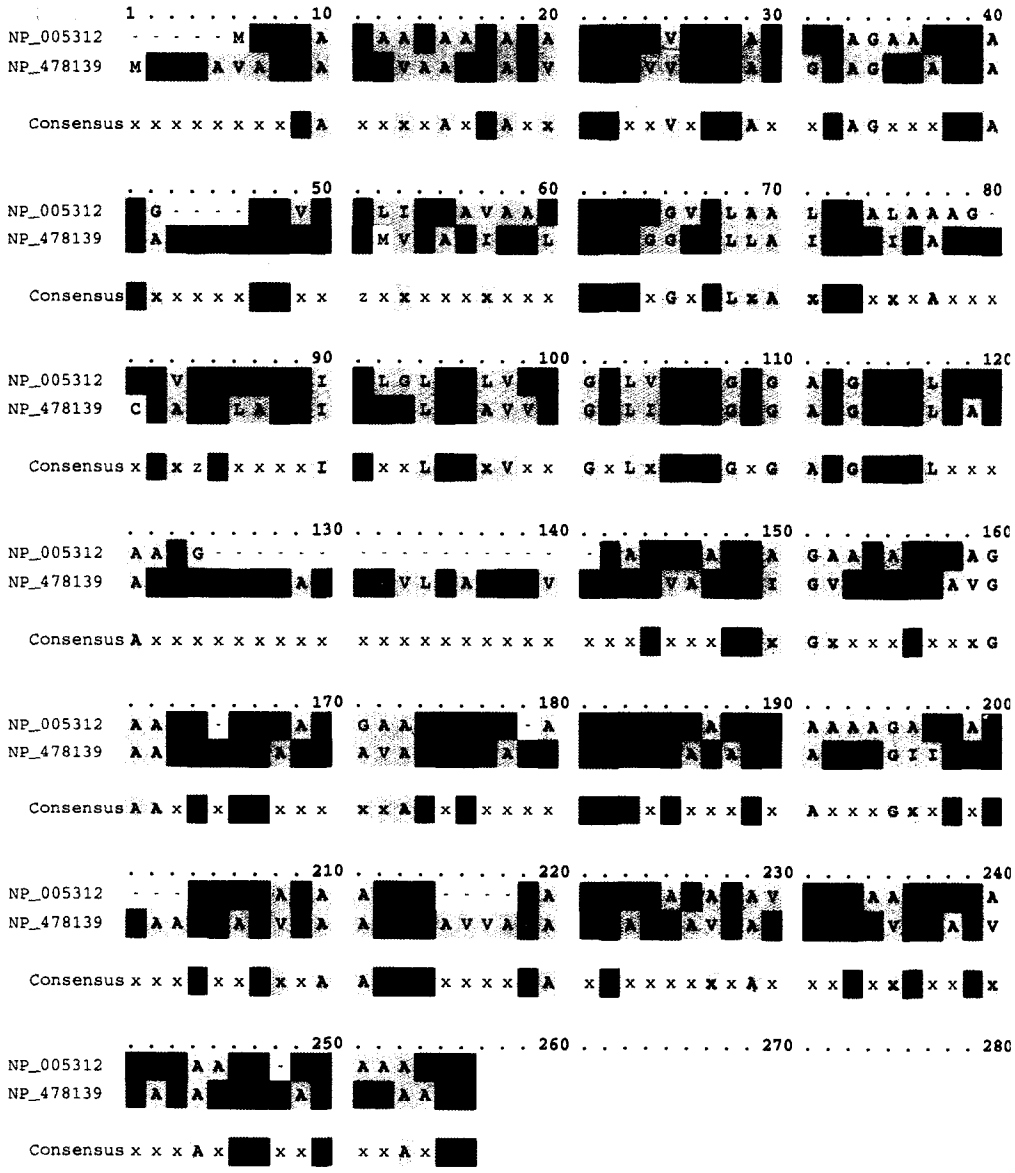

Figure 3.1. Sequence alignment of *Drosophila* H1 compared to mammalian H1^{s}-4. The top sequence is H1^{s}-4 and the bottom sequence represents *Drosophila* H1. The consensus amino acids are indicated below the aligned sequences. There is a 46% similarity in amino acid composition with 36% being identical between species.

Reproduced with permission of the copyright owner. Further reproduction prohibited without permission.

The degree of chromatin assembly is measured by a change from relaxed plasmid DNA to assembled supercoiled DNA (123). As the core histone to DNA mass ratio is increased, nucleosomes form on the relaxed plasmid template. The addition of each nucleosome puts one negative supercoil in the relaxed DNA, which subsequently alters its migration in electrophoresis. Therefore, the presence of mostly supercoiled DNA suggests the template is assembled into chromatin.

Histone H1 could be added to the assembly reaction either at the beginning of assembly or two hours post-assembly and not interfere with chromatin assembly, as measured by topological analysis. However, supercoiling occurred at a lower core histone to DNA ratio in the presence of H1 as compared to that from templates without H1 (Figure 3.2, compare top & bottom panel). This experiment merely suggests incorporation of H1, as binding of the linker histone increases the DNA associated with each nucleosome (4, 89). In the presence of H1, we would expect fewer nucleosomes to occupy the plasmid DNA template. Therefore, the core histone to DNA ratio at which templates are best assembled in the presence of linker histone should be less than the ratio from chromatin assembled in the absence of H1.

Reproduced with permission of the copyright owner. Further reproduction prohibited without permission.

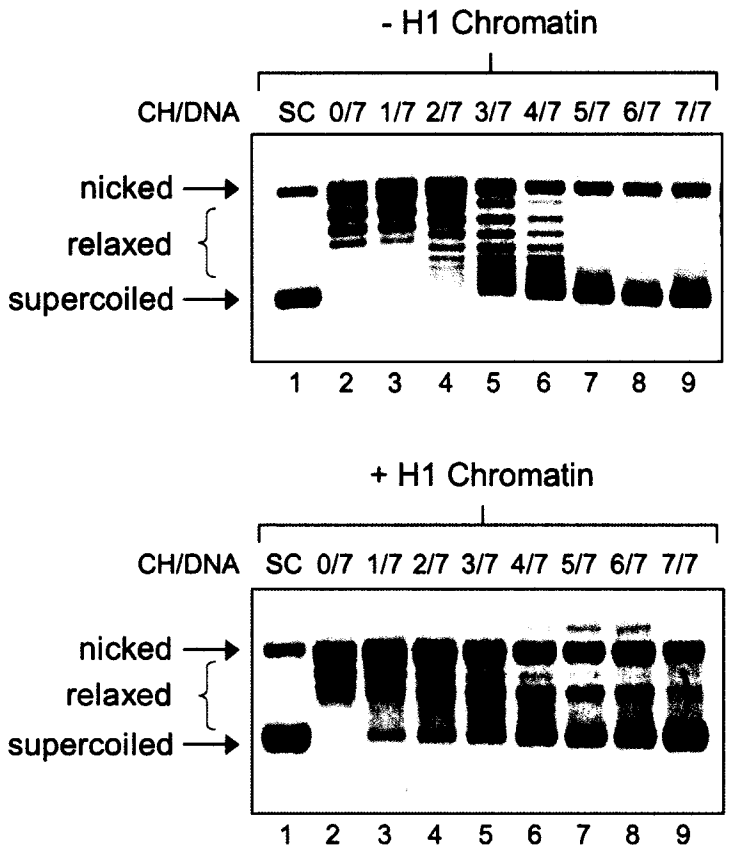

Figure 3.2. Chromatin assembles at a lower core histone to DNA ratio upon addition of histone H1. Relaxed plasmid DNA was assembled into chromatin without (-) or with (+) histone H1. Core histones were titrated onto the DNA template to form nucleosomes. The core histone to DNA (CH/DNA) mass ratios are indicated. The resulting change in DNA topology was resolved using 1%TBE agarose gel electrophoresis. Nucleic acids were visualized with SYBR gold staining and STORM imaging. The positions of nicked, relaxed and supercoiled (SC) DNA are illustrated.

Reproduced with permission of the copyright owner. Further reproduction prohibited without permission.

3.3c Micrococcal Nuclease Digestion Assays

Topological assays only assess the extent to which chromatin assembly occurs. Therefore, micrococcal nuclease (MNase) digestion assays were performed to examine the quality of the *in vitro* assembled chromatin and to confirm H1 incorporation (123). Since a nucleosome containing H1 protects 10-20 additional base pairs from micrococcal nuclease digestion (89), increased nucleosome repeat length was used to verify proper addition of linker histone. The repeat length increased from 149 (+/- 6) base pairs in the absence of H1 to 160 (+/-4) base pairs upon H1 incorporation (Figure 3.3). In this assay, the increased nucleosome repeat length only occurred if H1 was added 1.5-2 hours post-assembly to the reactions, establishing that the time H1 was added to the assembly is crucial for proper incorporation. Furthermore, the presence of several nucleosomes (greater than six) on each chromatin template confirmed the quality of chromatin formed using this system (Figure 3.3).

Additionally, we tested if mammalian H1 isolated from an uninfected T-cell line (CEM) could be incorporated into chromatin using this protocol. Figure 3.4 demonstrates CEM H1 is incorporated into the chromatin template, producing a nucleosome repeat length similar to that observed with incorporation of *Drosophila* H1.

Reproduced with permission of the copyright owner. Further reproduction prohibited without permission.

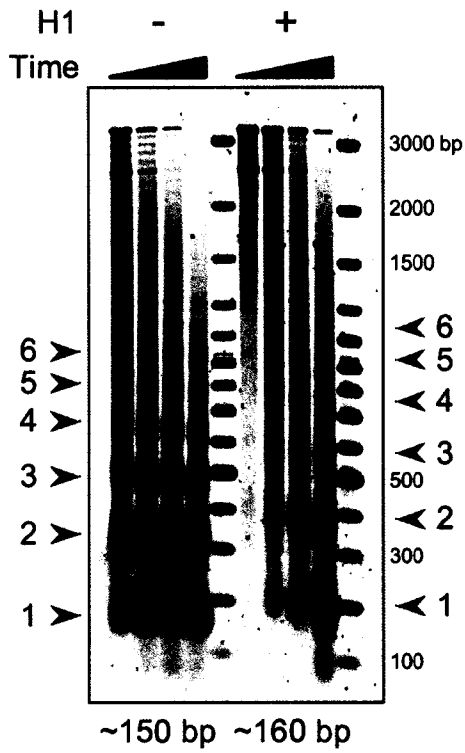

Figure 3.3. Incorporation of histone H1 into chromatin using a recombinant assembly system. Chromatin was assembled in the absence (-) or presence (+) of histone H1 and digested with micrococcal nuclease for 1, 2, 4 & 8 minutes. DNA was extracted, precipitated and resolved on a 1.2% agarose gel. The positions of nucleosomes are numerically indicated for each chromatin template (1=mononucleosome, 2=dinucleosome, etc.). Chromatin assembled without histone H1 has a nucleosome repeat length of 149 (+/- 6 bp) compared to a repeat length of 160 (+/- 4 bp) for H1 chromatin. The calculations were based on three independent experiments and determined as described in Chapter 2 (Materials & Methods). Base pair markers from Fermentas (100 bp DNA ladder plus) are indicated to the right.

Reproduced with permission of the copyright owner. Further reproduction prohibited without permission.

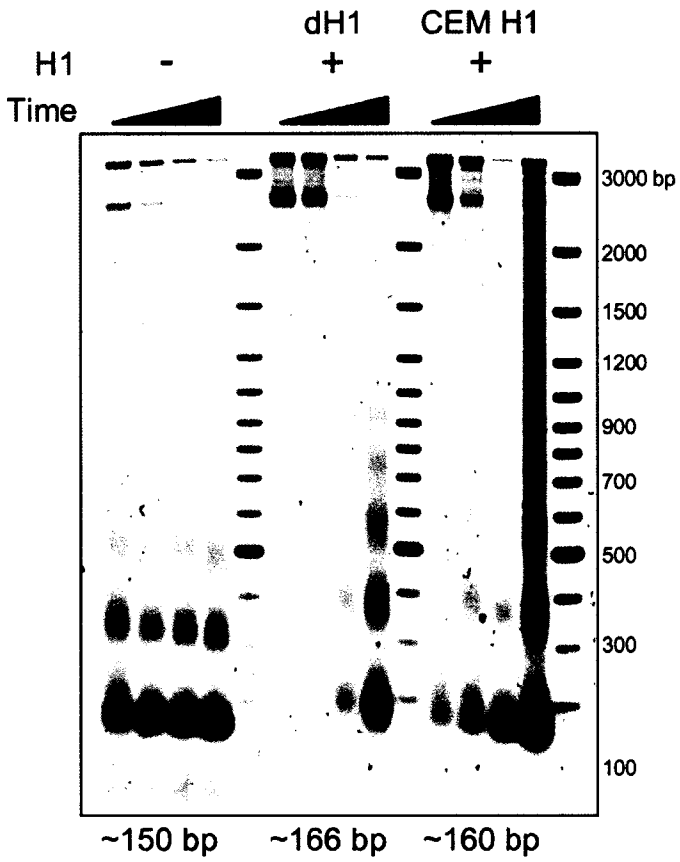

Figure 3.4. Mammalian H1 is incorporated into chromatin using a recombinant assembly system. Chromatin was assembled in the absence (-) or presence (+) of histone H1 and digested with micrococcal nuclease as described previously. The nucleosome repeat lengths have been calculated for each assembly and are as follows: no H1 - 150 (+/- 9 bp), dH1 - 166 (+/- 8 bp), and CEM H1 – 159 (+/- 10 bp). Base pair markers from Fermentas (100 bp DNA ladder plus) are indicated to the right.

Reproduced with permission of the copyright owner. Further reproduction prohibited without permission.

3.3d Stoichiometric Incorporation of Histone H1

One molecule of H1 typically binds per core histone octamer *in vivo* (16); therefore, it is critical to assemble chromatin with stoichiometric levels of histone H1. H1 incorporation was further optimized by assembling chromatin samples at different H1 to core histone octamer ratios. The resulting samples were purified using 15-40% sucrose gradients and ultracentrifugation. A slight molar excess of histone H1 (1.25) relative to core histone octamer was needed to achieve stoichiometric incorporation of H1 (Figure 3.5). Proteins were visualized using SYPRO ruby, which allowed quantification of H1 relative to the core histones more accurately than detection with coomassie brilliant blue. The addition of too much H1 at ratios of 1.75 or greater resulted in an aggregate of chromatin that sedimented to the very bottom of the gradient. Therefore, templates were assembled with an H1 to octamer ratio of 1.25 for subsequent experiments.

3.3e Comparison of the Histone Chaperones – yNAP-1 and dNAP-1 in Chromatin Assembly

Because yNAP-1 is much easier to purify than dNAP-1, the ability of yNAP-1 to assemble chromatin that contains linker histone was compared to dNAP-1. Interestingly, full-length yNAP-1 failed to form H1-chromatin with an increased nucleosome repeat length. Non-specific interactions between full–length yNAP-1 and the core histones are minimized upon truncation of yNAP-1 by deletion of amino acids within the N- and C-terminal regions (truncated yNAP-1 74-365 aa was engineered by Dr. Steven McBryant) (106). Therefore,

Reproduced with permission of the copyright owner. Further reproduction prohibited without permission.

truncated yNAP-1 was tested for its ability to assemble chromatin containing linker histone. While there appeared to be no difference between dNAP-1 and truncated yNAP-1 in their ability to assemble chromatin containing H1 as measured by MNase and sucrose gradient analysis (Figure 3.6), there were functional differences between templates assembled with these histone chaperones. Specifically, H1-chromatin assembled with yNAP-1 failed to repress Tax-mediated transcriptional activation, an observed characteristic of H1-chromatin assembled with dNAP-1. Thus dNAP-1 was used as the histone chaperone protein.

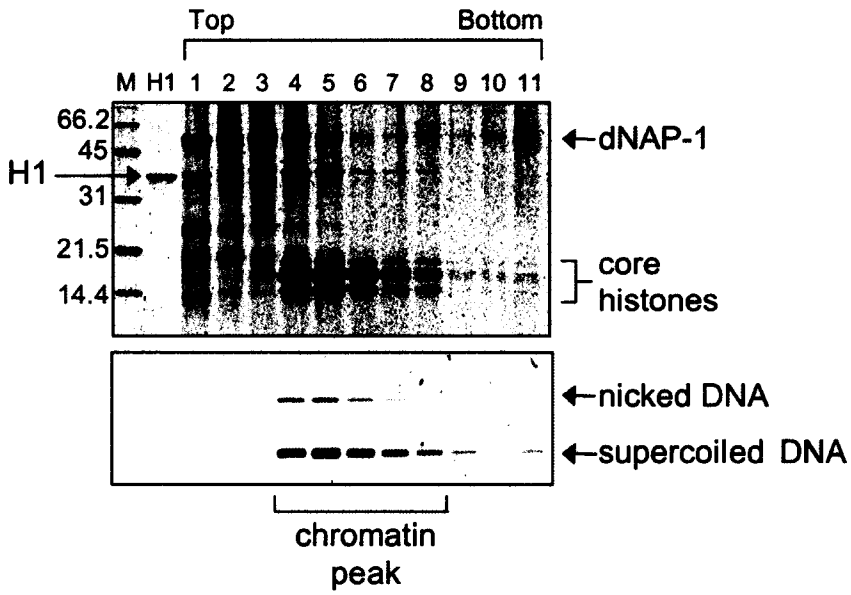

Figure 3.5. Histone H1 is stoichiometrically incorporated into chromatin. Chromatin was assembled with an H1 to core histone octamer ratio of 1.25. The chromatin sample was purified over a 13 ml 15-40% sucrose gradient. Proteins were precipitated using TCA/DOC and resolved on 15% SDS-PAGE. Following staining with SYPRO ruby, proteins were quantified using Image Quant 5.1 software. DNA was extracted, precipitated and resolved on a 1% agarose gel. Molecular weight markers (M) are indicated in kilodaltons on the left.

Reproduced with permission of the copyright owner. Further reproduction prohibited without permission.

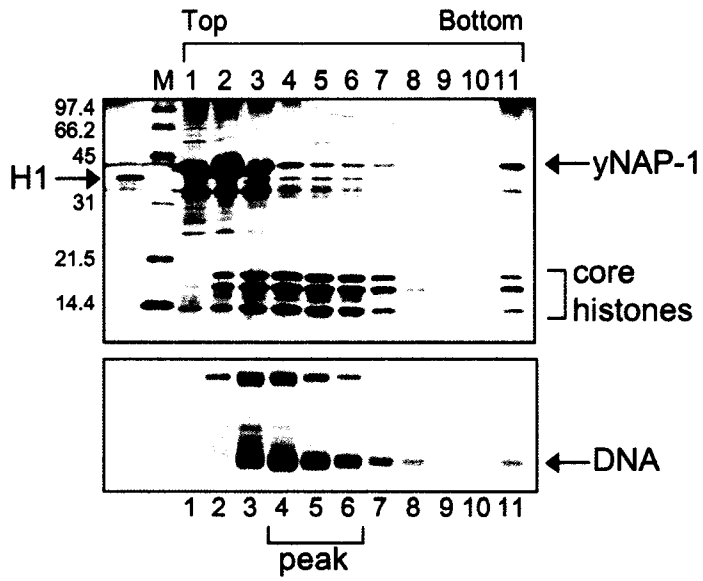

Figure 3.6. Truncated yNAP-1 (74-365 aa) assembles chromatin containing H1. Chromatin was assembled with histone H1 using the truncated histone chaperone yNAP-1 and purified using 15-40% sucrose gradients as previously described. Proteins were TCA/DOC precipitated and visualized by silver-staining. The DNA was extracted, precipitated and resolved using agarose gel electrophoreisis. Molecular weight markers (M) in kilodaltons are indicated, as are the positions of H1, core histones and supercoiled DNA. The fractions corresponding to the chromatin peak are illustrated.

3.4 DISCUSSION

When this project began in 2001, histone H1 had only been incorporated into chromatin using salt dialysis (89) or S-190 cell extracts from *Drosophila* (23). While these methods are still widely used today, we wanted to take advantage of a recombinant system for assembling chromatin. However, use of this system to incorporate histone H1 had yet to be defined. Therefore, we tested whether the

Reproduced with permission of the copyright owner. Further reproduction prohibited without permission.

recombinant assembly factors, dNAP-1 and ACF, could properly assemble chromatin that contained linker histones.

We found the time histone H1 was added to the assembly reaction to be a crucial step for H1 incorporation. During our optimization of H1 incorporation using dNAP-1 and ACF, the Kadonaga laboratory published a method for assembling chromatin containing H1 using the recombinant assembly system (45). They added histone H1 to the initial assembly reaction when forming chromatin containing linker histone. We attribute this difference, in part, to the activities of ACF and dNAP-1, and believe our assembly factors are not as active as those in the Kadonaga laboratory. As a result, we only observed evenly spaced nucleosomes and increased repeat length if the assembly was allowed to proceed, at first, in the absence of histone H1. Also, we were able to use this system to incorporate H1 isolated from mammalian T-cells. Interestingly, NAP-1 was recently identified as a linker histone chaperone in *Xenopus*, depositing H1 onto the linker DNA at physiological pH and ionic strengths (142), which supports a role for dNAP-1 as an H1 chaperone in our system.

Since dNAP-1 is expressed and purified from Sf9 cells, we wanted to test yNAP-1, which is expressed and more easily purified from bacteria, in assembling chromatin with histone H1. We found truncated yNAP-1 as effective as dNAP-1 for assembling histone H1 into chromatin, even though yeast only contain a putative H1 (122). However, H1-chromatin assembled with yNAP-1 did not repress Tax-mediated transcriptional activation, where as we observed repression from H1-chromatin assembled with dNAP-1. We attribute the

Reproduced with permission of the copyright owner. Further reproduction prohibited without permission.

difference seen with yNAP-1 to its ability to exchange histone H2A/H2B dimers (118). We propose this function of yNAP-1 increases the off-rate of histone H1, thereby alleviating the transcriptional repression observed with dNAP-1. As a result, extensive optimization of H1 incorporation using yNAP-1 was not performed, and dNAP-1 served as the sole histone chaperone for our studies. Additionally, comparison of the sequences for yNAP-1 and dNAP-1 revealed only a 30% similarity, suggesting that their functions may be different.

A concern with using a recombinant assembly system to form chromatin containing H1 was whether H1 could be properly incorporated. Not only did MNase experiments confirm an increase in the nucleosome repeat length, but we also found H1 could be incorporated stoichiometrically when added in slight molar excess compared to histone octamer. At this ratio, the final concentration of H1 in our assembly reactions was approximately 170nM, which is higher than the optimal concentration of 50-100nM found by other researchers (32). However, in their study, chromatin containing linker histone was formed using *Drosophila* S-190 extracts, which are very crude and also contain endogenous H1. Therefore the endogenous H1 could skew the amount of exogenously added H1 required for apparent saturation of the chromatin template. Thus, we are confident that despite having a higher concentration of histone H1 in our assembly reactions, we have formed chromatin containing *in vivo* levels of H1 with approximately one histone H1 per nucleosome.

The necessity for adding excess histone H1 to core histone octamer for stoichiometric H1 incorporation may be, in part, due to slight differences in the

Reproduced with permission of the copyright owner. Further reproduction prohibited without permission.

concentration of each protein. Additionally, the dynamic behavior of H1 may play a role, and addition of extra H1 could help ensure that most of the nucleosomes contain a molecule of linker histone at any given time. Also, the concentration of proteins within a cell is much greater than that *in vitro*. Regardless, these experiments confirm use of a recombinant assembly system in the formation of chromatin containing linker histones, and upon optimization, produce chromatin templates that better resemble those found *in vivo* as compared to chromatin assembled in the absence of linker histone.

Reproduced with permission of the copyright owner. Further reproduction prohibited without permission.

Chapter 4

Tax Abolishes Histone H1 Repression of p300 Acetyltransferase Activity at the HTLV-1 Promoter

This work has been submitted for publication to the *Journal of Virology*. The results cited as "data not shown" in the text are provided here as supplemental figures. The Materials and Methods for this section have been included in Chapter 2. The citation for the manuscript is as follows:

Konesky, K., Nyborg, J.K. & Laybourn, P.J. 2006. Tax abolishes histone H1 repression of p300 acetyltransferase activity at the HTLV-1 promoter.

Reproduced with permission of the copyright owner. Further reproduction prohibited without permission.

4.1 ABSTRACT

Upon infection of human T-cell leukemia virus type-1 (HTLV-1), the provirus is integrated into the host cell genome and subsequently packaged into chromatin that contains histone H1. Consequently, transcriptional activation of the virus requires overcoming the environment of chromatin and H1. To efficiently activate transcription, HTLV-1 requires the virally-encoded protein Tax and cellular transcription factor CREB. Together Tax and CREB interact with three *cis*-acting promoter elements called viral cyclic-AMP response elements (vCREs). Binding of Tax and CREB to the vCREs promotes association of p300/CBP into the complex and leads to transcriptional activation. Therefore, to fully understand the mechanism of Tax transactivation, it is necessary to examine transcriptional activation from chromatin assembled with H1. Using a DNA template harboring complete HTLV-1 promoter sequence and a highly defined recombinant assembly system, we demonstrate proper and stoichiometric incorporation of histone H1 into chromatin. Addition of H1 to the chromatin template reduces HTLV-1 transcriptional activation two-fold through a novel mechanism. Specifically, H1 does not inhibit CREB or Tax binding to the viral CREs or p300 recruitment to the promoter. Rather, H1 directly targets p300 acetyltransferase activity. Interestingly, in determining the mechanism of H1 repression, we have discovered a previously undefined function of Tax, which is to overcome the repressive effects of H1-chromatin. Tax specifically abrogates the H1 repression of p300 enzymatic activity in a manner independent of p300 recruitment and without displacement of H1 from the promoter.

Reproduced with permission of the copyright owner. Further reproduction prohibited without permission.

4.2 INTRODUCTION

Human T-cell leukemia virus type-1 (HTLV-1) was first isolated in 1979 (125), and since has been identified as the etiologic agent of adult T-cell leukemia (ATL) and HTLV-1 associated myelopathy/tropical spastic paraparesis (HAM/TSP) (48, 116, 154, 166). Upon infection, the provirus is nearly randomly integrated into the host cell chromosome and subsequently packaged into chromatin (90). Of the estimated 12 million worldwide carriers, roughly 4% eventually develop ATL or HAM/TSP often decades after the initial infection (147). The events that mediate transformation remain largely unknown. However, activation of transcription from the integrated provirus assembled into chromatin is a necessary step for the production of virally-encoded proteins, including Tax. Tax is essential for efficient transcription of the viral genome (17, 162, 163, 165, 167), and contributes to malignant transformation through effects on other genes and cell components (53, 54).

Tax associates with the HTLV-1 promoter through protein-protein interactions between CREB (or other ATF/CREB family members) and protein-DNA contacts. The Tax/CREB complex interacts with three *cis*-acting DNA elements called viral cyclic AMP-response elements (vCREs) located within the U3 region of the HTLV-1 LTR (1, 43, 52). Specifically, CREB binds as a dimer to the 8 nucleotide, off-consensus CRE core within each 21 base pair vCRE (77). Tax interacts with CREB and the GC-rich sequences flanking the core CRE within the DNA minor groove, forming a ternary complex on the promoter (82, 97, 103). Several studies have shown Tax and CREB binding to viral DNA promotes

Reproduced with permission of the copyright owner. Further reproduction prohibited without permission.

association of the pleiotropic coactivators p300 and CBP, forming a quaternary complex (50, 81, 86, 88).

CBP and p300 are cellular coactivators that likely regulate transcription in all metazoans (reviewed in 51). Their effect on transcription is, at least in part, through their intrinsic acetyltransferase activity that targets lysine residues within each of the four core histone proteins (112), as well as non-histone targets (46). Chromatin regions enriched with acetylated nucleosomes correlate with areas of active chromatin (70). *In vivo* studies on the HTLV-1 LTR provide direct evidence for p300 and CBP promoter occupancy contributing to increased levels of histone H3 and H4 acetylation (95). Furthermore, inhibition of histone deacetylase complexes (HDACs) led to even greater levels of histone acetylation and increased viral RNA transcripts (95, 96, 100). Therefore, it is no surprise that we and others observe a requirement for p300 and acetyl CoA in potentiating the effects of Tax transactivation from chromatin templates *in vitro* (47, 99).

Nucleosomes form the basic repeating unit of chromatin and consist of a core histone octamer (two H2B/H2A dimers and one H3/H3 tetramer) wrapped by 146 base pairs of DNA (102). In addition to the core histones, a fifth or "linker" histone, H1 also contributes to the structure and function of chromatin. Approximately one histone H1 is associated per nucleosome *in vivo* (16); however, the precise location of H1 on the nucleosome remains to be determined. The linker histone acts, in part, to stabilize higher order chromatin structure, but is not required for chromatin condensation (27). Functionally, H1 is

Reproduced with permission of the copyright owner. Further reproduction prohibited without permission.

classified as a transcriptional repressor, but no general mechanism for H1 repression has emerged from the literature. Rather, chromatin containing histone H1 has been shown to inhibit various steps associated with transcriptional activation and even initiation (32, 63, 78, 79, 157, 158).

In cells, nucleosomes on the HTLV-1 promoter contain histone H1 (94). Therefore, it is critical to examine the mechanism of Tax activation biochemically on chromatin containing H1. In this study, we investigated the effects of H1-containing chromatin on HTLV-1 transcriptional activation using a defined, recombinant assembly system, extending previous work examining viral activation in the context of chromatin (46, 47, 99). Upon optimization of H1 incorporation into chromatin, we observed a two-fold reduction in HTLV-1 transcriptional activation. We demonstrated that H1 represses transcription through inhibition of p300 activity. Furthermore, we determined H1-chromatin directly represses p300 acetyltransferase activity, as p300 recruitment was not affected by linker histone. In determining the mechanism behind H1 repression, we uncovered a previously undefined function of Tax. Specifically, Tax abrogated H1-mediated inhibition of p300 enzymatic activity in a manner independent of p300 recruitment and without displacing H1 from the promoter. We propose a model where transcriptional activation at the HTLV-1 promoter is tightly regulated through the opposing effects of Tax and H1 on p300 acetyltransferase activity.

Reproduced with permission of the copyright owner. Further reproduction prohibited without permission.

4.3 RESULTS

4.3a Proper and Stoichiometric Incorporation of Histone H1 Into *in vitro* Assembled Chromatin Templates

H1-containing chromatin was assembled with purified H1 and core histones (Figure 4.1A) using a well-characterized, highly defined assembly system (45). Histones were deposited onto a plasmid harboring natural HTLV-1 promoter sequence (Figure 4.2A) using nucleosome assembly protein-1 (NAP-1) and ATP-utilizing chromatin assembly and remodeling factor (ACF). Since a nucleosome containing histone H1 protects 10–20 additional base pairs from micrococcal nuclease digestion (89), we used increased nucleosome repeat length to verify proper H1 incorporation. The nucleosomal repeat length increased from 149 (+/- 6) base pairs in the absence of H1 to 160 (+/- 4) base pairs upon H1 addition, confirming linker histone incorporation (Figure 4.1B).

Typically, one molecule of H1 binds per core histone octamer *in vivo* (16); therefore, it is critical to assemble chromatin with stoichiometric levels of histone H1. Chromatin samples were assembled at different H1 to core histone octamer ratios, and unincorporated linker histone was separated from assembled chromatin templates using 15-40% sucrose gradients. Proteins from sucrose gradient purified chromatin were visualized using SYPRO ruby, which quantitatively stains proteins. H1 was quantified relative to the core histones, and we found a slight molar excess of histone H1 (1.25) to histone octamer was needed to achieve stoichiometric incorporation (Figure 4.1C, lanes 4-8). As the

Reproduced with permission of the copyright owner. Further reproduction prohibited without permission.

Reproduced with permission of the copyright owner. Further reproduction prohibited without permission.

Figure 4.1. Histone H1 is properly incorporated into chromatin using a recombinant assembly system. (A) Purified H1 and core histones isolated from *Drosophila* embryos were analyzed by 15% SDS-PAGE and visualized by staining with coomassie blue. The positions of each histone are labeled, while the masses of molecular weight markers (M) in kilodaltons, are indicated to the left. (B) Histone H1 incorporation increases nucleosome repeat length from 149 (+/- 6 bp) to 160 (+/- 4 bp) base pairs. Chromatin was assembled on the p-306/G-less template (0.94 pmol) using recombinant NAP-1 and ACF assembly factors in the absence or presence of histone H1 as indicated and digested with MNase for 1, 2, 4, & 8 minutes. Nucleosomal DNA was resolved on a 1.2% agarose gel and visualized by SYBR gold staining. Number and position of nucleosomes for each template are labeled numerically. Base pair size markers are indicated to the right. (C) Histone H1 is stoichiometrically incorporated into chromatin. Chromatin containing H1 (1.25 molar excess to octamer) was purified over 15-40% sucrose gradients. Proteins from each fraction were resolved on 15% SDS-PAGE and visualized with SYPRO ruby (top). Molecular weight markers, (M), are shown on the left. Positions of H1, core histones and the major chromatin peak are also indicated. Relative H1 and core histone protein levels from each fraction were quantified using Image Quant. DNA from each fraction was also resolved using agarose gel electrophoresis and SYBR gold (bottom).

Reproduced with permission of the copyright owner. Further reproduction prohibited without permission.

H1 to octamer ratios were increased past 1.25, we observed significant levels of free, unassembled H1 (data not shown). Therefore, we chose templates assembled with an H1 to octamer ratio of 1.25 for subsequent experiments. Together, these experiments confirm proper and stoichiometric incorporation of histone H1 into the chromatin template using a recombinant assembly system.

4.3b H1-Chromatin Represses HTLV-1 Transcriptional Activation

Having optimized H1 incorporation, we next examined the effects of chromatin containing linker histone on HTLV-1 transcriptional activation. Plasmid templates containing the HTLV-1 viral promoter upstream of a G-less cassette (Figure 4.2A) were assembled into chromatin both in the absence and presence of histone H1. Exogenous Tax, CREB and p300 were added after chromatin assembly and H1 incorporation to the transcription reactions where indicated. All reactions contained AcCoA and nuclear extract prepared from an uninfected T-cell line (CEM), which contains the RNA polymerase II transcription machinery.

H1-chromatin reduced relative transcription from the HTLV-1 promoter as compared to that from chromatin lacking the linker histone (Figure 4.2B, lanes 2-4 vs. 5-7, Figure 4.2C). Basal and Tax/CREB-mediated transcription were reduced about 3-fold (Figure 4.2B, lanes 2 vs. 5 & 3 vs. 6, Figure 4.2C), while Tax/CREB/p300-mediated transcription was reduced two-fold (Figure 4.2B, lanes 4 vs. 7, Figure 4.2C). The effects of H1 were chromatin-specific, as H1 addition to free (unassembled) DNA at levels used in chromatin assembly had no significant impact on transcription (data not shown).

Reproduced with permission of the copyright owner. Further reproduction prohibited without permission.

Reproduced with permission of the copyright owner. Further reproduction prohibited without permission.

C.

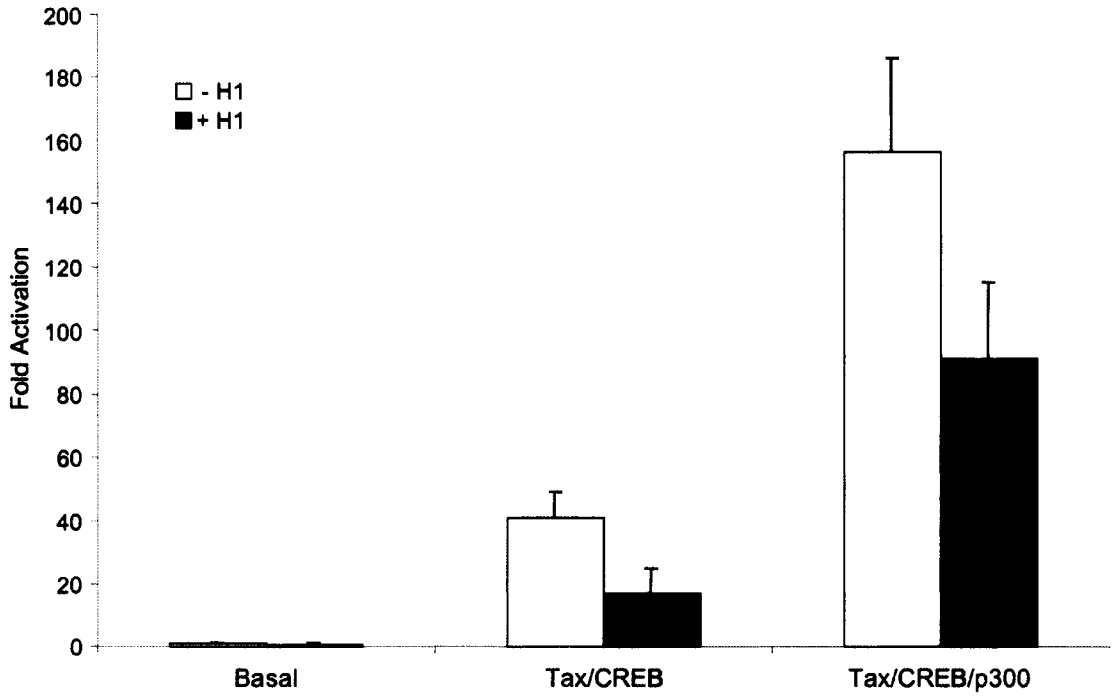

Figure 4.2. Incorporation of histone H1 into chromatin represses HTLV-1 transcriptional activation. (A) Promoter schematic of the p-306/G-less construct relative to the HTLV-1 genome. The approximate positions of the TATA box and vCREs are indicated relative to the transcription start site at +1. (B) *In vitro* transcriptional analysis of chromatin containing histone H1. Chromatin (67 fmol p-306/G-less DNA) was assembled without or with H1 and transcription was assayed in the presence (+) or absence (-) of recombinant CREB (1.6 pmol), Tax (1.6 pmol) and p300 (0.3 pmol) as indicated. CREB, Tax and p300 were added to transcription reactions after chromatin assembly. All reactions contained 50 μM AcCoA and ~40 μg CEM T-cell (uninfected) nuclear extract. Transcription reactions were performed in duplicate and the values shown are averages of transcript levels measured for the duplicate lanes. Transcription was expressed relative to the maximally activated Tax/CREB/p300-dependent transcripts, which are set to 100 (lane 4). The positions of RNA transcript and labeled DNA recovery standard are indicated to the right, while labeled DNA size markers (in nucleotides) are indicated to the left of the gel. (C) Graphical representation of five independent transcription experiments from chromatin either lacking (open bars) or containing (gray bars) histone H1. The fold activation was calculated relative to basal transcription from chromatin assembled in the absence of H1, which is set to 1.

Reproduced with permission of the copyright owner. Further reproduction prohibited without permission.

4.3c Tax Counteracts H1-chromatin Repression of Transcriptional Activation

As a primary step in elucidating the mechanism of H1 repression at the HTLV-1 promoter, we examined the ability of Tax and CREB to compete with H1. For these experiments, chromatin was either assembled without or with H1. Tax and CREB (or CREB alone) were added either after the 4-hour chromatin assembly (AA) or during assembly (DA) after 1.5 hours along with H1 (Figure 4.3A). H1 was added at 1.5 hours to achieve proper incorporation. Upon complete assembly (4 hrs), chromatin templates were incubated with AcCoA and nuclear extract, and transcription was initiated with the addition of rNTPs (Figure 4.3A). Where indicated, exogenous p300 was added to the transcription reactions after chromatin assembly.

As before, H1-chromatin repressed Tax/CREB-mediated transcriptional activation two-fold when added after assembly (AA) (Figure 4.3B, lanes 3 vs. 8). When CREB alone was added after chromatin assembly (AA), transcription also decreased two-fold in the presence H1-chromatin (Figure 4.3B, lanes 2 vs. 7). Even when added during chromatin assembly (DA), CREB-alone activation was repressed two-fold by chromatin containing H1 (Figure 4.3B, lanes 4 vs. 9). However, addition of Tax together with CREB during chromatin assembly (DA) completely counteracted the H1-chromatin repression of CREB transcriptional activation (Figure 4.3B, lanes 5 vs. 10, Figure 4.3D).

The relative level of transcription from templates assembled with CREB or Tax/CREB increased with the addition of exogenous p300 (after assembly,

Reproduced with permission of the copyright owner. Further reproduction prohibited without permission.

Figure 4.3A) on both chromatin templates (Figure 4.3C). However, H1 incorporation still produced a two-fold reduction in CREB/p300-mediated transcription (Figure 4.3C, lanes 2 vs. 6, Figure 4.3D), indicating that p300 cannot counteract H1 repression and that the effects of H1-chromatin may be through inhibition of CREB binding. While p300 addition to chromatin templates assembled with Tax/CREB augmented transcriptional activation in the presence of H1 (Figure 4.3C, lanes 7 vs. 8), exogenous p300 was not required for Tax and CREB to completely counteract H1-chromatin repression (Figure 4.3C, lanes 3 vs. 7, Figure 4.3D).

We performed micrococcal nuclease digestion analysis to verify Tax and CREB addition during assembly did not compromise the integrity of our chromatin templates, and obtained the same quality ladders as seen from chromatin assembled in the absence of transcription factors (data not shown).

Reproduced with permission of the copyright owner. Further reproduction prohibited without permission.

Reproduced with permission of the copyright owner. Further reproduction prohibited without permission.

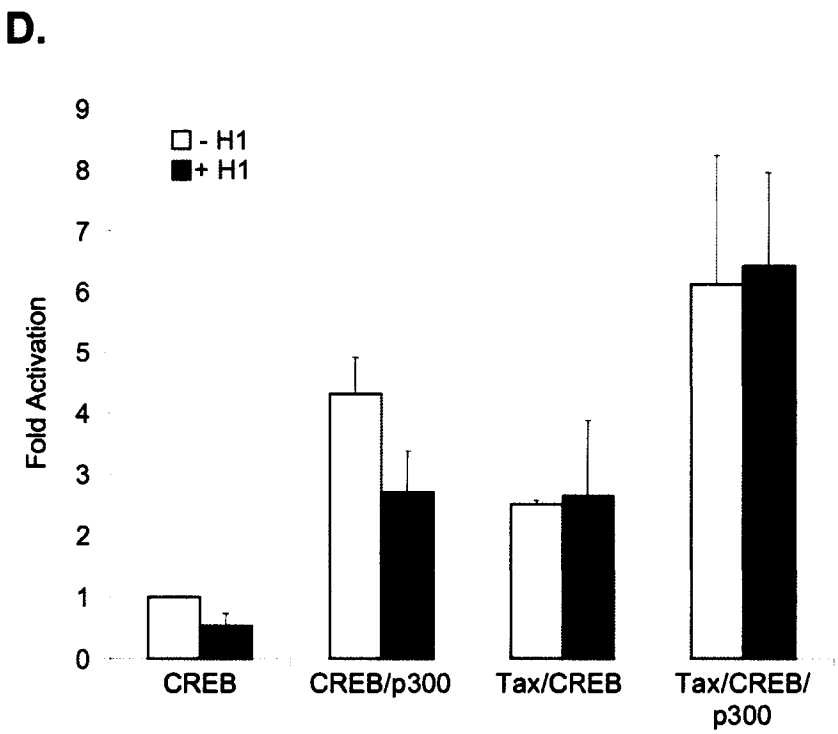

Figure 4.3. Tax counteracts the H1-chromatin repression of transcriptional activation. (A) Timeline of chromatin assembly and factor addition for *in vitro* transcription reactions. (B) Tax and CREB but not CREB alone overcome H1 repression of transcriptional activation. Chromatin (67 fmol p-306/G-less DNA) was assembled without or with histone H1. Equivalent amounts of Tax and CREB (1.6 pmol each) were added either after (AA) or during chromatin assembly (DA) as indicated for each chromatin template. Transcript levels are an average of duplicate lanes and were calculated relative to lane 3, which was set to 100. (C) Addition of p300 does not overcome H1 repression of CREB-mediated transcriptional activation. Chromatin was assembled as described above. Tax and CREB (1.6 pmol each) were added during chromatin assembly (DA), while p300 (0.3 pmol) was added after chromatin assembly (AA) to the transcription reactions as indicated. Transcript levels are an average of duplicate lanes and were calculated relative to lane 4, which was set to 100. (D) Graphical representation of three independent transcription experiments from chromatin lacking (open bars) or containing (gray bars) histone H1 assembled with factors added during chromatin assembly. The fold activation was calculated relative to CREB-alone transcription from chromatin assembled without H1, which is set to 1.

Reproduced with permission of the copyright owner. Further reproduction prohibited without permission.

4.3d CREB Binding to the vCREs is Not Reduced in the Context of H1-Chromatin

To directly test the hypothesis that H1-chromatin represses transcription through an inhibition of CREB binding to the vCREs, DNase I primer extension footprinting analysis was performed. CREB binding was determined using the same templates and salt conditions as in transcription studies. Chromatin was assembled without or with histone H1, followed by incubation with increasing concentrations of CREB. The templates were digested with DNase I, and DNA cleavage was analyzed by primer extension.

Surprisingly, incorporation of H1 into chromatin produced no measurable decrease in CREB binding at the vCREs. At the lowest ratio of CREB per vCRE binding site (same four-fold molar excess as that used in transcription reactions), CREB addition after chromatin assembly resulted in similar DNase I protection on either chromatin template (Figure 4.4 lanes 3 vs. 10). As CREB concentrations were increased to a 40-fold molar excess relative to binding sites, DNase I protection continued to increase by essentially equal levels on both chromatin templates (Figure 4.4 lanes 6 vs. 13). We have also footprinted the promoter proximal vCRE and found no change in the ability of CREB to bind upon H1 incorporation (data not shown). Based on these data, we concluded the mechanism by which H1-chromatin represses transcriptional activation is not through an effect on CREB binding.

As would be expected, when CREB was added during chromatin assembly, H1 incorporation had no effect on CREB binding. Also, addition of

Reproduced with permission of the copyright owner. Further reproduction prohibited without permission.

Tax during assembly did not increase CREB binding to H1-chromatin (data not shown). Therefore, Tax functions at a step downstream of CREB binding in counteracting H1-chromatin repression.

4.3e Chromatin Containing Histone H1 Inhibits p300 Activity

Previous *in vitro* and *in vivo* studies have demonstrated the importance of p300 in HTLV-1 transcriptional activation (46, 47, 95, 99). Therefore, we tested if H1-chromatin affected Tax/CREB stimulation of p300 activity using histone acetyltransferase (HAT) assays. The same plasmid template (Figure 4.2A) used in transcription and footprinting studies was assembled into chromatin containing or lacking linker histone. Upon assembly, chromatin was incubated with Tax, CREB, p300 and ^{14}C-labeled AcCoA. The core histone proteins were resolved using SDS-PAGE and ^{14}C incorporation was analyzed as described in the Materials and Methods.

Addition of Tax/CREB after chromatin assembly (AA) increased relative acetylation above basal levels from both chromatin templates (Figure 4.5A). However, incorporation of H1 decreased basal histone acetylation (Figure 4.5A, lanes 2 vs. 4), as well as Tax/CREB-stimulated acetylation about three-fold (Figure 4.5A, lanes 3 vs. 5). Repression of p300 histone acetylation parallels the reduction in transcription observed from chromatin containing H1 (Figure 4.2B, lanes 4 vs. 7). We found H1 that was not incorporated into nucleosomes had no effect on p300 HAT activity (data not shown).

Reproduced with permission of the copyright owner. Further reproduction prohibited without permission.

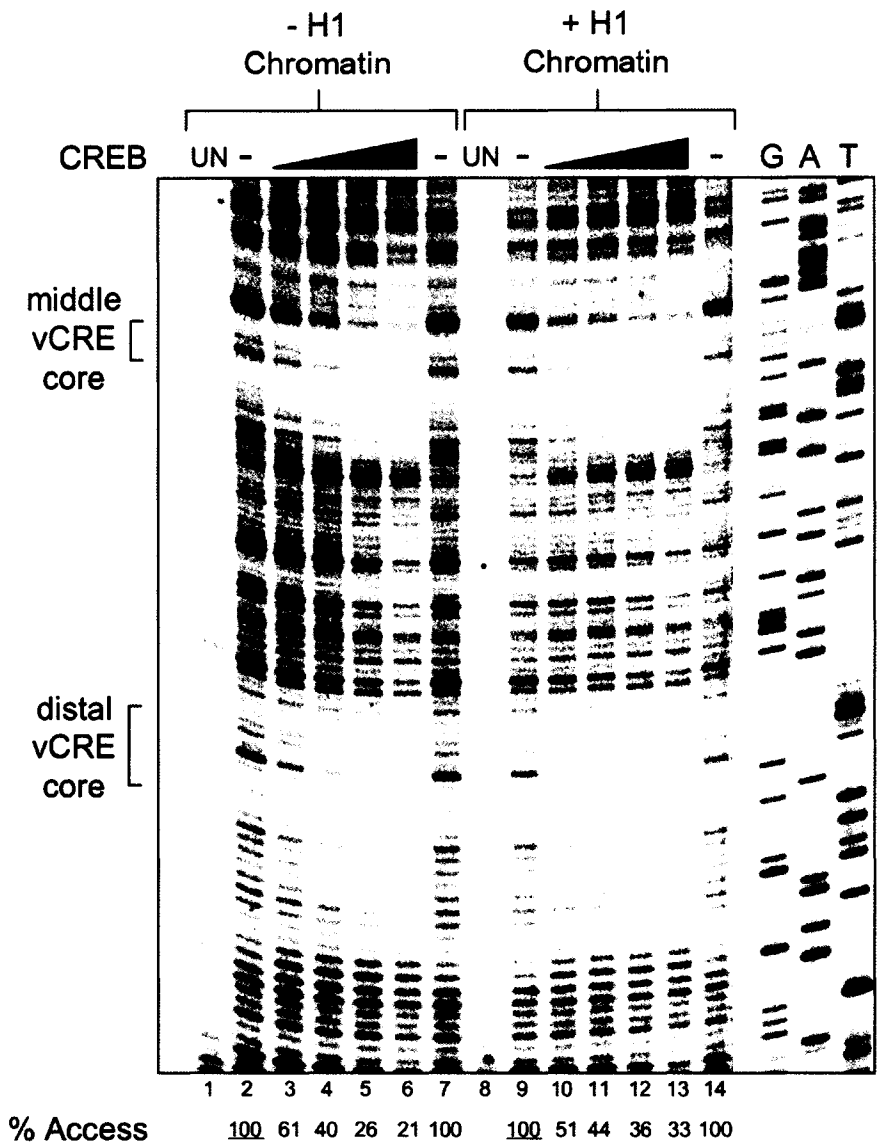

Figure 4.4. H1-chromatin repression is not through inhibition of CREB binding. DNase I primer extension footprinting analysis of CREB binding on chromatin templates (56 fmol p-306/G-less DNA) assembled in the absence and presence of histone H1. CREB was added after chromatin assembly to each template and titrated from a 4 to 40-fold molar excess as indicated by triangles (1.3, 2.7, 6.7 & 13.4 pmol of CREB respectively). Undigested DNA (UN) and no protein (-) lanes are labeled for both chromatin templates. Digested, ^{32}P-labeled DNA products from the primer extension reaction were resolved on an 8% sequencing gel. Protection was observed at both the middle and distal vCRE core regions as CREB was titrated onto the DNA. Protein binding was measured as a percent of DNA accessibility with the digested, no-protein lanes set as 100 percent accessible. The percent accessibility was calculated for the distal vCRE, although similar levels of protection were calculated for the middle and proximal vCREs.

Reproduced with permission of the copyright owner. Further reproduction prohibited without permission.

Reproduced with permission of the copyright owner. Further reproduction prohibited without permission.

C.

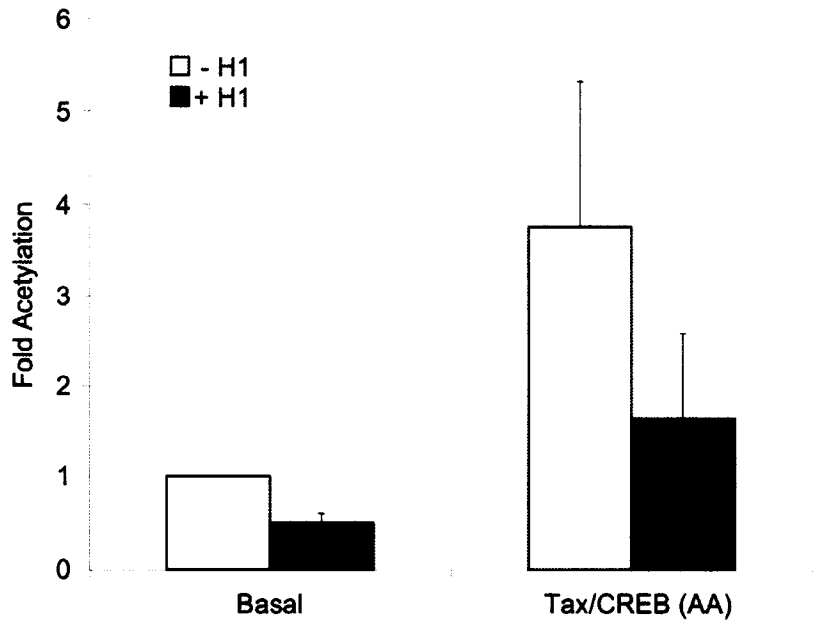

Figure 4.5. H1-chromatin repression is through an effect on p300 activity. (A) *In vitro* histone acetyltransferase activity of p300 was measured by ^{14}C-labeled AcCoA incorporation into histones present on chromatin templates (1.26 pmol p-306/G-less DNA) assembled in the absence or presence of linker histone. Acetylation reactions were performed with recombinant p300 (8.4 pmol) in the presence (+) or absence (-) of Tax and CREB (30 pmol each) added after chromatin assembly. Histones were resolved via 18% SDS-PAGE. Free histones were acetylated by p300 for size markers and positions of each core histone are indicated on the left. Acetylation levels are calculated relative to chromatin lacking H1 in the absence of Tax and CREB (set to 1) and displayed as the average values between duplicate lanes. (B) Tax/CREB-mediated acetylation by p300 is vCRE dependent. The p-52/G-less construct (Figure 4.2A, 1.26 pmol DNA) was assembled into chromatin without or with histone H1 and acetylation reactions were performed as above. (C) Graphical representation of acetylation levels on chromatin assembled without (open bars) or with (gray bars) linker histone. Tax and CREB were added after chromatin assembly (AA). Data were calculated from three independent experiments and acetylation levels are relative to basal from templates lacking H1, which is set to 1.

Reproduced with permission of the copyright owner. Further reproduction prohibited without permission.

To verify that the increase in acetylation required vCRE-mediated recruitment of Tax and CREB, we assembled a plasmid carrying the HTLV-1 promoter deleted to -52 (Figure 4.2A). This construct, which lacks the vCREs, was assembled into chromatin in the absence or presence of linker histone. The results obtained demonstrated that p300-mediated histone acetylation requires Tax/CREB binding to the vCREs (Figure 4.5B). These data indicate H1-chromatin reduces Tax/CREB-mediated transcriptional activation through an effect on p300 at the HTLV-1 promoter. Furthermore, the data support a model where H1 inhibits either p300 recruitment and/or enzymatic activity.

4.3f Tax Completely Overcomes the H1-Chromatin Repression of p300 Activity

Having determined incorporation of linker histone into our chromatin templates affects p300 function, we turned our focus to the mechanism of Tax in overcoming H1-chromatin transcriptional repression. This ability of Tax is most pronounced when it is added together with CREB during chromatin assembly. Therefore, we examined the ability of Tax and CREB to stimulate p300 HAT activity when added during chromatin assembly (DA) either in the absence or presence of histone H1 (Figure 4.3A).

In this context, Tax/CREB addition abrogated H1-chromatin repression of p300 histone tail acetylation (Figure 4.6A, lanes 3 & 5). The degree to which these results mirror the derepression observed in transcriptional activation with Tax/CREB addition during chromatin assembly is striking (Figure 4.3C, lanes 4

Reproduced with permission of the copyright owner. Further reproduction prohibited without permission.

vs. 8), suggesting Tax functions through effects on p300 in counteracting H1-repression. Unlike transcription reactions, HAT assays were performed using only purified proteins (no nuclear extract). Therefore, we can be certain that only Tax is required together with CREB to overcome the repressive effects of H1-chromatin.

Phosphorylation of CREB at Ser133 is a necessary step in the recruitment of p300 and subsequent transcriptional activation of cellular promoters (87, 108). Recently, we have determined that CREB is phosphorylated in our transcription nuclear extract, potentially recruiting p300 independently of Tax (N. Sharma, personal communication). Tax is thought to bypass the need for CREB phosphorylation in p300 recruitment (86). By extension, CREB phosphorylation may have the same effect as Tax in counteracting H1-chromatin repression of p300. To test the ability of phosphorylated-CREB (P-CREB) alone to overcome the effects of H1-chromatin, P-CREB was added during chromatin assembly (DA) without and with H1 and p300 HAT activity was assayed as before. We observed a two-fold reduction in p300 HAT activity mediated by P-CREB in the presence of H1 (Figure 4.6B, lanes 4 vs. 7), demonstrating P-CREB is not sufficient for counteracting the repressive effects of H1-chromatin on p300.

Reproduced with permission of the copyright owner. Further reproduction prohibited without permission.

Reproduced with permission of the copyright owner. Further reproduction prohibited without permission.

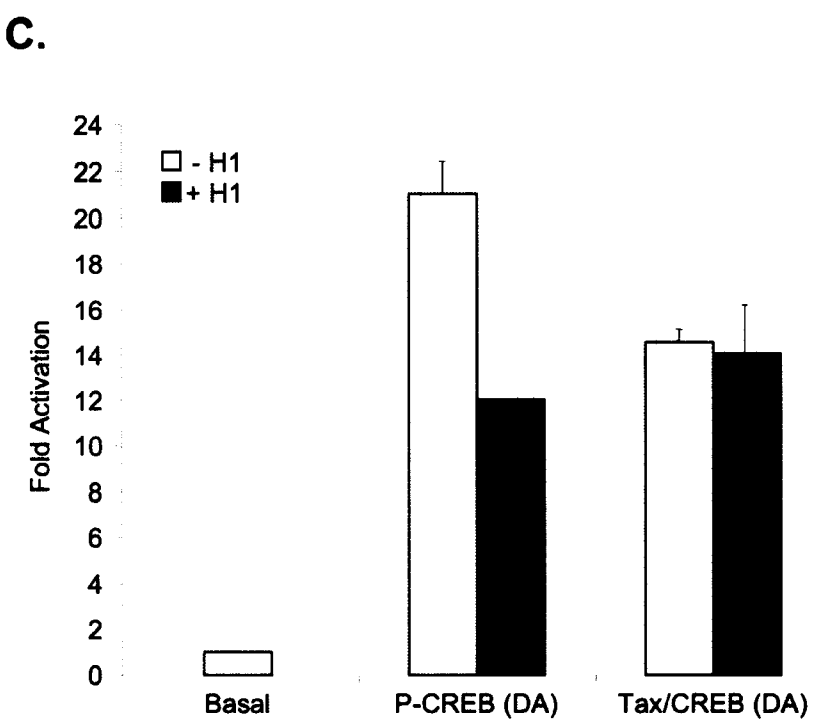

Figure 4.6. Tax completely overcomes H1-repression of p300. (A) Addition of Tax and CREB during chromatin assembly (DA) reverses the effect of histone H1 on p300. *In vitro* histone acetyltransferase activity of p300 was measured by ^{14}C-labeled AcCoA incorporation onto chromatin templates (1.26 pmol p-306/G-less DNA). Acetylation reactions were performed with recombinant p300 (8.4 pmol) in the presence (+) or absence (-) of Tax and CREB (30 pmol each) added during chromatin assembly on chromatin templates containing (+) or lacking histone H1 (-) where indicated. Free histones were acetylated by p300 for size markers and positions of each histone are labeled on the left. Acetylation levels were calculated relative to chromatin lacking H1 in the absence of Tax and CREB (lane 2, set to 1). (B) Chromatin containing H1 represses P-CREB-mediated p300 HAT activity. Acetylation reactions were performed as above except that either P-CREB or CREB (30 pmol each) were added without Tax to each reaction during chromatin assembly (DA) on chromatin templates assembled without or with histone H1. The positions of acetylated free histones are labeled on the left. Acetylation levels were calculated relative to chromatin lacking H1 in the absence of CREB and P-CREB (lane 2, set to 1). (C) Graphical representation of acetylation levels from factor addition during chromatin assembly (DA) on templates lacking (open bars) or containing (gray bars) histone H1. Data was calculated from two independent experiments for P-CREB and from three independent experiments for Tax/CREB. Acetylation levels are relative to basal from chromatin lacking H1, which is set to 1.

Reproduced with permission of the copyright owner. Further reproduction prohibited without permission.

4.3g p300 Acetyltransferase Activity, Not Recruitment, Is Inhibited By Chromatin Containing H1

To further define the mechanism of H1 repression, we used immobilized chromatin templates containing HTLV-1 DNA. The promoter fragment (P) carries the three viral CREs, while the control fragment (C) lacks viral CREs (Figure 4.2A). First, each fragment was bound through a 5' biotin moiety to magnetic streptavidin beads. These bead-bound fragments were then assembled into chromatin without or with H1 using the recombinant assembly system. Tax and P-CREB were added either after (AA) or during (DA) chromatin assembly and p300 was added after chromatin assembly where indicated. The templates were isolated using magnetic separation, washed, and the remaining bound proteins were resolved by SDS-PAGE and quantified by western blot analysis. The difference in Tax, P-CREB and p300 binding to the promoter fragment (P) versus the control fragment (C) demonstrated that their binding is vCRE specific (Figure 4.7A).

To determine the effects of H1, we compared p300 promoter occupancy in the presence of P-CREB alone or P-CREB plus Tax added during (DA) or after (AA) assembly on chromatin templates without and with histone H1. In the absence of Tax and P-CREB, there was no significant binding of p300 to the promoter (Figure 4.7B, lanes 1 & 2). A significant increase in p300 recruitment was observed in the presence P-CREB (Figure 4.7B, lanes 3-6). Addition of Tax together with P-CREB further enhanced p300 promoter occupancy above that of P-CREB alone (Figure 4.7B, compare lanes 3-6 to 7-10). Despite the differences

Reproduced with permission of the copyright owner. Further reproduction prohibited without permission.

in the amounts of p300 recruited to the promoter by P-CREB and Tax/P-CREB, p300 promoter occupancy was unaffected by chromatin assembled with H1 (Figure 4.7B). These results clearly demonstrate that assembly of chromatin with H1 does not inhibit p300 recruitment to the promoter. Therefore, our data strongly support a model where H1 carries out its repressive effects via inhibition of p300 acetyltransferase activity. And, Tax/CREB, but not CREB alone, reverses this inhibition resulting in a high degree of HTLV-1 transcriptional activation.

4.3h Tax and CREB Do Not displace Histone H1 From the Promoter

We tested the hypothesis that Tax functions in counteracting H1 repression by displacing H1 from the promoter during chromatin assembly. Although micrococcal nuclease digestion experiments verified that global H1 incorporation was preserved, this assay could not detect a highly localized loss of H1 molecules at the promoter (data not shown). In contrast, approximately 3 chromatosomes form on each 700 base pair bead-bound promoter fragment. Therefore, if Tax caused localized H1 displacement, the reduction would be detected by western blot. Surprisingly, the amount of linker histone assembled into chromatin does not change when Tax is added together with P-CREB either during (DA) or after (AA) chromatin assembly (Figure 4.7B, lanes 8 vs. 10). Thus, Tax does not function in counteracting H1-repression through displacement of histone H1.

Reproduced with permission of the copyright owner. Further reproduction prohibited without permission.

Reproduced with permission of the copyright owner. Further reproduction prohibited without permission.

Figure 4.7. Recruitment of p300 is not affected by chromatin containing H1. (A) Factor binding is vCRE-dependent. Chromatin was assembled in the absence of linker histone on promoter (P, three vCREs) or control (C, no vCREs) DNA (2 pmol biotinylated fragment DNA). Recombinant Tax (18 pmol), P-CREB (12 pmol) and p300 (0.75 pmol) were added to the assembled chromatin templates. Upon isolation and washing of each template, the bound proteins were analyzed by western blot. Antibodies are indicated to the left of each blot. (B) Factor binding to the promoter fragment assembled into chromatin either in the absence (-) or presence (+) of histone H1. Tax and P-CREB were added during (DA) or after (AA) chromatin assembly, as indicated. All reactions contained p300, which was added after chromatin assembly. Bound proteins were detected using western blot analysis with the indicated antibodies. (C) Graphical representation of p300 binding from either Tax/P-CREB or P-CREB-mediated recruitment in the context of chromatin lacking (open bars) or containing linker histone (gray bars). Data was averaged between three independent experiments and p300 binding is relative to chromatin assembled without H1 for each condition, which are set to 1.

Reproduced with permission of the copyright owner. Further reproduction prohibited without permission.

4.4 DISCUSSION

Despite the general characterization of histone H1 as a transcriptional repressor (89, 139), there is no clearly defined mechanism for H1 repression. Rather, the data presented to date suggest the effects of chromatin containing histone H1 are, to some degree, promoter-specific (32, 37, 78, 83, 92, 131). Additionally, recent microarray data collected from mice embryonic stem cells null for three H1 isoforms demonstrated mammalian H1 acts both negatively and positively in gene regulation (41).

In this study, we examined the effect of histone H1 on Tax-mediated activation of HTLV-1 transcription. Incorporation of H1 into the chromatin template repressed HTLV-1 transcriptional activation. The reduction in transcription was not attributable to decreased transcription factor binding, as we observed no change in either CREB or Tax promoter occupancy upon H1 incorporation. Rather, chromatin containing H1 inhibited p300 acetyltransferase activity directly without affecting p300 recruitment to the promoter. Additionally, we have discovered a previously undefined function of Tax, which is to overcome H1-mediated inhibition of p300 enzymatic activity.

4.4a H1 Represses CREB Transcriptional Activation but Not CREB Binding

Although the histones, including H1, are evicted from the HTLV-1 promoter region upon Tax transactivation, Tax must first interact with chromatin that contains linker histone (94). Therefore, we examined steps prior to transcription initiation and RNA polymerase II recruitment in determining the role

Reproduced with permission of the copyright owner. Further reproduction prohibited without permission.

of H1 at the HTLV-1 promoter. Since H1-chromatin reduced transcriptional activation, we performed competition studies between CREB, Tax and H1 and indirectly assayed factor binding using transcription assays. When Tax and CREB were added at the same time as histone H1 during chromatin assembly, the activators completely counteracted the repressive effects of H1-chromatin on transcriptional activation. However, CREB, in the absence of Tax, was not capable of overcoming H1-repression (Figure 4.3B). Additionally, exogenous p300 failed to reverse the repressive effects of histone H1 on CREB-mediated activation (Figure 4.3C).

Previous studies have shown that H1 interferes with transcription factor binding to the DNA (78, 137). We directly tested this possibility and found, through DNase I footprinting, that the repressive effects of H1 do not result from inhibition of CREB/vCRE interactions (Figure 4.4). Additionally, we found no change in CREB or Tax binding to the vCREs on immobilized chromatin templates assembled in the absence or presence H1 (Figure 4.7B). These data are in agreement with Cheung et al. (2002), where it was demonstrated that estrogen receptor-α (ER-α) binding is not affected by chromatin containing histone H1 (32). Further, Koop et al. (2003) found that H1 did not inhibit progesterone receptor (PR) binding to the MMTV promoter. Instead, H1 increased the efficiency of PR binding (83).

Reproduced with permission of the copyright owner. Further reproduction prohibited without permission.

4.4b H1 Represses Transcription Through Inhibition of p300 Activity

Additional mechanisms for H1-transcriptional repression include effects on factors with HAT activity (63). Given the presence of p300/CBP on the HTLV-1 promoter *in vivo* and the role of these coactivators in transcriptional activation, we examined the effects of H1-containing chromatin on p300 enzymatic activity and recruitment (47, 95, 99). While we have shown that the histone tails are not the primary target of p300 in HTLV-1 activation, the non-histone target(s) remains to be identified (46). Therefore, we used HAT assays as a general measure of p300 enzymatic activity. We found H1-chromatin inhibited both Tax/CREB-mediated (targeted) and basal (non-targeted) p300 HAT activity (Figure 4.5A). Thus, the two-fold reduction in transcriptional activation observed could be attributed to the effects of H1-chromatin on p300 acetyltransferase activity (Figure 4.2B). In agreement with our HAT data, others have previously demonstrated linker histone repression of non-targeted, recombinant PCAF (p300/CBP-associated factor) HAT activity (63). In contrast, Cheung et al. (2002) found no affect of H1 on ERα-mediated stimulation of p300 HAT activity (32).

Intriguingly, we discovered that Tax and CREB addition during chromatin assembly abolished the repressive effects of H1-chromatin on p300 HAT activity (Figure 4.6A), consistent with the derepression of transcription observed from H1-chromatin in this context (Figure 4.3B & C). These data pinpoint the function of Tax in counteracting histone H1 to an effect on p300, and suggest that Tax antagonizes H1 repression of HTLV-1 transcription via modulation of p300 function.

Reproduced with permission of the copyright owner. Further reproduction prohibited without permission.

4.4c H1-Chromatin Directly Represses p300 Acetyltransferase Activity

Herrera et al. (2000) attributed H1 repression of PCAF activity to steric hindrance of H3 accessibility by the H1 tails, but they did not examine if PCAF interactions with the chromatin template were altered by H1 incorporation. To determine if H1-chromatin directly inhibited p300 acetyltransferase activity, or if the observed repression was through an indirect affect on p300 recruitment, we used immobilized chromatin templates. H1 incorporation into chromatin did not decrease P-CREB-mediated or Tax/P-CREB-mediated p300 recruitment, confirming histone H1 inhibits p300 acetyltransferase activity at the HTLV-1 promoter.

4.4d Tax Counteracts H1-Chromatin Repression of p300 Enzymatic Activity

Having defined the step in HTLV-1 transcriptional activation that H1 represses, we further probed the mechanism of Tax function in this process. Using immobilized chromatin templates, we demonstrated that Tax does not simply function through displacement of histone H1 at the promoter (Figure 4.7B). Intriguingly, we observed a three-fold increase in Tax promoter occupancy with addition during chromatin assembly (DA) relative to Tax occupancy when added after chromatin assembly (AA) (Figure 4.7B). However, we did not observe a concomitant increase in p300 binding. In fact, the level of p300 recruited remained constant, regardless of when Tax and P-CREB were added to the assembly reactions. Furthermore, the increase in p300 recruitment observed with Tax/P-CREB over that of P-CREB alone, is not sufficient to

Reproduced with permission of the copyright owner. Further reproduction prohibited without permission.

counteract H1 repression of p300 activity or transcriptional activation. Therefore, the simplest interpretation is that Tax directly targets the inhibition of p300 enzymatic activity to abrogate H1-chromatin repression of HTLV-1 transcription.

4.4e H1 and Tax Regulation of the HTLV-1 Promoter

We propose a model that defines a role for histone H1 in regulation of the HTLV-1 promoter during early events in transcriptional activation (Figure 4.8). Incorporation of linker histone into chromatin does not affect CREB, Tax or p300 association with the promoter. Rather, H1 inhibits p300 directly through reduction of acetyltransferase activity, apparently resulting in the 2-fold repression of HTLV-1 transcription. In addition, when Tax is present with CREB during chromatin assembly, the effects of H1 on p300 acetyltransferase activity are alleviated (Figure 4.8). While the exact mechanism has yet to be elucidated, we propose several models for Tax function in overcoming H1-repression of p300 HAT activity. Tax may alter p300 substrate accessibility. Addition of Tax during assembly could also affect higher order chromatin structure, which, in turn, could lead to effects on protein-protein and protein-DNA interactions. Additionally or alternatively, Tax could disrupt H1 interactions that allosterically inhibit p300 activity, as acetyl CoA has been shown to allosterically regulate p300 inhibitory activity (129). Either mechanism is consistent with previous finding that the globular domain of H1/H5 is not sufficient for inhibition of HAT activity, rather the tails of H1 are responsible for mediating decreased acetylation (63). Coupled with our finding that histone H1 is not displaced, these data suggest

Reproduced with permission of the copyright owner. Further reproduction prohibited without permission.

p300 repression is mediated by the H1 tails, rather than the globular domain. Future experiments will be directed at differentiating between these possible mechanisms.

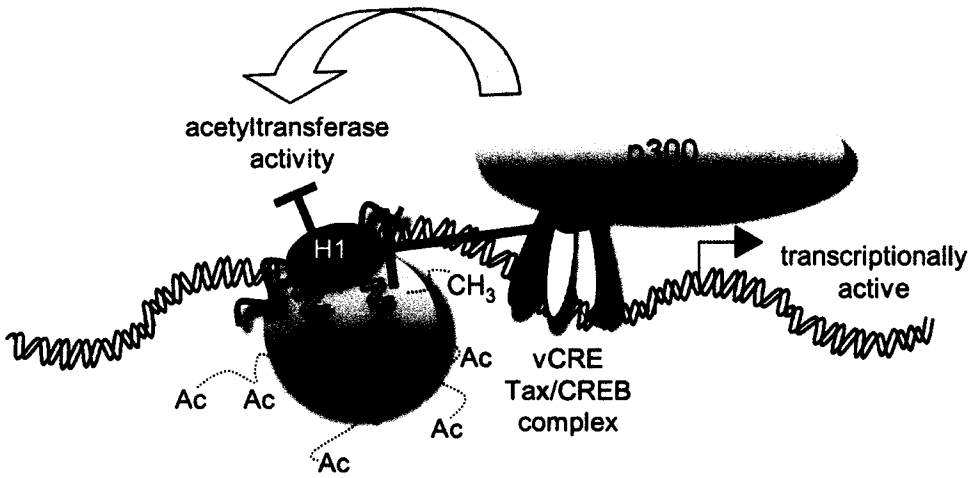

Figure 4.8. Model for HTLV-1 transcriptional regulation in a chromatin context. H1 incorporation into nucleosomes inhibits p300 enzymatic activity and Tax functions to abolish the H1-chromatin repression, providing a means for tighter control of HTLV-1 transcription.

Reproduced with permission of the copyright owner. Further reproduction prohibited without permission.

SUPPLEMENTAL FIGURES

Reproduced with permission of the copyright owner. Further reproduction prohibited without permission.

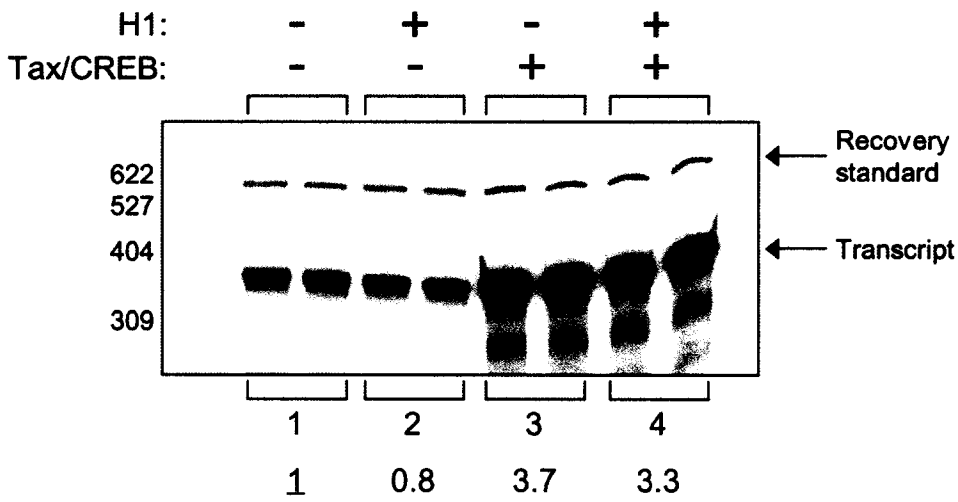

Figure 4.9. Addition of free histone H1 does not repress transcription of naked HTLV-1 DNA templates. The same level of linker histone added to previous transcription experiments with chromatin containing H1 was added to unassembled DNA. Tax and CREB were added as indicated. Transcription levels are averages of duplicate lanes and were calculated relative to lane 1, which is set to 1.

Reproduced with permission of the copyright owner. Further reproduction prohibited without permission.

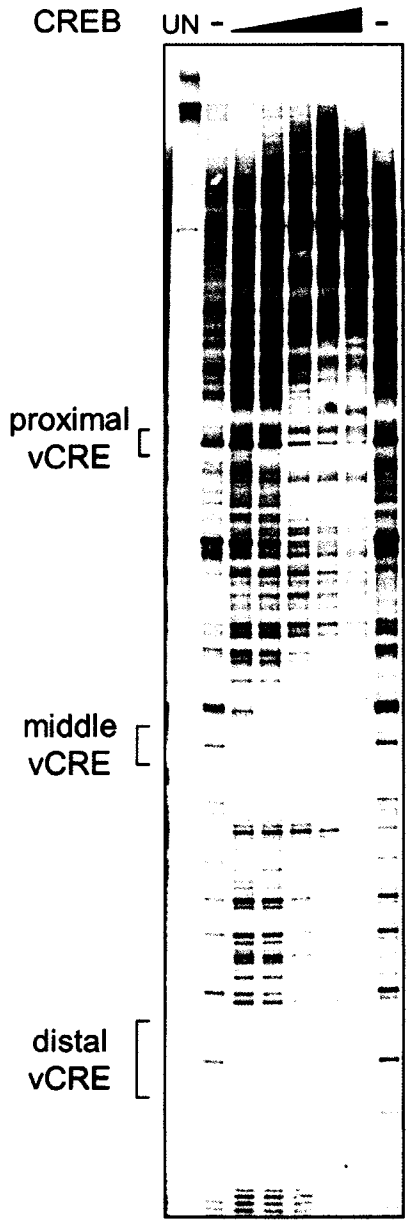

Figure 4.10. CREB binds to all three vCREs. CREB was titrated onto naked DNA (50, 100, 250, 500 1000 ng) starting with a 20-fold molar excess of CREB to vCRE binding site. The positions of each vCRE are indicated.

Reproduced with permission of the copyright owner. Further reproduction prohibited without permission.

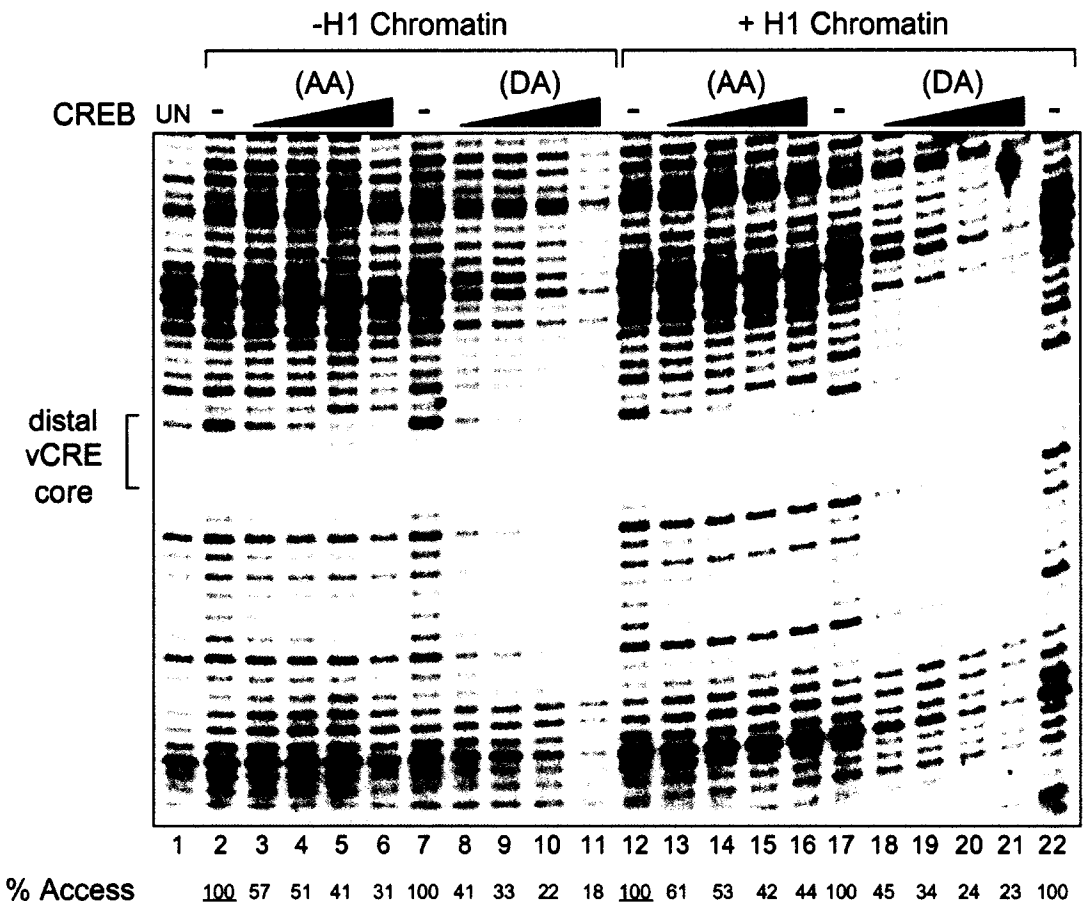

Figure 4.11. CREB binds similarly to both chromatin templates when added either after (AA) or during (DA) chromatin assembly. CREB was added as indicated and titrated from a 4 to 40-fold molar excess per binding site. Only the distal vCRE is shown and the percent accessibility was calculated relative to the no protein (-) lane for each chromatin template, which is set to 100. At the lowest molar ratio (4-fold) for each condition, the accessibility of CREB is similar when added either AA or DA on both chromatin templates. As the concentration of CREB is increased to the 40-fold molar excess, CREB binding DA is twice that added AA.

Reproduced with permission of the copyright owner. Further reproduction prohibited without permission.

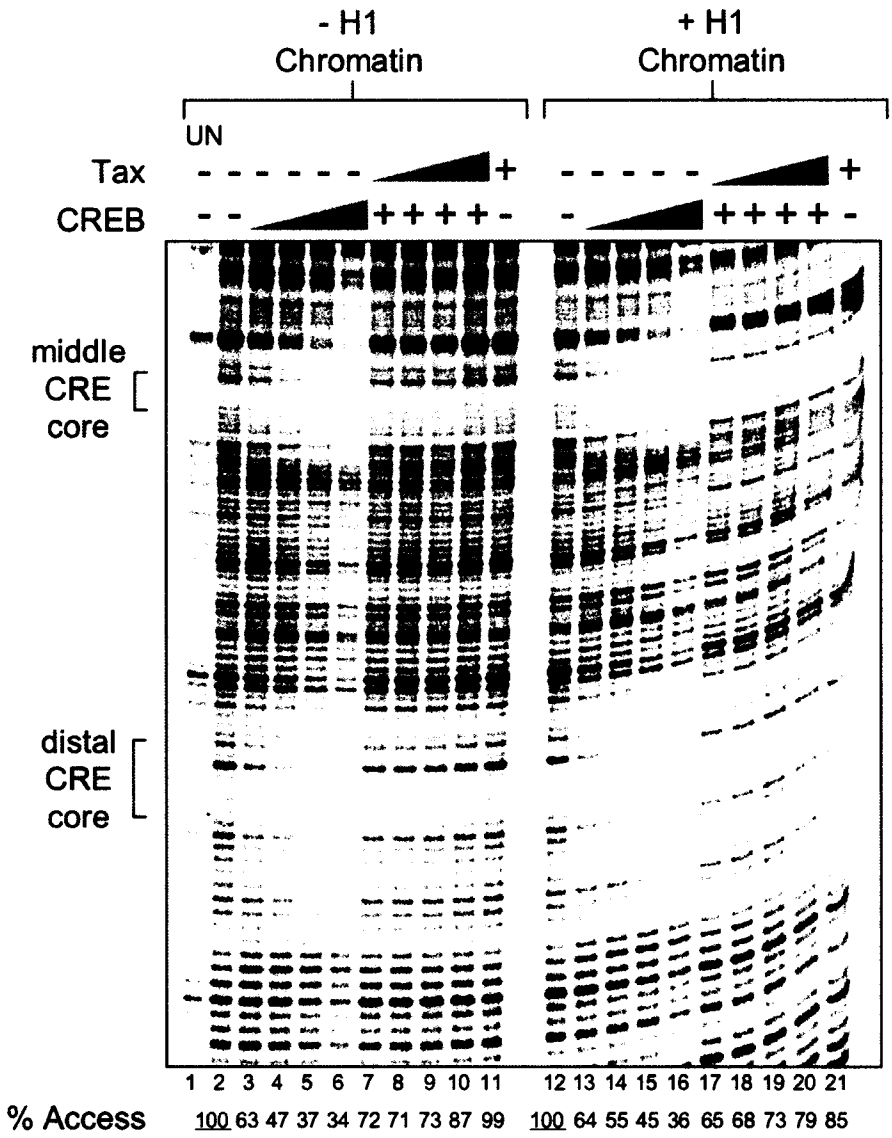

Figure 4.12. Tax does not aid CREB binding in the presence of H1-chromatin. Tax was added during assembly (DA) and titrated from a 4-fold to 40-fold molar excess (triangles) on chromatin assembled without or with H1 as indicated. CREB was either absent (-) or added during assembly in a four-fold excess (+) where indicated. Tax was either absent (-) from the reactions or added in a 40-fold molar excess (+) as labeled. Undigested DNA (UN) is labeled. Digested, ^{32}P-labeled DNA product from the primer extension reaction was resolved on a 8% sequencing gel. Protein binding was measured as a percent of DNA accessibility with the digested, no-protein lanes being 100 percent accessible. The percent accessibility corresponds to that from the distal vCRE.

Reproduced with permission of the copyright owner. Further reproduction prohibited without permission.

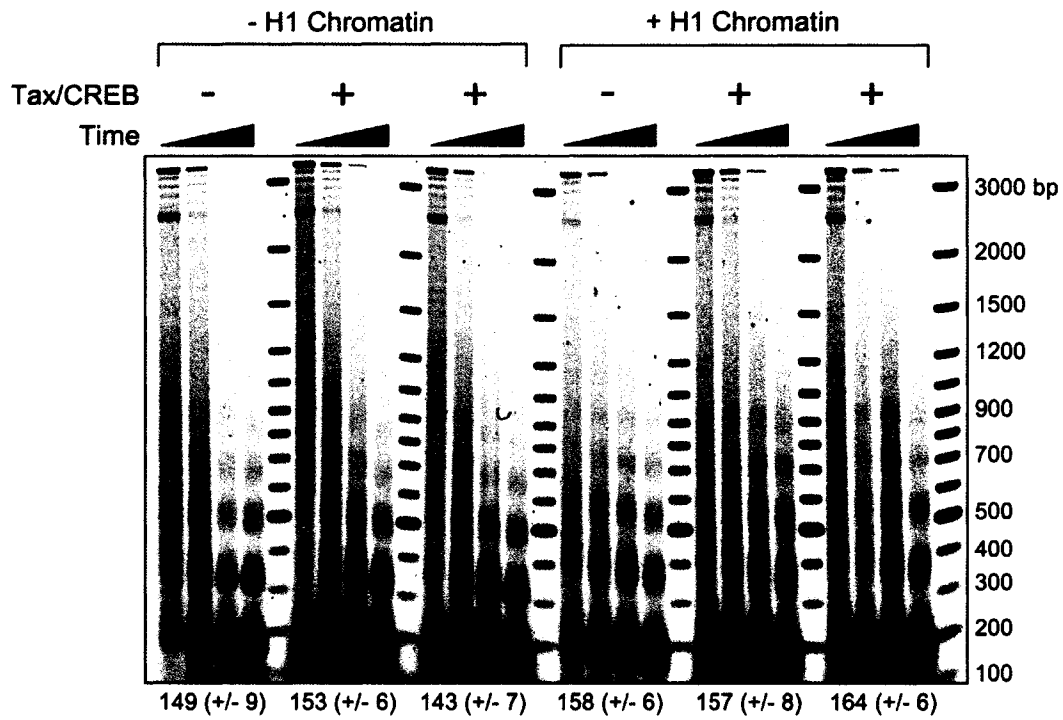

Figure 4.13. Tax and CREB addition during chromatin assembly (DA) does not interfere with chromatin formation or H1 incorporation. Chromatin was assembled with Tax/CREB as indicated (performed in duplicate) on templates lacking or containing histone H1 and digested with MNase. The approximate nucleosome repeat length in base pairs is given for each template. DNA was extracted and resolved using 1.2% TBE agarose gel electrophoresis and visualized with SYBR gold staining and STORM imaging. Base pair markers are indicated to the right (Fermentas 100 base pair DNA ladder plus).

Reproduced with permission of the copyright owner. Further reproduction prohibited without permission.

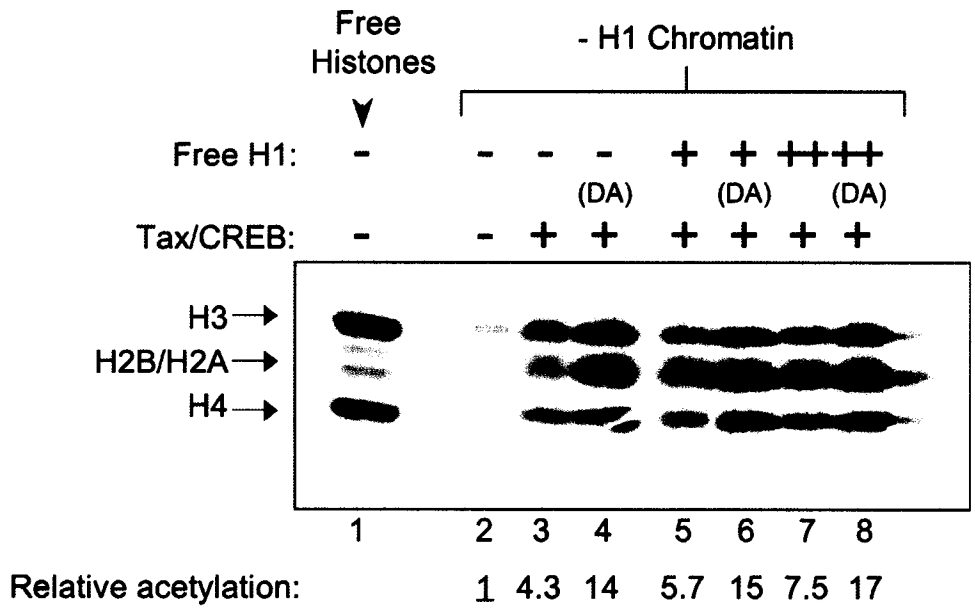

Figure 4.14. Addition of free H1 does not inhibit p300 activity. *In vitro* histone acetyltransferase activity of p300 was measured by ^{14}C-labeled AcCoA incorporation onto chromatin templates (1.26 pmol p-306/G-less DNA). Acetylation reactions were performed with recombinant p300 (8.4 pmol) in the presence (+) or absence (-) of Tax and CREB (30 pmol each) added during chromatin assembly (DA) where indicated or otherwise after assembly on chromatin templates lacking histone H1. Free (unassembled H1) was added after chromatin assembly to acetylation reactions as illustrated. H1 was added at the same amount used for H1-chromatin (+) or twice that normally used (++). Free histones were acetylated by p300 for size markers and positions of each histone are labeled on the left. Acetylation levels were calculated relative to chromatin lacking H1 in the absence of Tax and CREB (lane 2, set to 1).

Reproduced with permission of the copyright owner. Further reproduction prohibited without permission.

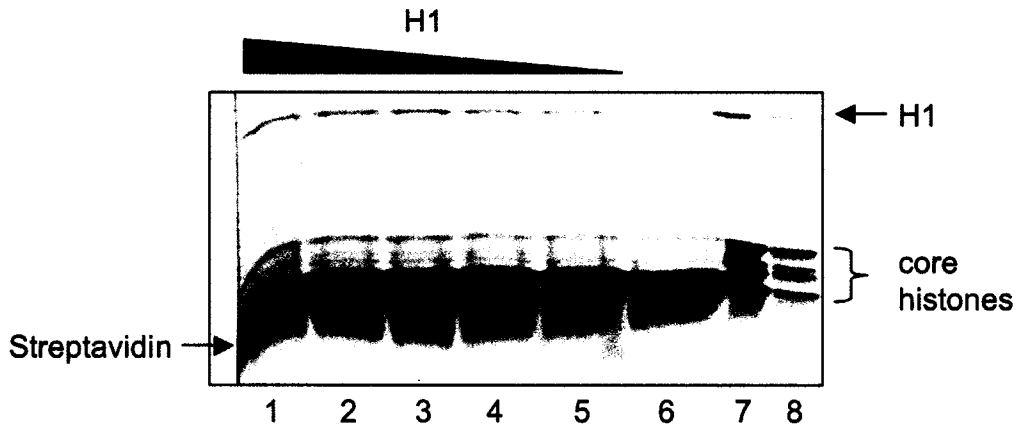

Figure 4.15. Histone H1 incorporation into chromatin assembled on an immobilized bead-bound DNA fragment. Linker histone was titrated (120, 150, 180, 210 to 240 ng) into chromatin assembled with 500 ng core histones and 700 ng bead-bound promoter DNA fragment. After assembly, the chromatin was washed and resolved on 15% SDS-PAGE and visualized using SYPRO ruby. Quantification of lanes 1-5 reveal a 1:2 stoichiometry between H1 and H3, suggesting H1 is binding to the chromatin and not non-specifically. Lanes 7 & 8 are histone markers. The streptavidin bead dissociates into monomers upon boiling and runs at 13 kilodaltons (dark black band).

Reproduced with permission of the copyright owner. Further reproduction prohibited without permission.

CHAPTER 5

FUTURE DIRECTIONS

Reproduced with permission of the copyright owner. Further reproduction prohibited without permission.

We have optimized a recombinant assembly system to properly incorporate histone H1 into a chromatin template harboring natural HTLV-1 promoter DNA. Use of this template better mimics the environment within the cell. In addition, we have discovered a new function of Tax that is only apparent in the context of chromatin containing histone H1. We observed a typical effect of H1, which was to repress transcriptional activation. Unexpectedly, we found the H1-mediated repression could be alleviated by the addition of Tax together with CREB during chromatin assembly. Furthermore, CREB, in the absence of Tax, failed to overcome the repressive effects of H1-chromatin, demonstrating the strong Tax requirement. The data presented within this dissertation reveal that transcriptional activation at the HTLV-1 promoter is tightly regulated through the opposing effects of Tax and H1 on p300 acetyltransferase activity. To better understand the ability of Tax to overcome histone H1 repression, a series of intricate experiments is needed. Here we discuss several hypotheses and suggest approaches to test them.

5.1 How Does Tax Affect p300 in Overcoming H1 Repression?

First, we propose Tax could affect p300 allosterically. Previous data suggest that AcCoA allosterically regulates an inhibitory activity of p300 that is chromatin dependent (129). Therefore, it is reasonable to hypothesize Tax could function in this manner, allowing p300 to overcome H1-mediated repression. Proving Tax affects p300 allosterically would be a definite challenge and would require examination of specific protein-protein contacts between Tax and p300.

Reproduced with permission of the copyright owner. Further reproduction prohibited without permission.

But, the real challenge with these experiments would be performing them in the context of chromatin and comparing the effects of Tax on p300 with Tax and CREB addition both during and after chromatin assembly.

Second, perhaps Tax acts to alter the tail positions of histone H1, since it is possible that linker histone tails are responsible for the inhibition of p300 enzymatic activity. This hypothesis could be tested using only the globular domain of histone H1. Incorporation of the globular domain of H1 is required for increased nucleosome repeat length and it would be interesting to see if this tailless form of H1 could repress transcription similarly to wild type. As a more conservative approach, gradual H1 tail deletions could be engineered and tested functionally.

In addition, Tax could increase the chance for core histone tail acetylation. This could be tested using tailless chromatin and histones mutated at specific lysine residues. Perhaps mass spectrometry analysis could be used to verify a change in the acetylation levels when Tax and CREB are added either after or during chromatin assembly and the chromatin template is subsequently incubated with p300. Alternatively, nucleosomes could be formed that are preacetylated with p300.

The Tax mutant M47 has been shown to interact with both CREB and p300 but is defective in transactivation. The steps in transcriptional activation M47 affects are currently unknown. Use of this mutant with our system could further define the mechanism of Tax transcriptional activation in the context of

Reproduced with permission of the copyright owner. Further reproduction prohibited without permission.

H1-chromatin. For example, does M47 function like wild-type Tax in overcoming the repressive effects of H1-containing chromatin?

Tax addition during chromatin assembly could also affect the higher order structure of chromatin. Again, tailless templates would be useful since tail deletion abolishes the ability of the core histones to form higher order structures (57). Additionally, analytical ultracentrifugation could also be employed to examine the effects on higher order chromatin structure.

5.2 Is There a Difference in the Ability of CREB to Bind Chromatin *in vitro* Versus *in vivo*?

Recent studies observe minimal CREB binding to the promoter region in cells in the absence of Tax, and CREB binding increases significantly upon Tax transfection (94). In contrast, we observe CREB binding to the vCREs assembled into chromatin in our *in vitro* experiments. Further, we do not see an increase in CREB binding with Tax addition. Given the *in vivo* evidence that CREB is not constitutively bound at CRE regions (29), we propose CREB is "actively displaced" *in vivo*. In the absence of Tax, we hypothesize that the presence of SWI/SNF at the promoter functions, in part, to keep factors from interacting with the promoter. When Tax is present, SWI/SNF leaves the promoter and CREB binding increases. Interestingly, M47 does not displace SWI/SNF but does increase CREB binding (94).

In my experiments, we lack this "active displacement" function of factors present within the cell. Therefore, we propose CREB is not inhibited from

Reproduced with permission of the copyright owner. Further reproduction prohibited without permission.

binding nucleosomal DNA in this context, explaining the lack of a Tax effect in stabilizing CREB binding. To address these quandaries a fully defined transcription system is needed with purified transcription factors. As a complimentary approach, an inducible Tax expression system would allow factor binding to be measured in discreet time intervals, providing a better picture of the order of events prior to transcriptional activation in cells.

5.3 Can We Correlate H1 Structure With Function?

We have H1 mutants readily available in the department from the Hansen laboratory. They have correlated regions of linker histone with the ability to stabilize higher order chromatin structures (101). I think it would be interesting to test these mutants functionally with our model transcription system. Are there certain regions of H1 that are involved in stabilizing higher order structures that also contribute to transcriptional repression? Of course, these mutants could also be used to test our hypothesis that H1 and Tax function allosterically in regulating p300 acetyltransferase activity.

Reproduced with permission of the copyright owner. Further reproduction prohibited without permission.

APPENDIX A

Histone Variant H2A.Bbd

This section was possible through collaboration with Yunhe Bao and Karolin Luger, which resulted in a co-author publication. The citation for the manuscript is as follows. I performed the experiments presented in Figure 8, which are shown here.

Bao, Y., Konesky, K., Park, Y-J., Rosu, S., Dyer, P.N., Rangasamy, D., Tremethick, D.J., Laybourn, P.J., & Luger, K.L. 2004. Nucleosomes containing the histone variant H2A.Bbd organize only 118 base pairs of DNA. The EMBO Journal. **23**, 3314-3324.

Reproduced with permission of the copyright owner. Further reproduction prohibited without permission.

A.1 ABSTRACT

In addition to the major core histones, histone variants contribute to the structure and function of chromatin. Using a defined recombinant assembly system, chromatin was assembled with the histone variant, H2A.Bbd. Micrococcal nuclease digestion of nucleosomal arrays assembled with H2A.Bbd protected less DNA than canonical nucleosomes. The nucleosomal repeat length decreased from ~150 base pairs to ~120 base pairs upon H2A.Bbd substitution. Additional studies revealed that the distance between the DNA ends of H2A.Bbd nucleosomes was significantly increased over wild type nucleosomes, suggesting a more relaxed structure. To determine a functional significance of this confirmation, transcription studies were performed using nucleosomal arrays containing H2A.Bbd. Using our model HTLV-1 transcription system, we found H2A.Bbd arrays to repress transcription, which could be alleviated upon addition of the transcriptional activators Tax and CREB and the coactivator p300. These findings support a model where H2A.Bbd plays a role in transcriptionally active chromatin.

A.2 INTRODUCTION

How cells manage to perform biological functions in the complex but organized nature of chromatin remains a central question in molecular biology. A method for overcoming chromatin repression is through exchange of the major core histones for histone variants. Interestingly, the H2A variant, H2A.Bbd, has been found to overlap regions of chromatin that are acetylated, giving rise to the

Reproduced with permission of the copyright owner. Further reproduction prohibited without permission.

possibility that this variant localizes to transcriptionally active areas within the genome (30). H2A.Bbd is largely excluded from the inactive X chromosome, and is therefore labeled Barr-body deficient (Bbd) (30). Interestingly, this variant is only 48% identical to the major type H2A, which suggests H2A.Bbd function may not overlap with major H2A.

To better understand H2A.Bbd both structurally and functionally Dr. Yunhe Bao and Dr. Karolin Luger collaborated with Dr. Paul Laybourn and myself. My focus in this effort involved optimizing our recombinant assembly system to incorporate the core histone variant H2A.Bbd into nucleosomal arrays. After which, we examined arrays containing the variant functionally using our model transcription system.

H2A.Bbd that was incorporated into arrays protected only ~120 base pairs of DNA, consistent with Yunhe's studies at the mononucleosome level. Additionally, nucleosomes containing H2A.Bbd repressed transcription of the natural HTLV-1 promoter, and the repression was alleviated upon addition of transcriptional activators Tax, CREB and p300. Our findings support a model where H2A.Bbd plays a role in transcriptionally active chromatin and the loose structure of H2A.Bbd nucleosomes may contribute to this function.

A.3 RESULTS & DISCUSSION

A.3a Chromatin Containing H2A.Bbd Protects Less DNA

Nucleosomal arrays were formed on a plasmid template harboring complete HTLV-1 promoter sequence (Figure 2.7) as previously described in the

Reproduced with permission of the copyright owner. Further reproduction prohibited without permission.

Materials and Methods section of Chapter 2. However, H2A.Bbd was substituted for major H2A. Micrococcal nuclease digestion of templates assembled with the variant histone produced nucleosomal repeat lengths of only ~120 base pairs, significantly shorter than the typical repeat lengths of ~150 base pairs we observed using major histones (Figure A.1). These results strongly supported Yunhe's findings at the mononucleosome level, which demonstrated only 118 base pairs of DNA were associated with H2A.Bbd nucleosomes. Additionally, he found the DNA ends were farther apart than with wild-type mononucleosomes, suggesting a looser confirmation, which could explain the decreased nucleosomal repeat length.

A.3b H2A.Bbd Nucleosomal Arrays Repress Transcription of a Natural Promoter

Previous data demonstrated H2A.Bbd localized to regions of transcriptionally active chromatin (30). Therefore, we tested nucleosomal arrays containing H2A.Bbd in transcriptional activation of the HTLV-1 promoter. While these arrays repressed transcriptional activation, they were not as effective as wild-type arrays in repressing basal transcription (Figure A.2). Additionally, the templates assembled with H2A.Bbd were less responsive to addition of the transcription factors Tax and CREB and coactivator p300, supporting a model in which H2A.Bbd functions in actively transcribed regions.

Reproduced with permission of the copyright owner. Further reproduction prohibited without permission.

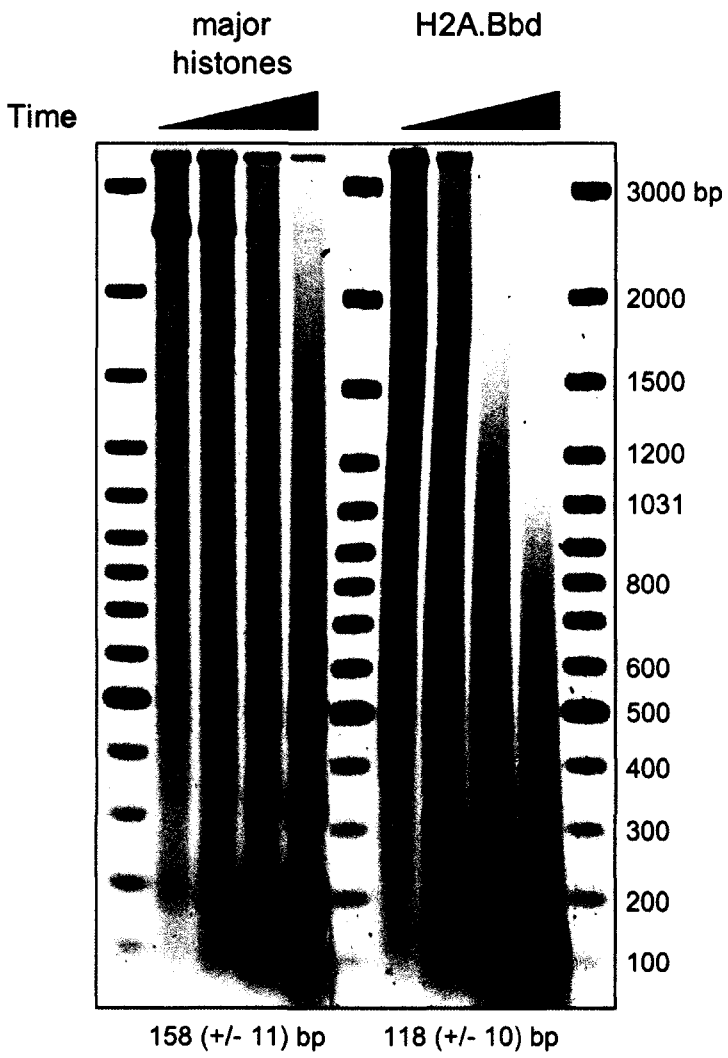

Figure A.1. Nucleosomes containing H2A.Bbd have a shorter repeat length than major type nucleosomes. Chromatin was assembled using native *Drosophila* (major histones) or recombinant mouse histones with H2A.Bbd as indicated and digested with MNase. Calculation of each nucleosome repeat length, based on the migration of DNA size markers, confirmed the much shorter repeat length of H2A.Bbd containing nucleosomes at ~120 base pairs.

Reproduced with permission of the copyright owner. Further reproduction prohibited without permission.

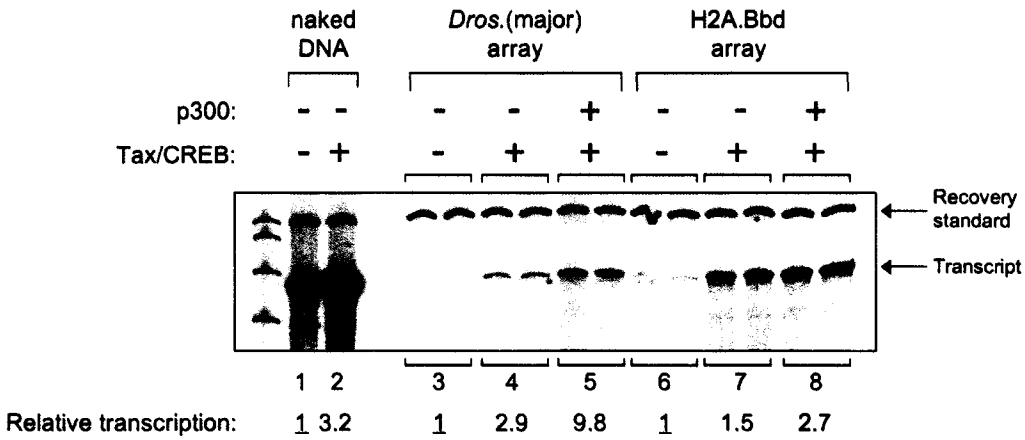

Figure A.2. Templates assembled with H2A.Bbd are less repressive. Chromatin was assembled and transcribed as previously described. Tax, CREB, and p300 were added as indicated. Transcript levels are relative to basal for each template, which is set to one. Duplicate lanes were averaged.

Reproduced with permission of the copyright owner. Further reproduction prohibited without permission.

APPENDIX B

Mass Spectrometry Analysis of *Drosophila* Histones

Reproduced with permission of the copyright owner. Further reproduction prohibited without permission.

Upon formation of chromatin containing H1, we initiated a collaboration with Natalie Ahn at the University of Colorado in Boulder. The purpose of this collaboration was to examine whether incorporation of H1 resulted in preferential selection of core histone variants using mass spectrometry. Mass spectrometry analysis revealed that the core histone variants present in *Drosophila* that were assembled into chromatin were insignificantly represented compared to the major types, as no peaks were observed that corresponded to any variants. However, we did learn that a portion of the H3 within our core histones was methylated, which generally corresponds with a repressive modification. No other modifications were present in quantities such that they could be detected. Because there is no data to show for this project, this section is only being briefly mentioned. Perhaps the most important aspect of this collaboration was optimizing the extraction of the histones, including histone H1 from our recombinant assembled chromatin before performing mass spectrometry. These protocols have been outlined in Chapter 2, section 2.3e.

We also performed mass spectrometry analysis on our purified, native *Drosophila* histone H1 using the MRF facilities here at CSU. While *Drosophila* contain only one H1 isoform, we determined some of the protein is phosphorylated. Additionally, we confirmed by mass spectrometry that H1 could be treated with λ-phosphatase to remove the phosphate groups. Interestingly, we found no difference in our functional assays between the phosphatased or untreated forms of H1, suggesting an equilibrium is reached in transcription studies between the actions of kinases and phosphatases. Again, the most

Reproduced with permission of the copyright owner. Further reproduction prohibited without permission.

important aspect of these experiments was determining a method for precipitating H1 that was compatible with mass spectrometry, which is explained in great detail in Chapter 2, section 2.3f.

Reproduced with permission of the copyright owner. Further reproduction prohibited without permission.

REFERENCES

1. **Adya, N., and C. Z. Giam.** 1995. Distinct regions in human T-cell lymphotropic virus type I tax mediate interactions with activator protein CREB and basal transcription factors. J. Virol. **69:**1834-1841.

2. **Adya, N., L. J. Zhao, W. Huang, I. Boros, and C. Z. Giam.** 1994. Expansion of CREB's DNA recognition specificity by Tax results from interaction with Ala-Ala-Arg at positions 282-284 near the conserved DNA-binding domain of CREB. Proc. Natl. Acad. Sci. USA **91:**5642-5646.

3. **Ahmad, K., and S. Henikoff.** 2002. The histone variant H3.3 marks active chromatin by replication-independent nucleosome assembly. Mol Cell **9:**1191-200.

4. **Allan, J., P. G. Hartman, C. Crane-Robinson, and F. X. Aviles.** 1980. The structure of histone H1 and its location in chromatin. Nature **288:**675-9.

5. **Allan, J., T. Mitchell, N. Harborne, L. Bohm, and C. Crane-Robinson.** 1986. Roles of H1 domains in determining higher order chromatin structure and H1 location. J Mol Biol **187:**591-601.

6. **Anderson, M. G., and W. S. Dynan.** 1994. Quantitative studies of the effect of HTLV-I Tax protein on CREB-proteins-DNA binding. Nucleic Acids Res. **22:**3194-3201.

7. **Anderson, M. G., K. E. Scoggin, C. M. Simbulan-Rosenthal, and J. A. Steadman.** 2000. Identification of Poly(ADP-ribose) polymerase as a transcriptional coactivator of the human T-cell leukemia virus type 1 tax protein. J. Virol. **74:**2169-2177.

8. **Angelov, D., A. Molla, P. Y. Perche, F. Hans, J. Cote, S. Khochbin, P. Bouvet, and S. Dimitrov.** 2003. The histone variant macroH2A interferes with transcription factor binding and SWI/SNF nucleosome remodeling. Mol Cell **11:**1033-41.

Reproduced with permission of the copyright owner. Further reproduction prohibited without permission.

9. **Angelov, D., A. Verdel, W. An, V. Bondarenko, F. Hans, C. M. Doyen, V. M. Studitsky, A. Hamiche, R. G. Roeder, P. Bouvet, and S. Dimitrov.** 2004. SWI/SNF remodeling and p300-dependent transcription of histone variant H2ABbd nucleosomal arrays. Embo J **23:**3815-24.

10. **Arias, J., A. S. Alberts, P. Brindle, F. X. Claret, T. Smeal, M. Karin, J. Feramisco, and M. Montminy.** 1994. Activation of cAMP and mitogen responsive genes relies on a common nuclear factor. Nature **370:**226-9.

11. **Asquith, B., E. Hanon, G. P. Taylor, and C. R. Bangham.** 2000. Is human T-cell lymphotropic virus type I really silent? Philos Trans R Soc Lond B Biol Sci **355:**1013-9.

12. **Astier-Gin, T., J. P. Portail, D. Londos-Gagliardi, D. Moynet, S. Blanchard, R. Dalibart, J. F. Pouliquen, M. C. Georges-Courbot, C. Hajjar, S. Sainte-Foie, and B. Guillemain.** 1997. Neutralizing activity and antibody reactivity toward immunogenic regions of the human T cell leukemia virus type I surface glycoprotein in sera of infected patients with different clinical states. J Infect Dis **175:**716-9.

13. **Bangham, C. R.** 2003. Human T-lymphotropic virus type 1 (HTLV-1): persistence and immune control. Int J Hematol **78:**297-303.

14. **Bao, Y., K. Konesky, Y. J. Park, S. Rosu, P. N. Dyer, D. Rangasamy, D. J. Tremethick, P. J. Laybourn, and K. Luger.** 2004. Nucleosomes containing the histone variant H2A.Bbd organize only 118 base pairs of DNA. Embo J **23:**3314-24.

15. **Baranger, A. M., C. R. Palmer, M. K. Hamm, H. A. Giebler, A. Brauweiler, J. K. Nyborg, and A. Schepartz.** 1995. Mechanism of DNA binding enhancement by the HTLV-I transactivator Tax. Nature **376:**606-608.

16. **Bates, D. L., and J. O. Thomas.** 1981. Histones H1 and H5: one or two molecules per nucleosome? Nucleic Acids Res **9:**5883-94.

17. **Bex, F., and R. B. Gaynor.** 1998. Regulation of gene expression by HTLV-I Tax protein. Methods **16:**83-94.

18. **Bex, F., M. J. Yin, A. Burny, and R. B. Gaynor.** 1998. Differential transcriptional activation by human T-cell leukemia virus type 1 Tax mutants is mediated by distinct interactions with CREB binding protein and p300. Mol. Cell. Biol. **18:**2392-2405.

Reproduced with permission of the copyright owner. Further reproduction prohibited without permission.

19. **Bhattacharjee, R. N., G. C. Banks, K. W. Trotter, H. L. Lee, and T. K. Archer.** 2001. Histone H1 phosphorylation by Cdk2 selectively modulates mouse mammary tumor virus transcription through chromatin remodeling. Mol Cell Biol **21:**5417-25.

20. **Bradbury, E. M., R. J. Inglis, and H. R. Matthews.** 1974. Control of cell division by very lysine rich histone (F1) phosphorylation. Nature **247:**257-61.

21. **Brady, J., K. T. Jeang, J. Duvall, and G. Khoury.** 1987. Identification of p40x-responsive regulatory sequences within the human T-cell leukemia virus type I long terminal repeat. J Virol **61:**2175-81.

22. **Brauweiler, A., P. Garl, A. A. Franklin, H. A. Giebler, and J. K. Nyborg.** 1995. A molecular mechanism for HTLV-I latency and Tax transactivation. J. Biol. Chem. **270:**12814-12822.

23. **Bulger, M., and J. T. Kadonaga.** 1994. Biochemical reconstitution of chromatin with physiological nucleosome spacing. Methods in Molecular Genetics (ed.) K.W. Adolph **5:**241-262. Academic Press. San Diego.

24. **Bustin, M., F. Catez, and J. H. Lim.** 2005. The dynamics of histone H1 function in chromatin. Mol Cell **17:**617-20.

25. **Cameron, I. L., W. A. Pavlat, and J. R. Jeter, Jr.** 1979. Chromatin substructure: an electron microscopic study of thin-sectioned chromatin subjected to sequential protein extraction and water swelling procedures. Anat Rec **194:**547-62.

26. **Caron, C., G. Mengus, V. Dubrowskaya, A. Roisin, I. Davidson, and P. Jalinot.** 1997. Human TAF(II)28 interacts with the human T cell leukemia virus type I Tax transactivator and promotes its transcriptional activity. Proc Natl Acad Sci U S A **94:**3662-3667.

27. **Carruthers, L. M., J. Bednar, C. L. Woodcock, and J. C. Hansen.** 1998. Linker histones stabilize the intrinsic salt-dependent folding of nucleosomal arrays: mechanistic ramifications for higher-order chromatin folding. Biochemistry **37:**14776-87.

28. **Catez, F., D. T. Brown, T. Misteli, and M. Bustin.** 2002. Competition between histone H1 and HMGN proteins for chromatin binding sites. EMBO Rep **3:**760-6.

Reproduced with permission of the copyright owner. Further reproduction prohibited without permission.

29. **Cha-Molstad, H., D. M. Keller, G. S. Yochum, S. Impey, and R. H. Goodman.** 2004. Cell-type-specific binding of the transcription factor CREB to the cAMP-response element. Proc Natl Acad Sci U S A **101:**13572-7.

30. **Chadwick, B. P., and H. F. Willard.** 2001. A novel chromatin protein, distantly related to histone H2A, is largely excluded from the inactive X chromosome. J Cell Biol **152:**375-84.

31. **Chan, H. M., and N. B. La Thangue.** 2001. p300/CBP proteins: HATs for transcriptional bridges and scaffolds. J. Cell. Sci. **114:**2363-2373.

32. **Cheung, E., A. S. Zarifyan, and W. L. Kraus.** 2002. Histone H1 represses estrogen receptor alpha transcriptional activity by selectively inhibiting receptor-mediated transcription initiation. Mol Cell Biol **22:**2463-71.

33. **Clark, K. L., E. D. Halay, E. Lai, and S. K. Burley.** 1993. Co-crystal structure of the HNF-3/fork head DNA-recognition motif resembles histone H5. Nature **364:**412-20.

34. **Clemens, K. E., G. Piras, M. F. Radonovich, K. S. Choi, J. F. Duvall, J. DeJong, R. Roeder, and J. N. Brady.** 1996. Interaction of the human T-cell lymphotropic virus type 1 tax transactivator with transcription factor IIA. Mol. Cell. Biol. **16:**4656-4664.

35. **Contreras, A., T. K. Hale, D. L. Stenoien, J. M. Rosen, M. A. Mancini, and R. E. Herrera.** 2003. The dynamic mobility of histone H1 is regulated by cyclin/CDK phosphorylation. Mol Cell Biol **23:**8626-36.

36. **Croston, G. E., L. A. Kerrigan, L. M. Lira, D. R. Marshak, and J. T. Kadonaga.** 1991. Sequence-specific antirepression of histone H1-mediated inhibition of basal RNA polymerase II transcription. Science **251:**643-9.

37. **Dusserre, Y., and N. Mermod.** 1992. Purified cofactors and histone H1 mediate transcriptional regulation by CTF/NF-I. Mol Cell Biol **12:**5228-37.

38. **Dynan, W. S.** 1987. DNase I footprinting as an assay for mammalian gene regulatory proteins. Genet. Eng. **9:**75-87.

Reproduced with permission of the copyright owner. Further reproduction prohibited without permission.

39. **Edlich, R. F., J. A. Arnette, and F. M. Williams.** 2000. Global epidemic of human T-cell lymphotropic virus type-I (HTLV-I). J Emerg Med **18:**109-19.

40. **Fan, Y., T. Nikitina, E. M. Morin-Kensicki, J. Zhao, T. R. Magnuson, C. L. Woodcock, and A. I. Skoultchi.** 2003. H1 linker histones are essential for mouse development and affect nucleosome spacing in vivo. Mol Cell Biol **23:**4559-72.

41. **Fan, Y., T. Nikitina, J. Zhao, T. J. Fleury, R. Bhattacharyya, E. E. Bouhassira, A. Stein, C. L. Woodcock, and A. I. Skoultchi.** 2005. Histone H1 depletion in mammals alters global chromatin structure but causes specific changes in gene regulation. Cell **123:**1199-212.

42. **Felber, B. K., H. Paskalis, C. Kleinman-Ewing, F. Wong-Staal, and G. N. Pavlakis.** 1985. The pX protein of HTLV-I is a transcriptional activator of its long terminal repeats. Science **229:**675-679.

43. **Franklin, A. A., and J. K. Nyborg.** 1995. Mechanisms of Tax regulation of Human T-Cell Leukemia Virus Type I gene expression. J. Biomed Sci. **2:**17-29.

44. **Franklin, A. A., M. F. Kubik, M. N. Uittenbogaard, A. Brauweiler, P. Utaisincharoen, M. A. Matthews, W. S. Dynan, J. P. Hoeffler, and J. K. Nyborg.** 1993. Transactivation by the human T-cell leukemia virus Tax protein is mediated through enhanced binding of activating transcription factor-2 (ATF-2) ATF-2 response and cAMP element-binding protein (CREB). J. Biol. Chem. **268:**21225-21231.

45. **Fyodorov, D. V., and J. T. Kadonaga.** 2003. Chromatin assembly in vitro with purified recombinant ACF and NAP-1. Methods Enzymol **371:**499-515.

46. **Georges, S. A., H. A. Giebler, P. A. Cole, K. Luger, P. J. Laybourn, and J. K. Nyborg.** 2003. Tax Recruitment of CBP/p300, via the KIX Domain, Reveals a Potent Requirement for Acetyltransferase Activity that is Chromatin-Dependent and Histone Tail-Independent. Mol. Cell. Biol., **23:**3392-3404.

47. **Georges, S. A., W. L. Kraus, K. Luger, J. K. Nyborg, and P. J. Laybourn.** 2002. p300-mediated Tax transactivation from recombinant chromatin: histone tail deletion mimics coactivator function. Mol Cell Biol **22:**127-37.

Reproduced with permission of the copyright owner. Further reproduction prohibited without permission.

48. **Gessain, A., F. Barin, J. C. Vernant, O. Gout, L. Maurs, A. Calender, and G. de The.** 1985. Antibodies to human T-lymphotropic virus type I in patients with tropical spastic paraparesis. Lancet **ii:**407-410.

49. **Gessain, A., A. Louie, O. Gout, R. C. Gallo, and G. Franchini.** 1991. Human T-cell leukemia/lymphoma virus type I (HTLV-I) expression in fresh of peripheral blood mono-nuclear cells from patients with tropical spastic paraparesis/HTLV-1-associated myelopathy. J. Virol. **65:**1628-1633.

50. **Giebler, H. A., J. E. Loring, K. Van Orden, M. A. Colgin, J. E. Garrus, K. W. Escudero, A. Brauweiler, and J. K. Nyborg.** 1997. Anchoring of CREB binding protein to the human T-cell leukemia virus type 1 promoter: a molecular mechanism of Tax transactivation. Mol. Cell. Biol. **17:**5156-5164.

51. **Goodman, R. H., and S. Smolik.** 2000. CBP/p300 in cell growth, transformation, and development. Genes Dev. **14:**1553-1577.

52. **Goren, I., O. J. Semmes, K. T. Jeang, and K. Moelling.** 1995. The amino terminus of Tax is required for interaction with the cyclic AMP response element binding protein. J. Virol. **69:**5806-5811.

53. **Grassmann, R., S. Berchtold, I. Radant, M. Alt, B. Fleckenstein, J. G. Sodroski, W. A. Haseltine, and U. Ramstedt.** 1992. Role of human T-cell leukemia virus type 1 X region proteins in immortalization of primary human lymphocytes in culture. J Virol **66:**4570-5.

54. **Grassmann, R., C. Dengler, I. Muller-Fleckenstein, B. Fleckenstein, K. McGuire, M. C. Dokhelar, J. G. Sodroski, and W. A. Haseltine.** 1989. Transformation to continuous growth of primary human T lymphocytes by human T-cell leukemia virus type I X-region genes transduced by a Herpesvirus saimiri vector. Proc Natl Acad Sci U S A **86:**3351-5.

55. **Graziano, V., S. E. Gerchman, A. J. Wonacott, R. M. Sweet, J. R. Wells, S. W. White, and V. Ramakrishnan.** 1990. Crystallization of the globular domain of histone H5. J Mol Biol **212:**253-7.

56. **Hanchard, B., W. N. Gibbs, W. Lofters, M. Campbell, E. Williams, N. Williams, E. Jaffe, B. Cranston, L. D. Panchoosingh, L. LaGrenade, R. J. Wilks, E. Murphy, W. A. Blattner, and A. Manns.** 1990. Human Retrovirology: HTLV-1. Blattner, W.A. (ed). Raven Press: New York, pp. 173-183.

Reproduced with permission of the copyright owner. Further reproduction prohibited without permission.

57. **Hansen, J. C.** 2002. Conformational dynamics of the chromatin fiber in solution: Determinants, mechanisms, and functions. Annu. Rev. Biophys. Biomol. Struct. **31**:361-392.

58. **Hansen, J. C., C. Tse, and A. P. Wolffe.** 1998. Structure and function of the core histone N-termini: more than meets the eye. Biochemistry **37**:17637-17641.

59. **Hansen, J. C., and A. P. Wolffe.** 1994. A role for histones H2A/H2B in chromatin folding and transcriptional repression. Proc. Natl. Acad. Sci. USA **91**:2339-2343.

60. **Hansen, J. C., and A. P. Wolffe.** 1992. Influence of chromatin folding on transcription initiation and elongation by RNA polymerase III. Biochemistry **31**:7977-7988.

61. **Harrod, R., Y. Tang, C. Nicot, H. S. Lu, A. Vassilev, Y. Nakatani, and C. Z. Giam.** 1998. An exposed KID-like domain in human T-cell lymphotropic virus type 1 Tax is responsible for the recruitment of coactivators CBP/p300. Mol. Cell. Biol. **18**:5052-5061.

62. **Hartman, P. G., G. E. Chapman, T. Moss, and E. M. Bradbury.** 1977. Studies on the role and mode of operation of the very-lysine-rich histone H1 in eukaryote chromatin. The three structural regions of the histone H1 molecule. Eur J Biochem **77**:45-51.

63. **Herrera, J. E., K. L. West, R. L. Schiltz, Y. Nakatani, and M. Bustin.** 2000. Histone H1 is a specific repressor of core histone acetylation in chromatin. Mol Cell Biol **20**:523-9.

64. **Hidaka, M., J. Inoue, M. Yoshida, and M. Seiki.** 1988. Post-transcriptional regulator (rex) of HTLV-1 initiates expression of viral structural proteins but suppresses expression of regulatory proteins. Embo J **7**:519-23.

65. **Hill, D. A., and A. N. Imbalzano.** 2000. Human SWI/SNF nucleosome remodeling activity is partially inhibited by linker histone H1. Biochemistry **39**:11649-56.

66. **Hino, S., S. Katamine, K. Kawase, T. Miyamoto, H. Doi, Y. Tsuji, and T. Yamabe.** 1994. Intervention of maternal transmission of HTLV-1 in Nagasaki, Japan. Leukemia **8 Suppl 1**:S68-70.

Reproduced with permission of the copyright owner. Further reproduction prohibited without permission.

67. **Hinuma, Y., K. Nagata, M. Hanaoka, M. Nakai, T. Matsumoto, K. I. Kinoshita, S. Shirakawa, and I. Miyoshi.** 1981. Adult T-cell leukemia: antigen in an ATL cell line and detection of antibodies to the antigen in human sera. Proc Natl Acad Sci U S A **78:**6476-80.

68. **Hoeffler, J. P., J. W. Lustbader and C.-Y. Chen.** 1991. Identification of multiple nuclear factors that inter-act with Cyclic Adenosine 3',5'-Monophosphate Response Element-Binding Protein and Activating Transcription Factor-2 by protein-protein interactions. Mol. Endocrin **5:**256-266.

69. **Horn, P. J., L. M. Carruthers, C. Logie, D. A. Hill, M. J. Solomon, P. A. Wade, A. N. Imbalzano, J. C. Hansen, and C. L. Peterson.** 2002. Phosphorylation of linker histones regulates ATP-dependent chromatin remodeling enzymes. Nat Struct Biol **9:**263-7.

70. **Horn, P. J., and C. L. Peterson.** 2002. Chromatin Higher Order Folding: Wrapping up Transcription. Science **297:**1824-1827.

71. **Igakura, T., J. C. Stinchcombe, P. K. Goon, G. P. Taylor, J. N. Weber, G. M. Griffiths, Y. Tanaka, M. Osame, and C. R. Bangham.** 2003. Spread of HTLV-I between lymphocytes by virus-induced polarization of the cytoskeleton. Science **299:**1713-6.

72. **Ito, T., M. Bulger, R. Kobayashi, and J. T. Kadonaga.** 1996. Drosophila NAP-1 is a core histone chaperone that functions in ATP-facilitated assembly of regularly spaced nucleosomal arrays. Mol Cell Biol **16:**3112-24.

73. **Ito, T., M. Bulger, M. J. Pazin, R. Kobayashi, and J. T. Kadonaga.** 1997. ACF, an ISWI-containing and ATP-utilizing chromatin assembly and remodeling factor. Cell **90:**145-55.

74. **Ito, T., M. E. Levenstein, D. V. Fyodorov, A. K. Kutach, R. Kobayashi, and J. T. Kadonaga.** 1999. ACF consists of two subunits, Acf1 and ISWI, that function cooperatively in the ATP-dependent catalysis of chromatin assembly. Genes Dev **13:**1529-39.

75. **Iwasaki, Y.** 1993. Human T cell leukemia virus type I infection and chronic myelopathy. Brain Pathol **3:**1-10.

76. **Jarvis, D. L., and A. Garcia, Jr.** 1994. Long-term stability of baculoviruses stored under various conditions. Biotechniques **16:**508-13.

Reproduced with permission of the copyright owner. Further reproduction prohibited without permission.

77. **Jeang, K. T., I. Boros, J. Brady, M. Radonovich, and G. Khoury.** 1988. Characterization of cellular factors that interact with the human T-cell leukemia virus type I $p40^{x}$-responsive 21-base-pair sequence. J. Virol. **62:**4499-4509.

78. **Juan, L. J., R. T. Utley, C. C. Adams, M. Vettese-Dadey, and J. L. Workman.** 1994. Differential repression of transcription factor binding by histone H1 is regulated by the core histone amino termini. Embo J **13:**6031-40.

79. **Juan, L. J., R. T. Utley, M. Vignali, L. Bohm, and J. L. Workman.** 1997. H1-mediated repression of transcription factor binding to a stably positioned nucleosome. J Biol Chem **272:**3635-40.

80. **Kalkhoven, E.** 2004. CBP and p300: HATs for different occasions. Biochem Pharmacol **68:**1145-55.

81. **Kashanchi, F., J. F. Duvall, R. P. Kwok, J. R. Lundblad, R. H. Goodman, and J. N. Brady.** 1998. The coactivator CBP stimulates human T-cell lymphotrophic virus type I Tax transactivation in vitro. J. Biol. Chem. **273:**34646-34652.

82. **Kimzey, A. L., and W. S. Dynan.** 1998. Specific regions of contact between human T-cell leukemia virus type I Tax protein and DNA identified by photocross-linking. J. Biol. Chem. **273:**13768-13775.

83. **Koop, R., L. Di Croce, and M. Beato.** 2003. Histone H1 enhances synergistic activation of the MMTV promoter in chromatin. Embo J **22:**588-99.

84. **Kraus, W. L., and J. T. Kadonaga.** 1998. p300 and estrogen receptor cooperatively activate transcription via differential enhancement of initiation and reinitiation. Genes Dev **12:**331-42.

85. **Kuzmichev, A., T. Jenuwein, P. Tempst, and D. Reinberg.** 2004. Different EZH2-containing complexes target methylation of histone H1 or nucleosomal histone H3. Mol Cell **14:**183-93.

86. **Kwok, R. P., M. E. Laurance, J. R. Lundblad, P. S. Goldman, H. Shih, L. M. Connor, S. J. Marriott, and R. H. Goodman.** 1996. Control of cAMP-regulated enhancers by the viral transactivator Tax through CREB and the co-activator CBP. Nature **380:**642-6.

Reproduced with permission of the copyright owner. Further reproduction prohibited without permission.

87. **Kwok, R. P., J. R. Lundblad, J. C. Chrivia, J. P. Richards, H. P. Bachinger, R. G. Brennan, S. G. Roberts, M. R. Green, and R. H. Goodman.** 1994. Nuclear protein CBP is a coactivator for the transcription factor CREB. Nature **370:**223-226.

88. **Laurance, M. E., R. P. Kwok, M. S. Huang, J. P. Richards, J. R. Lundblad, and R. H. Goodman.** 1997. Differential activation of viral and cellular promoters by human T-cell lymphotropic virus-1 Tax and cAMP-responsive element modulator isoforms. J. Biol. Chem. **272:**2646-2651.

89. **Laybourn, P. J., and J. T. Kadonaga.** 1991. Role of nucleosomal cores and histone H1 in regulation of transcription by RNA polymerase II. Science **254:**238-45.

90. **Leclercq, I., F. Mortreux, M. Cavrois, A. Leroy, A. Gessain, S. Wain-Hobson, and E. Wattel.** 2000. Host sequences flanking the human T-cell leukemia virus type 1 provirus in vivo. J Virol **74:**2305-2312.

91. **Lee, H., R. Habas, and C. Abate-Shen.** 2004. MSX1 cooperates with histone H1b for inhibition of transcription and myogenesis. Science **304:**1675-8.

92. **Lee, H. L., and T. K. Archer.** 1998. Prolonged glucocorticoid exposure dephosphorylates histone H1 and inactivates the MMTV promoter. Embo J **17:**1454-66.

93. **Lemasson, I., and J. K. Nyborg.** 2001. Human T-cell leukemia virus type I Tax repression of p73beta is mediated through competition for the C/H1 domain of CBP. J. Biol. Chem. **276:**15720-15727.

94. **Lemasson, I., N. J. Polakowski, P. J. Laybourn, and J. K. Nyborg.** 2006. Tax-dependent displacement of nucleosomes during transcriptional activation of human T-cell leukemia virus, type 1. J Biol Chem **in press**.

95. **Lemasson, I., N. J. Polakowski, P. J. Laybourn, and J. K. Nyborg.** 2002. Transcription factor binding and histone modifications on the integrated proviral promoter in human T-cell leukemia virus-I-infected T-cells. J Biol Chem **277:**49459-65.

96. **Lemasson, I., N. J. Polakowski, P. J. Laybourn, and J. K. Nyborg.** 2004. Transcription regulatory complexes bind the human T-cell leukemia virus 5' and 3' long terminal repeats to control gene expression. Mol Cell Biol **24:**6117-26.

Reproduced with permission of the copyright owner. Further reproduction prohibited without permission.

97. **Lenzmeier, B. A., H. A. Giebler, and J. K. Nyborg.** 1998. Human T-cell leukemia virus type 1 Tax requires direct access to DNA for recruitment of CREB binding protein to the viral promoter. Mol Cell Biol **18:**721-31.

98. **Lever, M. A., J. P. Th'ng, X. Sun, and M. J. Hendzel.** 2000. Rapid exchange of histone H1.1 on chromatin in living human cells. Nature **408:**873-6.

99. **Lu, H., C. A. Pise-Masison, T. M. Fletcher, R. L. Schiltz, A. K. Nagaich, M. Radonovich, G. Hager, P. A. Cole, and J. N. Brady.** 2002. Acetylation of nucleosomal histones by p300 facilitates transcription from tax-responsive human T-cell leukemia virus type 1 chromatin template. Mol Cell Biol **22:**4450-62.

100. **Lu, H., C. A. Pise-Masison, R. Linton, H. U. Park, R. L. Schiltz, V. Sartorelli, and J. N. Brady.** 2004. Tax relieves transcriptional repression by promoting histone deacetylase 1 release from the human T-cell leukemia virus type 1 long terminal repeat. J Virol **78:**6735-43.

101. **Lu, X., and J. C. Hansen.** 2004. Identification of specific functional subdomains within the linker histone H10 C-terminal domain. J Biol Chem **279:**8701-7.

102. **Luger, K., A. W. Mader, R. K. Richmond, D. F. Sargent, and T. J. Richmond.** 1997. Crystal structure of the nucleosome core particle at 2.8 A resolution [see comments]. Nature **389:**251-60.

103. **Lundblad, J. R., R. P. Kwok, M. E. Laurance, M. S. Huang, J. P. Richards, R. G. Brennan, and R. H. Goodman.** 1998. The human T-cell leukemia virus-1 transcriptional activator Tax enhances cAMP-responsive element-binding protein (CREB) binding activity through interactions with the DNA minor groove. J. Biol. Chem. **273:**19251-19259.

104. **Manns, A., W. J. Miley, R. J. Wilks, O. S. Morgan, B. Hanchard, G. Wharfe, B. Cranston, E. Maloney, S. L. Welles, W. A. Blattner, and D. Waters.** 1999. Quantitative proviral DNA and antibody levels in the natural history of HTLV-I infection. J Infect Dis **180:**1487-93.

105. **Marsden, I., Y. Chen, C. Jin, and X. Liao.** 1997. Evidence that the DNA binding specificity of winged helix proteins is mediated by a structural change in the amino acid sequence adjacent to the principal DNA binding helix. Biochemistry **36:**13248-55.

Reproduced with permission of the copyright owner. Further reproduction prohibited without permission.

106. **McBryant, S. J., Y. J. Park, S. M. Abernathy, P. J. Laybourn, J. K. Nyborg, and K. Luger.** 2003. Preferential binding of the histone (H3-H4)2 tetramer by NAP1 is mediated by the amino-terminal histone tails. J Biol Chem **278:**44574-83.

107. **Misteli, T., A. Gunjan, R. Hock, M. Bustin, and D. T. Brown.** 2000. Dynamic binding of histone H1 to chromatin in living cells. Nature **408:**877-81.

108. **Montminy, M. R., and L. M. Bilezikjian.** 1987. Binding of a nuclear protein to the cyclic-AMP response element of the somatostatin gene. Nature **328:**175-8.

109. **Moritoyo, T., S. Izumo, H. Moritoyo, Y. Tanaka, Y. Kiyomatsu, M. Nagai, K. Usuku, M. Sorimachi, and M. Osame.** 1999. Detection of human T-lymphotropic virus type I p40tax protein in cerebrospinal fluid cells from patients with human T-lymphotropic virus type I-associated myelopathy/tropical spastic paraparesis. J Neurovirol **5:**241-8.

110. **Myers, F. A., D. R. Evans, A. L. Clayton, A. W. Thorne, and C. Crane-Robinson.** 2001. Targeted and extended acetylation of histones H4 and H3 at active and inactive genes in chicken embryo erythrocytes. J Biol Chem **276:**20197-20205.

111. **O'Reilly, D. R., L. K. Miller, and V. A. Luckow.** 1994. Baculovirus Expression Vectors: A Laboratory Manual. Oxford University Press, Inc., New York.

112. **Ogryzko, V. V., R. L. Schiltz, V. Russanova, B. H. Howard, and Y. Nakatani.** 1996. The transcriptional coactivators p300 and CBP are histone acetyltransferases. Cell **87:**953-9.

113. **Ohshima, K., A. Ohgami, M. Matsuoka, K. Etoh, A. Utsunomiya, T. Makino, M. Ishiguro, J. Suzumiya, and M. Kikuchi.** 1998. Random integration of HTLV-1 provirus: increasing chromosomal instability. Cancer Lett **132:**203-12.

114. **Okochi, K., H. Sato, and Y. Hinuma.** 1984. A retrospective study on transmission of adult T cell leukemia virus by blood transfusion: seroconversion in recipients. Vox Sang **46:**245-53.

Reproduced with permission of the copyright owner. Further reproduction prohibited without permission.

115. **Orland, J. R., J. Engstrom, J. Fridey, R. A. Sacher, J. W. Smith, C. Nass, G. Garratty, B. Newman, D. Smith, B. Wang, K. Loughlin, and E. L. Murphy.** 2003. Prevalence and clinical features of HTLV neurologic disease in the HTLV Outcomes Study. Neurology **61:**1588-94.

116. **Osame, M., K. Usuku, S. Izumo, N. Ijichi, H. Amitani, A. Igata, M. Matsumoto, and M. Tara.** 1986. HTLV-1 associated myelopathy: a new clinical entity. Lancet **1:**1031-1032.

117. **Paca-Uccaralertkun, S., L.-J. Zhao, N. Adya, J. V. Cross, B. R. Cullen, I. Boros, and C.-Z. Giam.** 1994. In vitro selection of DNA elements highly responsive to the Human T-Cell Lymphotropic Virus Type I transcriptional activator, Tax. Mol. Cell. Biol. **14:**456-462.

118. **Park, Y. J., J. V. Chodaparambil, Y. Bao, S. J. McBryant, and K. Luger.** 2005. Nucleosome assembly protein 1 exchanges histone H2A-H2B dimers and assists nucleosome sliding. J Biol Chem **280:**1817-25.

119. **Parseghian, M. H., and B. A. Hamkalo.** 2001. A compendium of the histone H1 family of somatic subtypes: an elusive cast of characters and their characteristics. Biochem Cell Biol **79:**289-304.

120. **Parseghian, M. H., A. H. Henschen, K. G. Krieglstein, and B. A. Hamkalo.** 1994. A proposal for a coherent mammalian histone H1 nomenclature correlated with amino acid sequences. Protein Sci **3:**575-87.

121. **Parseghian, M. H., R. L. Newcomb, S. T. Winokur, and B. A. Hamkalo.** 2000. The distribution of somatic H1 subtypes is non-random on active vs. inactive chromatin: distribution in human fetal fibroblasts. Chromosome Res **8:**405-24.

122. **Patterton, H. G., C. C. Landel, D. Landsman, C. L. Peterson, and R. T. Simpson.** 1998. The biochemical and phenotypic characterization of Hho1p, the putative linker histone H1 of Saccharomyces cerevisiae. J Biol Chem **273:**7268-76.

123. **Pazin, M. J., and J. T. Kadonaga.** "Transcriptional and structural analysis of chromatin assembled in vitro", in Gould, H. (Ed.), Chromatin: A practical approach. Oxford: Oxford University Press, 1998; pp 173-194. .

124. **Perini, G., S. Wagner, and M. R. Green.** 1995. Recognition of bZIP proteins by the human T-cell leukemia virus transactivator Tax. Nature **376:**602-605.

Reproduced with permission of the copyright owner. Further reproduction prohibited without permission.

125. **Poiesz, B. J., F. W. Ruscetti, A. F. Gazdar, P. A. Bunn, J. D. Minna, and R. C. Gallo.** 1980. Detection and isolation of type C retrovirus particle from fresh and cultured lymphocytes of a patient with cutaneous T-cell lymphoma. Proc. Natl. Acad. Sci. USA **77:**7415-7419.

126. **Pusarla, R. H., and P. Bhargava.** 2005. Histones in functional diversification. Core histone variants. Febs J **272:**5149-68.

127. **Radhakrishnan, I., G. C. Perez-Alvarado, D. Parker, H. J. Dyson, M. R. Montminy, and P. E. Wright.** 1997. Solution structure of the KIX domain of CBP bound to the transactivation domain of CREB: a model for activator:coactivator interactions. Cell **91:**741-52.

128. **Rosen, C. A., J. G. Sodroski, and W. A. Haseltine.** 1985. Location of *cis*-acting regulatory sequences in the human T-cell leukemia virus type I long terminal repeat. Proc. Natl. Acad. Sci. USA **82:**6502-6506.

129. **Santoso, B., and J. T. Kadonaga.** 2006. Reconstitution of chromatin transcription with purified components reveals a chromatin-specific repressive activity of p300. Nat Struct Mol Biol **13:**131-9.

130. **Sarg, B., W. Helliger, H. Talasz, B. Forg, and H. H. Lindner.** 2006. Histone H1 Phosphorylation Occurs Site-specifically during Interphase and Mitosis: IDENTIFICATION OF A NOVEL PHOSPHORYLATION SITE ON HISTONE H1. J Biol Chem **281:**6573-80.

131. **Schlissel, M. S., and D. D. Brown.** 1984. The transcriptional regulation of Xenopus 5s RNA genes in chromatin: the roles of active stable transcription complexes and histone H1. Cell **37:**903-13.

132. **Schwarz, P. M., A. Felthauser, T. M. Fletcher, and J. C. Hansen.** 1996. Reversible oligonucleosome self-association: dependence on divalent cations and core histone tail domains. Biochemistry **35:**4009-15.

133. **Scoggin, K. E., A. Ulloa, and J. K. Nyborg.** 2001. The oncoprotein Tax binds the SRC-1-interacting domain of CBP/p300 to mediate transcriptional activation. Mol Cell Biol **21:**5520-30.

134. **Seiki, M., S. Hattori, Y. Hirayama, and M. Yoshida.** 1983. Human adult T-cell leukemia virus: complete nucleotide sequence of the provirus genome integrated in leukemia cell DNA. Proc Natl Acad Sci U S A **80:**3618-22.

Reproduced with permission of the copyright owner. Further reproduction prohibited without permission.

135. **Seiki, M., J. Inoue, T. Takeda, and M. Yoshida.** 1986. Direct evidence that p40x of human T-cell leukemia virus type I is a trans-acting transcriptional activator. EMBO J. **5:**561-565.

136. **Seiki, M., S. Hattori, and M. Yoshida.** 1982. Human adult T-cell leukemia virus: molecular cloning of the provirus DNA and the unique terminal structure. Proc. Natl. Acad. Sci. USA **79:**6899-6902.

137. **Sera, T., and A. P. Wolffe.** 1998. Role of histone H1 as an architectural determinant of chromatin structure and as a specific repressor of transcription on Xenopus oocyte 5S rRNA genes. Mol Cell Biol **18:**3668-80.

138. **Shaiu, W. L., and T. S. Hsieh.** 1998. Targeting to transcriptionally active loci by the hydrophilic N-terminal domain of Drosophila DNA topoisomerase I. Mol Cell Biol **18:**4358-67.

139. **Shimamura, A., M. Sapp, A. Rodriguez-Campos, and A. Worcel.** 1989. Histone H1 represses transcription from minichromosomes assembled in vitro. Mol Cell Biol **9:**5573-84.

140. **Shimotohno, K., M. Takano, T. Teruuchi, and M. Miwa.** 1986. Requirement of multiple copies of a 21-nucleotide sequence in the U3 region of human T-cell leukemia virus type I and type II long terminal repeats for trans-acting activation of transcription. Proc Natl Acad Sci USA **83:**8112-8116.

141. **Shimoyama, M.** 1991. Diagnostic criteria and classification of clinical subtypes of adult T-cell leukaemia-lymphoma. A report from the Lymphoma Study Group (1984-87). Br. J. Haematol. **79:**428-437.

142. **Shintomi, K., M. Iwabuchi, H. Saeki, K. Ura, T. Kishimoto, and K. Ohsumi.** 2005. Nucleosome assembly protein-1 is a linker histone chaperone in Xenopus eggs. Proc Natl Acad Sci U S A **102:**8210-5.

143. **Sterner, D. E., and S. L. Berger.** 2000. Acetylation of histones and transcription-related factors. Microbiol. Mol. Biol. Rev. **64:**435-459.

144. **Sugiyama, H., H. Doi, K. Yamaguchi, Y. Tsuji, T. Miyamoto, and S. Hino.** 1986. Significance of postnatal mother-to-child transmission of human T-lymphotropic virus type-I on the development of adult T-cell leukemia/lymphoma. J Med Virol **20:**253-60.

Reproduced with permission of the copyright owner. Further reproduction prohibited without permission.

145. **Suto, R. K., M. J. Clarkson, D. J. Tremethick, and K. Luger.** 2000. Crystal structure of a nucleosome core particle containing the variant histone H2A.Z. Nat Struct Biol **7:**1121-4.

146. **Tajima, K.** 1990. The 4th nation-wide study of adult T-cell leukemia/lymphoma (ATL) in Japan: estimates of risk of ATL and its geographical and clinical features. The T- and B-cell Malignancy Study Group. Int J Cancer **45:**237-43.

147. **Tajima, K., and T. Kuroishi.** 1985. Estimation of rate of incidence of ATL among ATLV (HTLV-I) carriers in Kyushu, Japan. Jpn J Clin Oncol **15:**423-30.

148. **Tajima, K., S. Tominaga, T. Suchi, H. Fukui, H. Komoda, and Y. Hinuma.** 1986. HTLV-I carriers among migrants from an ATL-endemic area to ATL non-endemic metropolitan areas in Japan. Int J Cancer **37:**383-7.

149. **Takatsuki, K., K. Yamaguchi, and Y. Matsuoka.** 1996. Adult T-cell leukemia. In: Human T-Cell Lymphotropic Virus Type I. H.D. Holsberg P (ed), New York. .219-246.

150. **Talasz, H., W. Helliger, B. Puschendorf, and H. Lindner.** 1996. In vivo phosphorylation of histone H1 variants during the cell cycle. Biochemistry **35:**1761-7.

151. **Thoma, F., and T. Koller.** 1977. Influence of histone H1 on chromatin structure. Cell **12:**101-7.

152. **Thoma, F., T. Koller, and A. Klug.** 1979. Involvement of histone H1 in the organization of the nucleosome and of the salt-dependent superstructures of chromatin. J Cell Biol **83:**403-27.

153. **Travers, A.** 1999. The location of the linker histone on the nucleosome. Trends Biochem Sci **24:**4-7.

154. **Uchiyama, T., J. Yodoi, K. Sagawa, K. Takatsuki, and H. Uchino.** 1977. Adult T-cell leukemia: clinical and hematologic features of 16 cases. Blood **50:**481-492.

155. **Ulyanova, N. P., and G. R. Schnitzler.** 2005. Human SWI/SNF generates abundant, structurally altered dinucleosomes on polynucleosomal templates. Mol Cell Biol **25:**11156-70.

Reproduced with permission of the copyright owner. Further reproduction prohibited without permission.

156. **Varga-Weisz, P. D., T. A. Blank, and P. B. Becker.** 1995. Energy-dependent chromatin accessibility and nucleosome mobility in a cell-free system. Embo J **14:**2209-16.

157. **Wolffe, A. P.** 1989. Dominant and specific repression of Xenopus oocyte 5S RNA genes and satellite I DNA by histone H1. Embo J **8:**527-37.

158. **Wolffe, A. P.** 1989. Transcriptional activation of Xenopus class III genes in chromatin isolated from sperm and somatic nuclei. Nucleic Acids Res **17:**767-80.

159. **Yamaguchi, K., T. Kiyokawa, G. Futami, T. Ishii, and K. Takatsuki.** 1990. Human Retrovirology: HTLV-1. Blatter, W.A. (ed). Raven Press: New York, pp. 163-171.

160. **Yao, T. P., S. P. Oh, M. Fuchs, N. D. Zhou, L. E. Ch'ng, D. Newsome, R. T. Bronson, E. Li, D. M. Livingston, and R. Eckner.** 1998. Gene dosage-dependent embryonic development and proliferation defects in mice lacking the transcriptional integrator p300. Cell **93:**361-72.

161. **Yasunaga, J., T. Sakai, K. Nosaka, K. Etoh, S. Tamiya, S. Koga, S. Mita, M. Uchino, H. Mitsuya, and M. Matsuoka.** 2001. Impaired production of naive T lymphocytes in human T-cell leukemia virus type I-infected individuals: its implications in the immunodeficient state. Blood **97:**3177-83.

162. **Yoshida, M.** 1995. HTLV-1 oncoprotein Tax deregulates transcription of cellular genes through multiple mechanisms. J Cancer Res Clin Oncol **121:**521-8.

163. **Yoshida, M.** 1994. Mechanism of transcriptional activation of viral and cellular genes by oncogenic protein of HTLV-1. Leukemia **8 Suppl 1:**S51-3.

164. **Yoshida, M.** 2001. Multiple viral strategies of HTLV-1 for dysregulation of cell growth control. Annu Rev Immunol **19:**475-96.

165. **Yoshida, M., J. Inoue, J. Fujisawa, and M. Seiki.** 1989. Molecular mechanisms of regulation of HTLV-1 gene expression and its association with leukemogenesis. Genome **31:**662-7.

Reproduced with permission of the copyright owner. Further reproduction prohibited without permission.

166. **Yoshida, M., I. Miyoshi, and Y. Hinuma.** 1982. Isolation and characterization of retrovirus from cell lines of human adult T-cell leukemia and its implication in the disease. Proc Natl Acad Sci U S A **79:**2031-5.

167. **Yoshida, M., M. Seiki, K. Yamaguchi, and K. Takatsuki.** 1984. Monoclonal integration of human T-cell leukemia provirus in all primary tumors of adult T-cell leukemia suggests causative role of human T-cell leukemia virus in the disease. Proc. Natl. Acad. Sci. USA **81:**2534-2537.

168. **Zhao, L. J., and C. Z. Giam.** 1992. Human T-cell lymphotropic virus type I (HTLV-I) transcriptional activator, Tax, enhances CREB binding to HTLV-I 21-base-pair repeats by protein-protein interaction. Proc. Natl. Acad. Sci. USA **89:**7070-7074.

169. **Zhao, L. J., and C. Z. Giam.** 1991. Interaction of the human T-cell lymphotrophic virus type I (HTLV-I) transcriptional activator Tax with cellular factors that bind specifically to the 21-base-pair repeats in the HTLV-I enhancer. Proc Natl Acad Sci U S A **88:**11445-9.

Reproduced with permission of the copyright owner. Further reproduction prohibited without permission.